Mechanisms Generating Biliary Lipid Specificity

Lipid transport in the apical and basolateral domain of the plasma membrane of differentiated HepG2 cells

D I S S E R T A T I O N

zur Erlangung des akademischen Grades
doctor rerum naturalium
(Dr. rer. nat.)
im Fach Biophysik

eingereicht an der
Mathematisch-Naturwissenschaftlichen Fakultät I
Humboldt-Universität zu Berlin

von
Frau Dipl.-Biochem. Astrid Tannert
geboren am 07.04.1976 in Wolfen

Präsident der Humboldt-Universität zu Berlin:
Prof. Dr. Jürgen Mlynek

Dekan der Mathematisch-Naturwissenschaftlichen Fakultät I:
Prof. Dr. Michael Linscheid

Gutachter:

1. Prof. Dr. Andreas Herrmann
2. Prof. Dr. Hermann-Georg Holzhütter
3. Prof. Dr. Philippe Devaux

eingereicht am: 2. September 2003
Tag der mündlichen Prüfung: 18. Dezember 2003

Abstract

This thesis addresses the molecular processes which are important in the formation of bile fluid. The polar liver cells (hepatocytes) secrete the bile fluid at their apical (canalicular) membrane into tubular bile canaliculi (BC) which are formed between adjacent cells. The basolateral membrane of hepatocytes faces the blood vessel. Bile fluid possesses a remarkable specificity regarding its lipid composition. Even though phosphatidylcholine (PC) contributes to only 35 % of the phospholipids in the canalicular membrane, it constitutes 95 % of biliary phospholipids. In this thesis possible mechanism that might lead to the specificity in biliary lipid secretion are analysed and discussed.

Phospholipids are secreted from the outer leaflet of the canalicular membrane into bile by the effect of bile salts. The interaction of bile salts with phospholipids was shown to be independent of the phospholipid headgroup. Solubilisation of phosphatidylserine (PS) and phosphatidylethanolamine (PE) by bile salts could be prevented by the action of an aminophospholipid translocase (APLT) which actively pumps these lipids to the cytoplasmic leaflet of the membrane. Experiments to demonstrate a canalicular APLT activity were performed to proof this hypothesis. For this, the hepatoma cell line HepG2 which is able to polarise and to form a canalicular vacuole (BC) was utilised. A panel of fluorescent lipid analogues with different affinities to this transporter was used and first characterised at the basolateral membrane of HepG2 cells, where an APLT activity was already demonstrated. The rapid APLT mediated uptake of aminophospholipid analogues representing appropriate substrates of APLT was reduced by applying the inhibitor suramin. The affinity of a pair of PS analogues with diether NBD-PS as a poor APLT substrate and diacyl NBD-PS representing a suitable substrate was confirmed. In a next step the enrichment of the same phospholipid analogues in the BC was investigated. There was a striking correlation between APLT mediated uptake of phospholipid analogues at the basolateral membrane and absence of these analogues from the BC. In the case of phospholipid analogues that were no or poor substrates of APLT the BC appeared highly fluorescent, indicating that indeed a canalicular APLT is responsible and sufficient for biliary absence of aminophospholipids.

Further experiments were aimed on the investigation of the role of MDR proteins (as MDR3) in biliary lipid secretion. It has been proposed that MDR3, which is crucial for biliary phospholipid secretion, acts as a specific flippase for

PC. However, different MDR inhibitors did not completely abolish the enrichment of fluorescent phospholipid analogues in the BC in this study. This observation can be explained assuming that MDR3 is responsible for the exposure of PC at the lumenal side of the canalicular membrane rather than for its transport across the membrane. Such a "liftase" activity of MDR could make endogenous PC accessible to the detergent bile salts which is not necessary for its more hydrophilic fluorescent analogues.

The third part of this thesis addressed the role of sphingolipids and the formation of detergent resistant rafts in the canalicular membrane. Rafts are thought to prevent sphingolipid solubilisation into bile. Fluorescent sphingolipid analogues were found to enrich in the BC even at low temperatures, however. These experiments suggest that the applied analogues might not suitably represent the majority of sphingolipids in the canalicular membrane.

The final part of this study provides the basis for a method to investigate the physico-chemical processes occurring during lipid secretion at the canalicular membrane. The sensitivity of fluorescence life times on environmental changes was analysed using fluorescent lipid analogues in a set of model environments and its utility for predicting biliary lipid organisation is discussed. Especially the interaction of different bile salts with lipid analogues and fluorescence energy transfer between distinct lipid analogues was characterised. These data can be utilised for characterisation of the organisation of biliary enriched lipid analogues *in vivo* at a microscopic level in future.

Keywords:
bile fluid, aminophospholipid translocase, phospholipids, MDR, fluorescence

Zusammenfassung

Die vorliegende Arbeit beschäftigt sich mit den molekularen Prozessen der Lipidanreicherung in der Gallenflüssigkeit. Leberzellen (Hepatozyten) sind polare Zellen, die für die Sekretion der Gallenflüssigkeit verantwortlich sind. Die Anbindung an den Blutkreislauf besteht über die basolaterale Membran. Durch die gegenüberliegende, sogenannte apikale Membran werden zwischen benachbarten Leberzellen tubuläre Stukturen (bile canaliculi, BC) gebildet, in die die Gallenflüssigkeit abgesondert wird. Daher wird diese Membran auch als Canalicularmembran (CM) bezeichnet.

Die Gallenflüssigkeit besitzt hinsichtlich ihrer Lipidzusammensetzung eine bemerkenswerte Spezifität. Obwohl der Anteil von Phosphatidylcholin (PC) an den Phospholipiden der CM nur 35 % beträgt, macht es 95 % der Phospholipide der Gallenflüssigkeit aus. Mögliche Mechanismen, die zur Spezifität der Lipidsekretion in die Gallenflüssigkeit führen, werden untersucht und diskutiert.

Phospholipide werden aus der äußeren Lamelle der CM durch Gallensalze herausgelöst. Die Wechselwirkung von Gallensalzen mit Phospholipiden ist kopfgruppenunspezifisch. Eine Solubilisierung von Phosphatidylserin (PS) und Phosphatidylethanolamin (PE) durch Gallensalze könnte durch die Wirkung einer Aminophospholipidtranslokase (APLT) verhindert werden, die diese Lipide aktiv auf die zytoplasmatische Seite der Membran pumpt. Zur Überprüfung dieser Hypothese wurden Versuche durchgeführt, um die Aktivität einer APLT in der CM nachzuweisen. Dabei wurde die Hepatomazelllinie HepG2 eingesetzt, die in der Lage ist, Canalicularvakuolen (BC) zu bilden. Zunächst wurde die Einwärtsbewegung einer Reihe fluoreszierender Lipidanaloga mit unterschiedlicher Affinität zur APLT charakterisiert. Dies geschah an der basolateralen Membran von HepG2 Zellen, wo eine APLT-Aktivität bereits bekannt ist. Die Aufnahme geeigneter APLT-Substrate konnte durch den APLT-Inhibitor Suramin reduziert werden. Ebenso wurde die Affinität eines Paares von PS-Analoga bestätigt, von denen Diether PS ein „schlechtes“ und Diacyl PS ein „gutes“ APLT-Substrat darstellt. Im zweiten Schritt wurde die Anreicherung der gleichen Analoga in BC von HepG2 Zellen untersucht. Es ergab sich eine auffallende Korrelation zwischen einer APLT vermittelten Aufnahme von Phospholipidanaloga an der basolateralen Membran und dem Fehlen dieser Analoga im Lumen der BC. Wenn Zellen mit Phospholipiden markiert wurden, die keine oder nur „schlechte“ APLT-Substrate darstellen, erschienen

die BC stark fluoreszierend. Diese Beobachtungen zeigen, dass eine APLT-Aktivität in der CM von Hepatozyten vorhanden ist, welche das Fehlen der Aminophospholipide in der Gallenflüssigkeit erklärt.

Ein zweiter Schwerpunkt dieser Arbeit war die Untersuchung der Rolle von MDR-Proteinen (wie MDR3) bei der Lipidsekretion in die Gallenflüssigkeit. Aufgrund bisheriger Arbeiten wird vermutet, dass MDR3 daran als spezifischer Membrantransporter für PC beteiligt ist. In der vorliegenden Arbeit konnte jedoch gezeigt werden, dass verschiedene MDR-Inhibitoren die Anreicherung fluoreszierender Phospholipidanaloga in den BC von HepG2 Zellen nur wenig reduzieren. Diese Beobachtung kann unter der Annahme erklärt werden, dass MDR3 eher für die Exposition von PC an der lumenalen Seite der CM verantwortlich ist, als für den Tranport von PC über die Membran. Solche „Liftase"-Aktivität von MDR3 könnte endogenes PC der Detergenzwirkung von Gallensalzen zugänglich machen, ein Prozess, der für die hydrophileren fluoreszierenden PC-Analoga nicht nötig ist.

Im dritten Teil wird die Rolle von Sphingolipiden und die Bildung von „Rafts" in der CM behandelt. Solche Membrandomänen sollten die Solubilisierung von Spingolipiden in die Gallenflüssigkeit verhindern. Eine Anreicherung fluoreszierender Sphingolipidanaloga in den BC wurde jedoch nachgewiesen, was darauf hindeutet, dass die verwendeten Analoga das Verhalten endogener Sphingolipide in der CM nicht korrekt wiederspiegeln.

Im abschließenden Teil dieser Arbeit wurden die Grundlagen für eine Methode zur Aufklärung der physikochemischen Prozesse der Lipidsekretion an der Canalicularmembran gelegt. Die starke Umgebungsabhängigkeit der Fluoreszenzlebensdauer für verschiedene fluoreszierende Lipidanaloga wurde in einer Reihe von Modellumgebungen analysiert und deren Nutzbarkeit für die Vorhersage der Lipidorganisation geprüft. Insbesondere wurde die Wechselwirkung verschiedener Gallensalze mit Lipidanaloga und der Fluoreszenzresonanzenergietransfer zwischen verschiedenen Lipidanaloga charakterisiert. Diese Daten sind Ausgangsbasis für die mikroskopische Charakterisierung der Organisation von Lipidanaloga in den BC *in vivo*.

Schlagwörter:
Gallenflüssigkeit, Aminophospholipidtranslokase, Phospholipide, MDR, Fluoreszenz

Contents

Abbreviations

ABC ..... ATP binding cassette
APLT ..... aminophospholipid translocase
ATP ..... adenosin triphosphate
BC ..... bile canaliculus/bile canaliculi
BP ..... band pass
BSA ..... bovine serum albumin
BSEP ..... bile salt export pump
CCD ..... charge coupled device
CGamF ..... cholylglycylamidofluorescein
CLSM ..... confocal laser scanning microscopy / microscope
CM ..... canalicular membrane(s)
CMC ..... critical micellar concentration
DFP ..... diisopropyl fluorophosphate
DHC ..... sodium dehydrocholate
DHE ..... dehydroergosterol
DMEM ..... Dulbecco's modified eagle medium
DPBS ..... Dulbecco's modified phosphate buffered saline
$DPBS^{+}$ ..... DPBS supplemented with glucose, pyruvate, and HEPES
EDTA ..... ethylene diamine tetra-acetate
ER ..... endoplasmic reticulum
EYPC ..... egg yolk phosphatidylcholine
EYSM ..... egg yolk sphingomyelin
FCS ..... foetal bovine serum
FRET ..... fluorescence resonance energy transfer
FWHM ..... full width of half maximum
GalCer ..... galactosyl ceramide

GC ..... sodium glycocholate

GlcCer ..... glucosyl ceramide

HBSS ..... HANK's buffered salt solution

$HBSS^+$ ..... HBSS supplemented with Ca^{2+} and Mg^{2+}

HI ..... hydrophobicity index

IRF ..... instrument response function

iRNA ..... interference ribonucleic acid

LP ..... long pass

LUV ..... large unilamellar vesicle

MCP ..... micro channel plate

MDR ..... multidrug resistance

MRP ..... multidrug resistance related protein

NBD 7-nitrobenzo-2-oxa-1,3-diazol-4-yl

N-Fl-PE 1,2-dioleoyl-sn-glycero-3-phosphoethanolamine-N-carboxy-fluorescein

N-Rh-PE ..... L-α-phosphatidylethanolamine-*N*-(lissamine rhodamine B sulfonyl)

NTCP ..... sodium-dependent taurocholate cotransporting polypeptide

OATP ..... organic anion transport protein

OCT ..... organic cation transport protein

PA ..... phosphatidic acid

PBS ..... phosphate buffered saline

PC ..... phosphatidylcholine

PC-TP ..... phosphatidylcholine transfer protein

PE ..... phosphatidylethanolamine

PFIC ..... progressive familiar intrahepatic cholestasis

PI ..... phosphatidylinositol

PL ..... phospholipid(s)

PM ..... plasma membrane

PS ..... phosphatidylserine

PSC 833 ..... 3'-oxo-4-butenyl-4methyl-threonine1)-(Val^2)-cyclosporin

POPC 1-palmitoyl-2-oleoyl-*sn*-glycero-3-phosphocholine

Rho123 ..... rhodamine 123

SEM ..... standard error of mean

SHG ..... second harmonics generation

SM ..... sphingomyelin

SUV ..... small unilamellar vesicle

TC ..... sodium taurocholate

TCSPC ..... time correlated single photon counting

TDC ..... sodium taurodeoxycholate

TGN ..... trans-Golgi network

TLC ..... sodium taurolithocholate

TLChr ..... thin liquid chromatography

UDC-NBD ..... ursodeoxycholyl-(Nϵ-NBD)-lysine

λ_{em} ..... wavelength of emission

λ_{ex} ..... wavelength of excitation

τ, τ_{Fl} ..... experimental fluorescence life time

χ^2 ..... figure of merit parameter describing the goodness of a fit

1 Introduction

1.1 The Liver and the Genesis of Bile Fluid

The liver is the central organ of metabolism and fulfils a variety of functions. These are, among others, the synthesis of plasma proteins, urea, hormones, and lipids, detoxification, degradation and storage of a great number of substances, and secretion of bile fluid. The liver is therefore a multifunctional organ which comprises different cell types. Hepatocytes, the major liver cells, make up 60–70 % of the liver cell mass and are (like the cholangiocytes which form the bile duct) of epithelial origin [1]. They are organised into folded sheets that face the blood filled sinusoids at one side, which are separated from the hepatocytes by a single layer of endothelial cells. At their other side, hepatocytes form a system of minute channels called biliary canaliculi (BC) into which they secrete the bile fluid (see figure 1.1). The flow of blood and bile is always in opposite direction [2]. Besides their function in transporting the emulsifying bile, BC also serve to secrete waste products into the gut [2].

Bile that is secreted by the hepatocytes is called primary bile. During its passage through the bile duct to the gallbladder it is modified and concentrated by resorption of water and electrolytes forming the so called secondary bile. The primary bile is an aqueous solution containing lipids, proteins, and bilirubin conjugates. Lipids form the most abundant solid component of the bile fluid [2].

BC are surrounded by the canalicular membranes (CM), domains of the plasma membrane (PM) of adjacent cells. Secretion of bile from the hepatocytes occurs via these CM, usually by the action of specific membrane transport proteins. Biliary lipids may also be solubilised directly from the CM (see below).

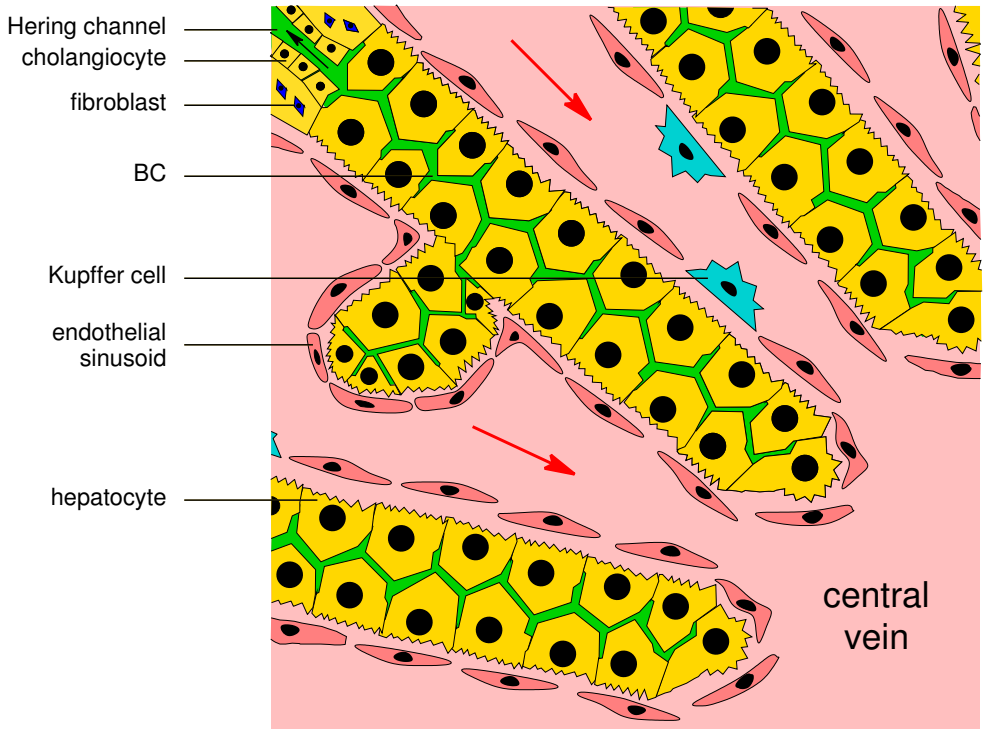

Figure 1.1: **Structure of the liver lobule.** (Schematic picture adapted from [2, 3, 4].) Hepatocytes are organised as plates of cells that form a layer which is about two cells thick. They are radially disposed from the central vein to the periphery of the lobule. A system of sinusoids interlaces the cells with mixed portal and arterial blood (red arrows). These sinusoids are separated from the hepatocytes by a single layer of endothelial cells and Kupffer cells. Kupffer cells are specialised macrophages that serve to eliminate cell fragments, bacteria etc. Hepatocytes form the BC (green) as minute channels between adjacent cells. Bile is collected in the opposite direction of blood flow into Hering channels (black arrow). The latter is the first part of the intrahepatic bile duct. At the edges of the hexagonal lobule the portal triad is located which consists of the interlobular vein (portal vein), the interlobular artery (hepatic artery), and the interlobular bile duct (not shown). [5]

1.2 Cellular Membranes

As biliary lipids are secreted from a specialised cellular membrane, it is worth to have a look on general features of biological membranes and the differences between certain types of them. Also membrane transport proteins shall be introduced in this section, with a special focus on those, which are involved in bile formation.

Biological membranes are build up by a bilayer of lipids (mainly phospholipids (PL), glycolipids and cholesterol) with embedded proteins. However, lipids have far more functions than forming the backbone of the membrane. The transbilayer distribution of lipids influences important physiological functions as cell viability, (phosphatidylserine (PS) is exposed to the exoplasmic leaflet of the PM of apoptotic cells) membrane fusion and cell - cell recognition.

The composition of the different cellular membranes is quite specific, with a lipid-to-protein ratio varying from 0.2–0.8 depending on the cell type and its function. The PM and the several intracellular membranes differ with respect to their lipid and protein composition. Even within one membrane the lipid composition may be different between separated domains as basolateral and apical domains of the PM of polarised cells. Even smaller domains (microdomains, rafts) were found, which are especially enriched in sphingomyelin and cholesterol and are defined by their insolubility in the detergent Triton X 100 [6]. Rafts might play a role in signalling processes, membrane sorting, membrane fusion etc.

As hepatocytes are polarised cells they have distinct PM domains. The apical or canalicular membrane which faces the BC is separated from the rest of the PM by tight junctions at the exoplasmic leaflet. The basolateral or sinusoidal membrane which faces the blood endothelial cells, and the lateral membrane domain which is located at the contact side between different hepatocytes form a continuum.

Within the membrane, lipids are able to move laterally (usually distances in the range of micrometres within seconds). However, spontaneous transversal movement of lipids carrying a polar head-group across a pure lipid bilayer is very rare (typical half-time of hours to days depending on the size and charge of the head group) [7]. In the presence of proteins, an increased transversal movement of lipids may occur due to a partial disturbance of the bilayer structure. Also, specific proteins involved in lipid transbilayer movement are embedded in biological membranes. The activity of these proteins may be highly selective (for instance for the head-group of PL) or unspecific. Some of these lipid transporters facilitate flip-flop of lipids and allow them to equilibrate between the two membrane leaflets independently of ATP (passive transport). Others specifically transport lipids against their concentration or electrochemical gradient consuming ATP and generating and/or maintaining a transbilayer lipid asymmetry in the membrane (active transport) [8].

Proteins are also responsible for the transport of non-lipid substances like amphiphatic drugs, ions, and nutrients across cellular membranes.

1.2.1 ABC Transport Proteins

Among others, ATP binding cassette (ABC) proteins play a role in active lipid transport across cellular membranes. Proteins belonging to this large superfamily found ubiquitously in prokaryotes and eukaryotes are responsible for the transport of a variety of substances across cellular membranes under the consumption of ATP. The ABC-proteins are characterised by their ATP binding domain of about 200–250 amino acids containing the conserved motifs Walker A and Walker B which are responsible for ATP binding [9].

In the past three decades, multidrug resistance (MDR) proteins belonging to the ABC transporter superfamily have been studied intensely. Their ability to transport cytotoxic drugs out of the cell makes them a medical challenge, for instance in chemotherapy. Their role in lipid transport has only recently

attracted interest in medical research. Now it becomes clear, that more ABC transporters may have a function in lipid transport than previously assumed.

In humans, 48 ABC proteins are currently known, which are classified into 7 families (A–G) according to sequence similarities [9]. Several of these were suggested to be involved in lipid transport after having been found to be mutated in lipid-linked diseases, involving members of the families A, B, C, D, and G. So far, direct transport of lipid substrates has only been shown for a small number of human ABC proteins.

The ABC transport proteins that are located in the hepatocyte PM shall be introduced in the following part. The role of the ABC transporters in hepatobiliary transport and bile secretion is only fully investigated for a few members of this family. Current research is focussed on the identification of the physiological role of newly investigated family members.

Most ABC proteins are relatively specific for a particular set of substrates. MDR1 Pgp (ABCB1), however, seems to be rather unspecific. In addition to the transport of a variety of structural unrelated compounds [10], it was also shown to transport lipid analogues [11, 12, 13, 14].

Due to its low substrate specificity, MDR1 Pgp might affect the transverse distribution of endogenous lipids, in particular of species which are normally predominant on the cytoplasmic PM leaflet, such as PS and PE [12, 14]. It was further shown to be involved in cholesterol redistribution across the PM [15]. MDR1 Pgp is also located in the apical plasma membrane of hepatocytes where it is thought to mediate the export of cationic cytotoxic drugs into the bile [16]. The protein is localised in low density membrane fractions enriched in sphingolipids and cholesterol. Cholesterol depletion, however, had no influence on its function in HepG2 cells [17].

ABCB4 (also termed MDR3 in human, corresponding to murine mdr2) is a close relative of MDR1 Pgp, sharing 75 % of its amino acid sequence. Unlike MDR1 Pgp, MDR3 is highly specific, exclusively transporting PC and

its analogues [11]. High accumulation of MDR3 is found in the canalicular membrane of hepatocytes, lower levels in the adrenal, heart, striated muscle, spleen, and tonsils [18, 19]. The physiological function of mdr2/MDR3 appears to be PC secretion into the bile [20, 21]. In some cases of progressive familiar intrahepatic cholestasis (PFIC), type III, MDR3 has indeed been found to be defective [22, 19].

ABCB11 which is also known as "sister of P-glycoprotein" (sPgp) or "bile salt export pump" (BSEP) was shown to act as an ATP-dependent canalicular bile salt transporter [23]. This protein is defective in PFIC, type II [24, 25] which is characterised by an accumulation of bile salts in the hepatocytes leading to injury, apoptosis and/or necrosis [24].

Members of the ABCC or MRP family, the so called "family of conjugate export pumps" are involved in the transport of a variety of conjugated substances out of the hepatocyte.

MRP1 and MRP2 (ABCC1 and ABCC2, respectively) are the best characterised members of this subfamily. They are closely related sharing about 49 % of amino acid sequence identity [26]. Both proteins function in detoxification of the cell and have a similar substrate specificity including glutathione-S-conjugates, oxidised gluthathione, and bilirubin diglucoronide [26, 27, 28]. MRP1 was also found to transport NBD labelled phospholipid analogues [29, 30, 31]. Transport of endogenous lipids was not reported for MRP1, however. While MRP1 is only expressed to a low amount in the liver (in the lateral membrane of hepatocytes [32]), MRP2 is abundant in the canalicular membrane of hepatocytes [33, 28]. MRP2 which is also known as canalicular multi organic anion transporter (cMOAT) is lacking in Dubin-Johnson syndrome, a conjugated hyperbilirubinemia, which is associated by a deficiency in the secretion of amphiphilic anions into bile [26, 34]. MRP2 was also shown to be involved in the secretion of sulfated and glucurunidated bile salts across the apical membrane [35, 36].

MRP3 (ABCC3) is expressed at the basolateral membrane of hepatocytes and mediates the transport of organic anions. It is upregulated when MRP2 is defective and might prevent the cell from toxic effects of substances that are normally excreted into the bile while sharing a similar substrate specificity with MRP2 [37, 38]. MRP3 was also shown to be able to transport bile salts and thus might prevent the cell from their emulsifying effects when the function of the bile salt exporters is disturbed [38].

MRP6 (ABCC6) which is highly expressed in the liver [39] was identified in the lateral and in the canalicular membrane of hepatocytes [27, 40]. Substrates are cyclic and linear hydrophobic peptides. Its physiological role, however, remains to be elucidated [40]. Among other possible functions it was also suggested to be involved in lipid transport and metabolism probably being a determinant of plasma lipoproteins [41].

Members of the ABCG family are associated with cholesterol and PL transport [42, 43]. ABCG5 and ABCG8 form a heterodimer in the membrane. When disrupted, mice show similar pathology as human patients with sitosterolemia, a disease that leads to the accumulation of plant sterols [44].

ABCG2, the human breast cancer resistance protein (BCRP) is abundant in the canalicular membrane of hepatocytes [45]. Its function is not yet fully understood. There is evidence that this protein is involved in sterol transport [46] and in the transport of PL across the PM (H. Woehlecke, unpublished observation).

1.2.2 P-type ATPases

The distribution of PL across the mammalian PM is not a random one. The aminophospholipids PS and phosphatidylethanolamine (PE) are enriched on the cytoplasmic side, whereas the PL containing a choline headgroup, PC and sphingomyelin (SM), are located almost exclusively on the exoplasmic leaflet of the PM [47]. The asymmetric distribution of PL across the PM seems

to be an important feature of living cells. A perturbation of the asymmetry is a signal in the process of apoptosis. The maintenance of this asymmetric distribution of PL is a function of a putative protein called aminophospholipid translocase (APLT). This protein transports the aminophospholipids PS and PE from the exoplasmic to the cytoplasmic leaflet of the PM, hydrolysing one molecule ATP per transported PL [48]. The affinity of APLT to PS is about tenfold higher than to PE [49]. Using spin labelled PL analogues, the half time of inward transport at the PM of red blood cells was found to be 2–5 min for PS and about 30 min for PE [50]. The PL that are typically found at the exoplasmic leaflet of the PM (e.g. PC, SM) are not recognised by APLT. APLT activity was first demonstrated in erythrocytes [51, 52, 53, 54] and was subsequently reported for a variety of mammalian cells [55, 56, 57, 58, 59, 60, 61, 62], including the basolateral membrane of hepatocytes [63, 64]. An APLT activity and thus an asymmetric distribution of PL in the apical PM domain of hepatocytes is assumed to be responsible for the almost complete absence of aminophospholipids from bile [65, 66] (see below), but has not yet been demonstrated.

Transport activity of APLT has been shown to be sensitive to vanadate [51], the sulfhydryl group modifying agent *N*-ethylmaleimide [53, 49], and to suramin, elaiophylin and eosin Y [67].

The activity of this protein has been known for about 20 years, but its molecular identity is still unknown. Recent results imply that it is very likely a member of the P-type ATPase family [67]. A possible candidate for APLT was cloned from bovine chromaffin granules [68], which was shown to be the first representative of a yet unknown subfamily of P-type ATPases. The homologue ALA1 in plants was also identified as a possible APLT [69]. Mutants in which the homologous protein in yeast (Drs2p) was defective were identified to lack low temperature uptake of fluorescent PS at the PM, which could not be confirmed by two independent groups [70, 71]. Later on Drs2p was shown to

be located to the late Golgi [72], so the identification of this protein as APLT is questioned. Recently, two other members of the P-type ATPase subfamily, Dnf1p and Dnf2p, have been found to be involved in transbilayer movement of fluorescent PL analogues of PS, PE, and PC in yeast [73]. Also other studies demonstrated that active uptake of PL in yeast is not restricted to aminophospholipids, but also includes PC [74]. It is thus likely that different types of P-type ATPase might function as PL translocases in different species. The protein Ros3p, which is unrelated to P-type ATPases, was also suggested to be involved in PL uptake in yeast, as deletions caused a reduced uptake of fluorescent PE and PC across the PM [75]. However, it is more likely to play another, perhaps regulative, role in the translocation machinery of the P-type ATPases [73].

Also the *Fic1* gene which is mutated in PFIC, type I was shown to code for a P-type ATPase [76]. It is located in the apical membrane of hepatocytes and cholangiocytes [77] and hence it was assumed to encode for an APLT in the canalicular membrane. Recently, Ujhazy et al [78] have demonstrated a Fic1 mediated PS translocation in transfected cells. However, as the authors did not investigate the translocation of non-aminophospholipids, it remains open whether Fic1 is a transporter specific for aminophospholipids. Fic1 might alternatively be involved in canalicular bile salt export as mutations in its gene show a similar pathology as PFIC II in which the canalicular BSEP is defective (see above). The bile of patients with PFIC I mainly lacks hydrophobic bile salts, so this protein might be a transporter for this type of bile salts [79]. At our current knowledge, the *Fic1* gene might encode for a bile salt pump by itself or for a protein that is necessary for the functional incorporation of bile salt pumps into the membrane [80, 77, 81].

1.2.3 Other Membrane Transporters in Hepatocytes

The basolateral uptake of a variety of bile salts is largely mediated by the sodium-dependent taurocholate cotransporting polypeptide (NTCP), which is also able to transport other organic anions. The driving force of the uptake of bile salts against the concentration gradient by this protein is the sodium gradient across the PM [80]. Sodium independent transport of organic anions including bile salts is performed by the family of organic anionic cotransporting polypeptides (OATPs). LST-1, another basolateral sodium independent organic anion transporter in humans was identified as a member of a new gene family [82] and is the predominant sodium independent bile salt uptake system in humans. LST-1 is also called OATP2 or OATPC although it is unrelated to rat Oatp2 [24].

Moreover, organic cation transporters (OCT) are localised in the basolateral membrane of hepatocytes, which are responsible for the hepatic clearance of substances as tetraethylammonium [34, 83, 25].

A summary of the proteins that are involved in membrane transport in hepatocytes is presented in figure 1.2.

1.3 Lipids in Bile

Biliary lipids comprise bile salts, phospholipids, and cholesterol. They function as detergents emulsifying dietary fats and make them accessible to the action of intestinal lipases.

As shown in table 1.1 the lipid composition of the bile varies between different species and is highly specific regarding the different constituents.

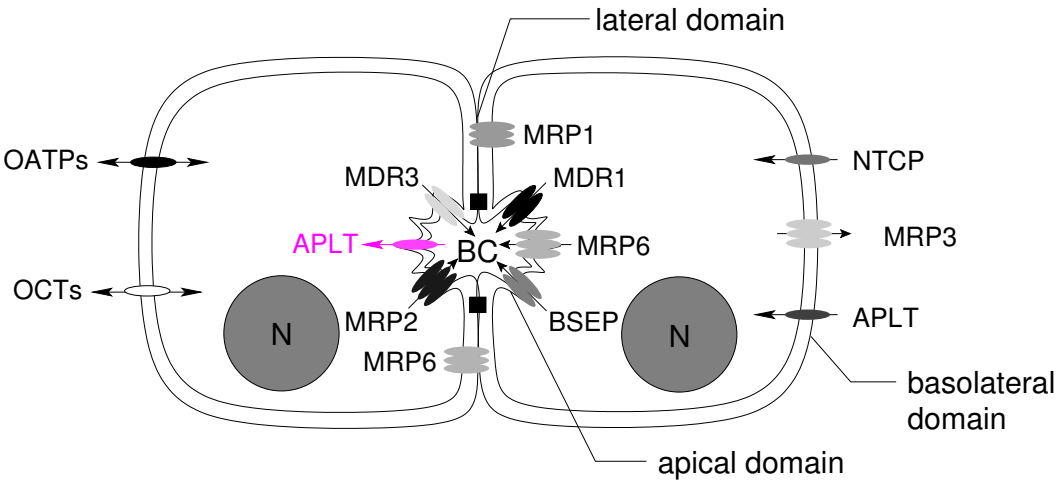

Figure 1.2: **Membrane transport proteins in hepatocytes.** Schematic picture of two hepatocytes forming a BC by a specialised apical membrane domain (adapted from [34, 83, 24, 80]). The localisation of the transport proteins in the different membrane domains is indicated. The putative APLT of the apical membrane is shown in pink. N-nucleus, black boxes represent tight junctions at the exoplasmic leaflet of the PM. See text for further explanation.

Table 1.1: **Comparison of lipid composition in different species.** BS-bile salts, PL-phospholipid, Ch-cholesterol; all values are given in mM. HI-hydrophobicity index of biliary bile salts according to Heuman [84]; data were taken from the literature [84, 85].

	Human	Rat	Mouse
BS	150–200	37	83
PL	46–58	7	22
Ch	5.3–20	0.6	4
HI	+0.32	-0.31	-0.45

1.3.1 Bile Salts

Bile salts are the major lipid species in the bile fluid and make up 60–70 % of the organic constituents of the bile in humans and most animals [85]. Bile salts that are secreted into the BC by hepatocytes are called primary bile salts. Only a small fraction of them is newly synthesised from cholesterol in hepatocytes. About 95 % of the bile salts are resorbed by the intestinal epithelium and redirected to the hepatocytes, a process called enterohepatic circulation [24]. During their passage through the intestine, bile salts are modified by bacteria becoming so called secondary bile salts. This process involves cleavage of an amino group (deconjugation) and several hydroxyl groups (dehydroxylation). The basolateral uptake of secondary bile salts is mediated by NTCP or OATPs (see section 1.2.3) [83]. Microsomal enzymes in hepatocytes are responsible for reconjugation and rehydroxylation of the secondary bile salts which are subsequently secreted into BC again [86]. Human bile salts are turned over about 6–10 times per day. About 0.5 g of the bile salts are lost through fecal excretion daily, corresponding to about 15 % of the human adult bile salt pool [24].

The intracellular transport of bile salts to the apical membrane is mediated by carrier proteins. If necessary (i. e. when bile salts are modified) these carrier proteins also interact with intracellular compartments like the ER. [86] Bile salts may also be transported through the cytoplasm in vesicles, especially when the intracellular bile salt concentration is high or bile salts are more hydrophobic [87, 24]. The active secretion against an about 1000 fold concentration gradient is mediated mainly by ABC proteins like BSEP and MRP2 (see above) [80, 83, 24].

1.3.2 Phospholipids

The PL composition of bile is very specific, as it mainly contains phosphatidylcholine (see table 1.2). Also the fatty acid composition of the PL in the bile is different from that of any cellular membrane. Biliary PL generally possess shorter fatty acid chains, as palmitic acid in *sn1*-position and oleic, linoleic, and arachidic acid in *sn2*-position [88].

Table 1.2: **Phospholipid composition of bile and the hepatocyte PM domains.** In contrast to its relative low content in the CM, PC is highly enriched in the bile fluid. BM-basolateral membrane. Data are given as % of total PL according to the literature [89].

	BM (%)	CM (%)	bile (%)
PC	44.6	35.5	94.8
SM	11.0	22.1	0.1
PE	28.4	23.8	4.5
PS	7.6	11.2	–
PI	6.4	4.4	–

Biliary PC is largely reabsorbed in the intestine. However, it is not completely recycled as described for bile salts, but rapidly degraded. The choline-head group is often reused to synthesise PC for biliary secretion. [90, 85]

The main fraction of biliary PC originates from a preformed intrahepatic microsomal pool, or is transported to the sinusoidal membrane in a HDL bound manner, where it is rapidly incorporated into the hepatocyte. Only about 14 % of biliary PC is formed from choline that is newly synthesised in the liver. [91, 92, 93] Two pathways exist for the intracellular transport of PC from the sinusoidal to the apical domain of the PM. This transport occurs either at the cytoplasmic leaflet of the PM or in vesicles through the cytoplasm [94]. A phosphatidyl transfer protein (PC-TP) has also been suggested to be involved in the intracellular transport of PC between the different membrane

domains [95]. No defects in biliary lipid secretion were found in the absence of PC-TP, however [96].

PL are secreted from the exoplasmic/lumenal leaflet of the canalicular membrane [65] into the lumen of the BC by the detergent capacity of lumenal bile salts. The interaction of bile salts with PL is independent of the head group but depends on the fatty acid composition of the PL [65, 66].

The ABC transporter MDR3 is essential for the enrichment of PC in the bile [21]. It is thus thought to represent a specific PC transporter which actively pumps PC from the cytoplasmic to the lumenal leaflet of the CM. This process makes PC accessible to the solubilising potential of bile salts (see section 1.2.1).

Even though Borst and his coworkers [20] showed a complete absence of PC from the bile of mdr2 knock out mice, also an ATP independent transport of PC across the canalicular membrane was reported [97, 98], which was not influenced by the general MDR inhibitor Verapamil [99].

1.3.3 Cholesterol

Cholesterol represents the third class of biliary lipids. In humans, biliary secretion is the only pathway for cholesterol elimination of the body. Newly synthesised cholesterol comprises only about 8 % of biliary cholesterol, the major part derives from preformed pools in the hepatocyte or from uptake at the sinusoidal membrane bound to lipoproteins [85]. Intracellular transport of cholesterol between the membrane domains and/or organelles is rapid and mainly independent of vesicles [100, 101]. The secretion of cholesterol into the BC is coupled to the secretion of PL which are solubilised from the apical membrane by the action of bile salts [85]. Biliary cholesterol secretion depends on the expression of the ABC transport proteins ABCG5 and ABCG8 which form a heterodimer [44] (see section 1.2.1). It is assumed that these proteins activate cholesterol in the CM and thus facilitate the disentanglement of cholesterol by bile salt/phospholipid micelles or vesicles. This scenario is more likely than a

cholesterol transport as cholesterol is able to cross the PM even without the help of proteins much faster than PL [102].

1.4 Model for Biliary Lipid Secretion

The active secretion of bile salts and other organic anions as glutathione and its conjugates into the BC is the major driving force of bile formation [25] and results in the secretion of other bile constituents. Mechanisms that lead to the specificity in biliary lipid contents, especially in its PL composition shall be discussed in this section as well as the physico-chemical processes of lipid secretion.

1.4.1 Phospholipid Asymmetry

The PL asymmetry of the PM (as described in section 1.2.2) which is most likely mediated by APLT was demonstrated for a variety of cells and is believed to be a general feature of mammalian cells. However, an APLT activity was not yet demonstrated in the canalicular membrane of hepatocytes, even though the Fic1 protein was suggested to harbour this function (see section 1.2.2) [78]. An asymmetric distribution of PL in the apical membrane might be responsible for the almost complete absence of aminophospholipids of the bile. As bile salts solubilise only PL in the outer leaflet [65] the action of a putative APLT in the canalicular membrane might prevent the aminophospholipids PS and PE from solubilisation by pumping them to the inner leaflet [94]. This would also explain the presence of a low amount of PE in the bile as APLT has a lower affinity to PE than to PS [50].

1.4.2 Bile Salt Resistance and Transbilayer Organisation of the Canalicular Membrane

The amount of SM in the apical membrane is about twofold higher than in the sinusoidal membrane of hepatocytes (see table 1.2). As sphingolipids and cholesterol are known to form detergent insoluble rafts (see section 1.2), the high amount of sphingolipids in the canalicular membrane might be necessary to prevent a complete solubilisation of this membrane by the bile salts in the lumen of the BC. The biliary PC (with its relatively short fatty acid chains) might be located at the cytoplasmic leaflet of the canalicular membrane. The transport activity of proteins like MDR3 (see section 1.3.2) would then be necessary to make PC accessible to the detergent potential of bile salts in the BC. This hypothesis is consistent with a lateral diffusion of PC at the cytoplasmic side of the PM from the basolateral to the apical domain or a transport of PC by PC-TP (see section 1.3.2). It would, however, also require an asymmetric phospholipid distribution in vesicles that are targeted to the canalicular membrane. PC synthesis takes place at the cytosolic leaflet of the ER [103] and SM is synthesised at the lumenal leaflet of the Golgi apparatus [104, 105, 106]. Contrary to SM, GlcCer is synthesised at the cytosolic leaflet of the Golgi [107, 105]. GlcCer is rapidly flipped across the Golgi membranes [64] which is necessary for further glycosylation at the lumenal side of the Golgi [108, 109]. Transport vesicles could contain sphingolipids at the lumenal leaflet whereas PC would be located at the cytoplasmic side [21, 110]. A fast flip-flop for PC in the ER has been demonstrated [111, 112, 113] making it unlikely that PC is restricted to the cytoplasmic leaflet of transport vesicles. However, if SM is restricted to the exoplasmic leaflet as flippase activity for SM in the Golgi is low [64], PC has to be located mainly at the cytoplasmic leaflet for sterical reasons. Indeed, a preferential localisation of SM and glycosphingolipids like GlcCer to the lumenal leaflet was demonstrated in TGN derived vesicles [114].

1.4.3 Supramolecular Organisation of Lipids in the BC

The mechanism of solubilisation of PL from the canalicular membrane by bile salts and the physico-chemical organisation of the lipids in the BC is still not completely elucidated. Two mechanisms have been proposed how PL are secreted into the bile: as vesicles or as micelles (see figure 1.3).

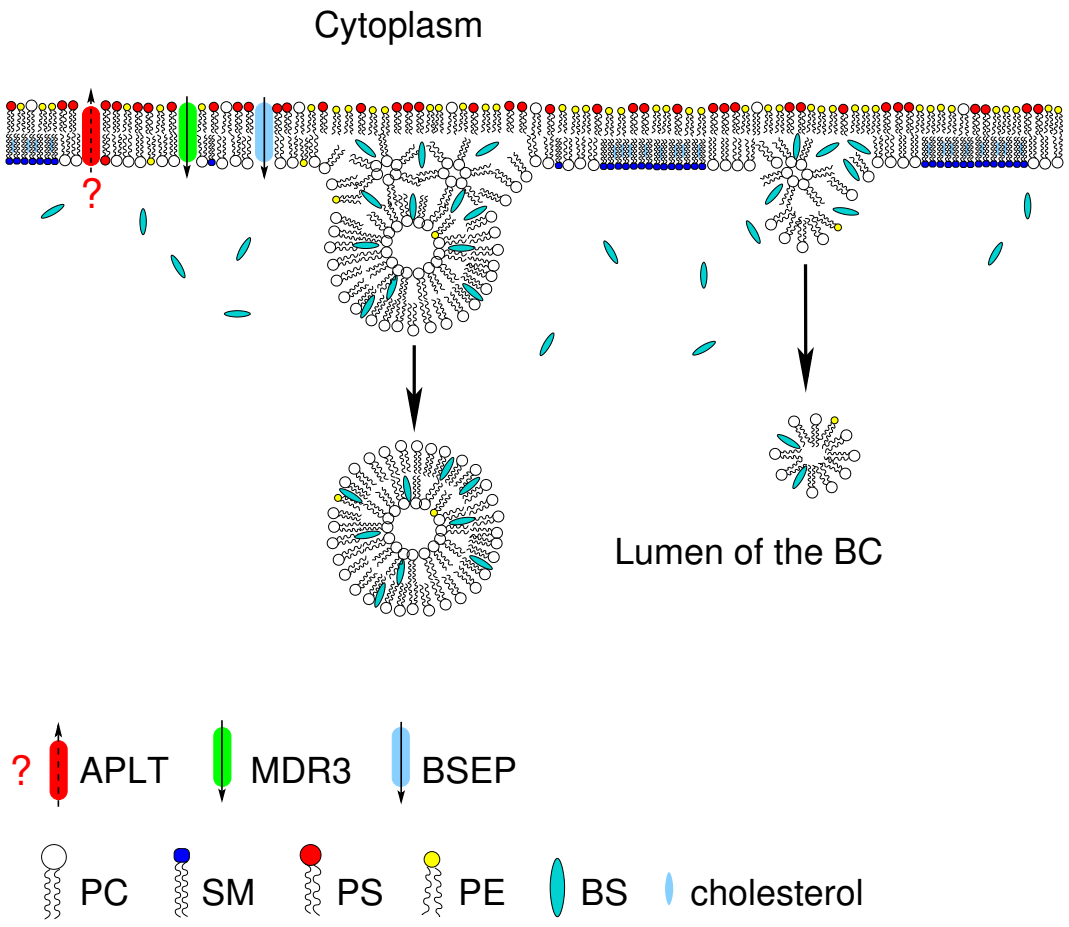

Figure 1.3: **Possible mechanisms of solubilisation of PL into the BC.** Bile salts induce the release of PL from the canalicular membrane either as vesicles (right) or micelles (left). Both way might also coexist in biliary PL secretion. Model adapted from [115] and [21].

First investigations on the secretion mechanism of PL suggested a micellar solubilisation, later experiments, however, preferred a vesiculation process

[116, 117, 118]. The high bile salt concentration in the BC was thought to mediate a rapid transformation of a part of those primary vesicles into micelles [116]. However, their is still some evidence for a micellation, especially in the process of cholesterol solubilisation [102]. It is also likely that both processes coexist during bile formation [119]. Micellation might take place besides vesiculation even if the vesicular solubilisation of lipids into the bile is the main path [120]. The mechanism of biliary PL secretion might further depend on the bile salt species in the lumen of the BC [85]. The general lipid composition of the bile and especially the composition of different bile salts and their hydrophobicity varies strongly between the different mammalian species (see table 1.1). Thus the physico-chemical processes underlying bile secretion could well be heterogeneous in different species.

Cholesterol is very poorly soluble by bile salts, addition of PL strongly increases its solubility. This fact might be responsible for the coupling of cholesterol to PL secretion (see section 1.3.3). If the secretion of PC is disturbed (as in the case of PFIC I), cholesterol is secreted to a very low extent, which most likely represents the amount of cholesterol that leads to saturation of the bile salts. Application of more hydrophilic bile salts enables a higher amount of cholesterol solubilisation [102].

One assumption about cholesterol solubilisation is that the main part of cholesterol that is exposed by ABCG5/ABCG8 in the CM is solubilised by mixed bile salt/phospholipid micelles. If the bile salt concentration in the BC is low, a solubilisation of cholesterol by mixed vesicles is supposed. [102].

The physico-chemical composition of bile is crucial for its functionality. The formation of gallstones from cholesterol crystals is dependent on the ratio of vesicles to micelles in bile as well as on the hydrophobicity of bile salts [121, 85]. The elucidation of the exact mechanism of biliary lipid secretion will be the basis for the treatment of hepato-biliary diseases.

1.5 Methods for Investigation of Lipid Enrichment and Organisation in Bile

The uptake of lipids at the sinusoidal membrane domain, their transport to the apical domain and the secretion of lipids into the bile fluid have been a subject of investigation for many years. Several methods have been used to investigate the enrichment of specific substances in the bile fluid, however they all have their specific advantages and disadvantages [88]. Only the combination of results and conclusions from different experimental designs might reveal the mechanism that leads to the specificity of bile composition.

One method involves radiolabelled precursors of biliary lipids that are fed to animals or applied to isolated perfused liver. The origin and metabolism of biliary lipids can be quantified. This allows mathematical analysis of vectorial solute movement, metabolic pathways and enterohepatic circulation. However, the data provide no insight into the mechanisms on a cellular level as measurement are possible only several orders of magnitude away from the scale of intracellular operations. Furthermore they can only provide informations on the "average" hepatocyte and do not take into account the differences arising from the situation of the hepatocyte within the liver lobule [88].

Another method is the isolation and analysis of subcellular fractions which also allows to trace radiolabelled substances. Organelle subfractions can then be analysed regarding lipid transport capacities, proteins involved in transport processes and lipid content. The latter gives indications about the origin of biliary lipids. However, the reliability of measurements on isolated organelles may be questionable as the *in vitro* environmental conditions might lack important factors that are present *in vivo*, such as membrane potential and cytoplasmic factors [88].

Morphological studies using microscopic techniques are another category of methods that is applied to study biliary secretion. Electron microscopy

provides detailed information on the structure and organisation of organelles. However, as cells have to be fixed, dynamic processes cannot be investigated. Fluorescence microscopy allows to monitor intracellular trafficking of fluorescence labelled substances. It is, however, often challenged that the fluorescence group might influence the behaviour of the investigated substance. Microscopic studies also require isolated cells and are characterised by the unability to study cellular functions *in situ* [88].

Isolated hepatocytes or hepatocytic cell lines are often used as model systems. The polarity of primary hepatocytes, however, is lost in cell culture making them improper objects for investigations on biliary lipid secretion. Alternatively, hepatocyte couplets can be isolated by incomplete separation of cells. These couplets reestablish their polarity when treated in a special way [122]. However, the life time of hepatocyte couplets in cell culture is limited.

Continuous cell lines avoid the disadvantage of a limited life time. However, as they are derived from carcinoma cells, they often have lost most of their cell type specific functions. Only a few cell lines are able to form polarised cells and mimic biliary secretion. One of them is the human hepatoma cell line HepG2 which was used for this study and which shall be introduced in more detail in the following part.

1.5.1 HepG2 Cells

HepG2 cells have been isolated from a liver tumour biopsy and were described as well differentiated epithelial carcinoma [123].

HepG2 cells are able to grow polarised and form a canalicular vacuole between two adjacent cells [124]. This vacuole resembles the BC of the liver in many ways [125, 126]. Synthesis and secretion of bile salts takes place in HepG2 cells and is similar to that of human hepatocytes [127, 128]. For this reason, HepG2 cells have been used for a variety of studies concerning biliary secretion.

1.5.2 Lipid Analogues

Phospholipid Analogues

To monitor lipid trafficking in cells and across membranes, lipids have to carry reporter groups that emit a detectable signal. For this study fluorescent lipid analogues were used. The most widely used fluorescence reporter group for lipids is the green fluorescent NBD that can be attached to phospholipids at a fatty acid chain or at the head group. Many studies use lipid analogues were the reporter group is attached to a short fatty acid chain in *sn2*-position making these phospholipids less hydrophobic. This enables easy incorporation in and extraction from membranes which is essential to introduce lipid analogues into living cells. Extraction of lipid analogues from the membrane allows to monitor the transbilayer distribution of the latter. Such short chain NBD labelled phospholipids were also applied to this study. A red fluorescent PC analogue carrying the BODIPY fluorophore at a short fatty acid chain was further used for colocalisation experiments. In addition, head-group labelled PE analogues carrying a fluorescein or rhodamine group were used. The chemical structure of some of the PL analogues used in this study is shown in figure 1.4.

The use of fluorescent lipid analogues is sometimes questioned regarding their ability to represent the behaviour of endogenous PL. Indeed, a so called "back looping" of the fatty acid chain that carries the fluorescent reporter group to the membrane surface has been described [129]. However, previous studies have shown that fluorescent lipid analogues are faithful reporters of the behaviour of endogenous lipids, as experiments with radioactive and spin labelled analogues gave similar results as those with fluorescent analogues in the erythrocyte membrane [54, 130, 51]. Moreover the use and comparison of lipid analogues carrying different fluorophores can rule out the influence that might derive from a fluorescent reporter group.

Another argument against the use of fluorescent PL analogues is their rapid

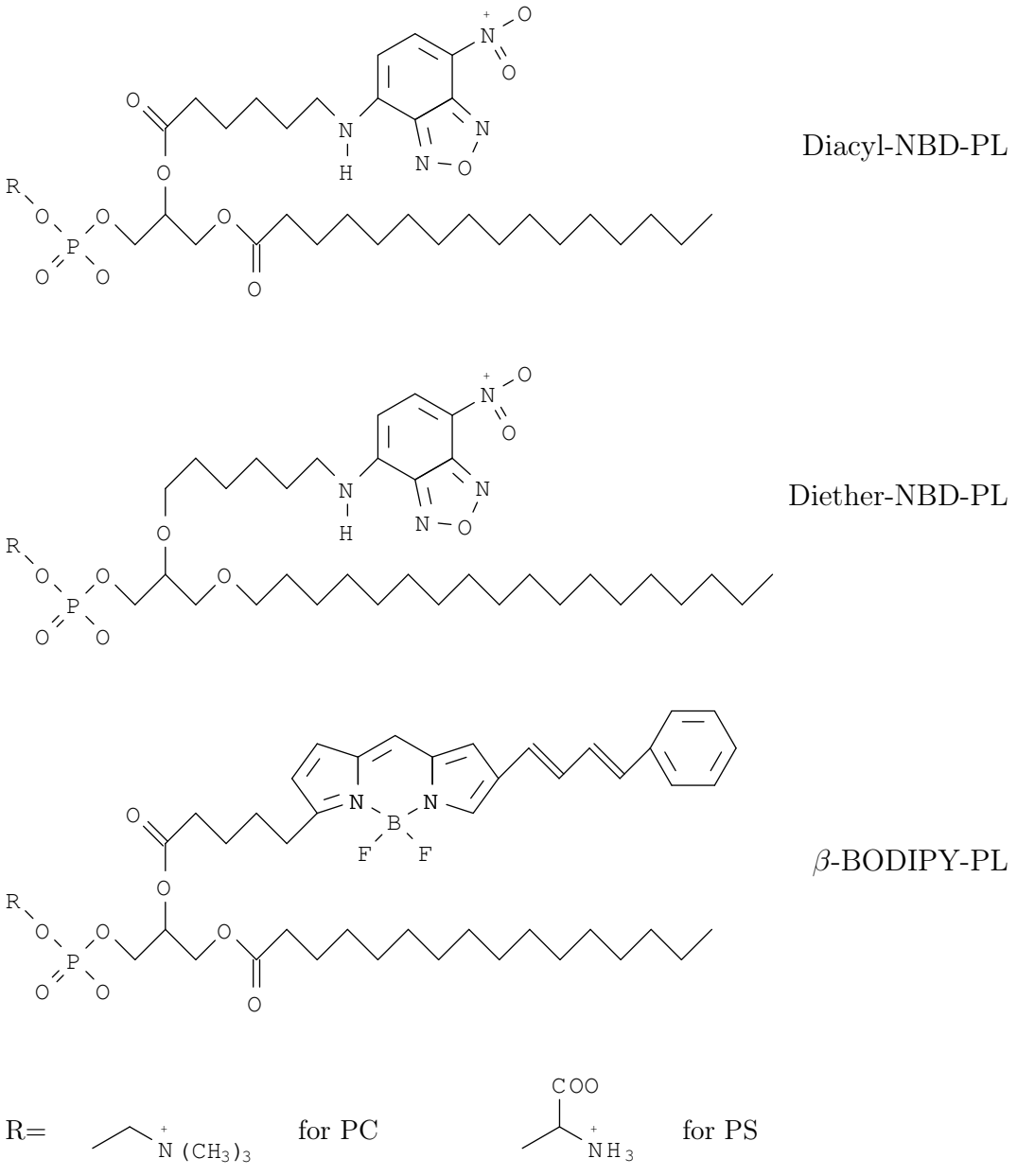

Figure 1.4: **Chemical structure of fluorescent PL analogues.** Some acyl chain labelled PL analogues which carry their fluorophore at a short fatty acid chain are shown. Both the diacyl and the diether green fluorescent NBD analogues were applied to this study. In addition a diacyl PC analogue labelled with the red fluorescent moiety BODIPY was used.

degradation by cellular phospholipases. This disadvantage can be overcome by the use of diether PL analogues which are not recognised by phospholipases [131]. Diether-NBD analogues of PC and PS have been used (see figure 1.4) in addition to diacyl analogues. The intracellular trafficking of diether analogues might be different from that of diacyl analogues in some cases due to the substitution of the ester bonds by ether bonds. Trafficking of diether NBD-PC and diacyl BODIPY-PC was compared by colocalisation experiments. The different affinities of analogues to APLT have furthermore been utilised. While the PC head group is not recognised by APLT the affinity of the transporter for aminophospholipid analogues is determined by the glycerol backbone as well as a modification of the head group [50]. This leads to a reduced affinity of diether PS to APLT [131] which was employed to study the influence of APLT to biliary lipid specificity.

Fluorescent Bile Salts

Fluorescent bile salts carrying a NBD or a fluorescein reporter groups were recently synthesised [132] (see figure 1.5). They were utilised to verify the functional polarity of adherent HepG2 cells and the integrity of their BC. Furthermore the change of their fluorescence life times upon interaction with unlabelled bile salts was investigated.

1.5.3 Fluorescence Life Time Analysis

The experimentally measured fluorescence life time is defined as the inverse rate of depopulation of the first excited singlet state after optical excitation from the ground state. Different decay pathways, radiative and non-radiative ones, compete in this process, which depend on the microenvironment of the fluorophore [133]. This causes a strong dependency of the fluorescence life time of a given chromophore on its physico-chemical environment which can be

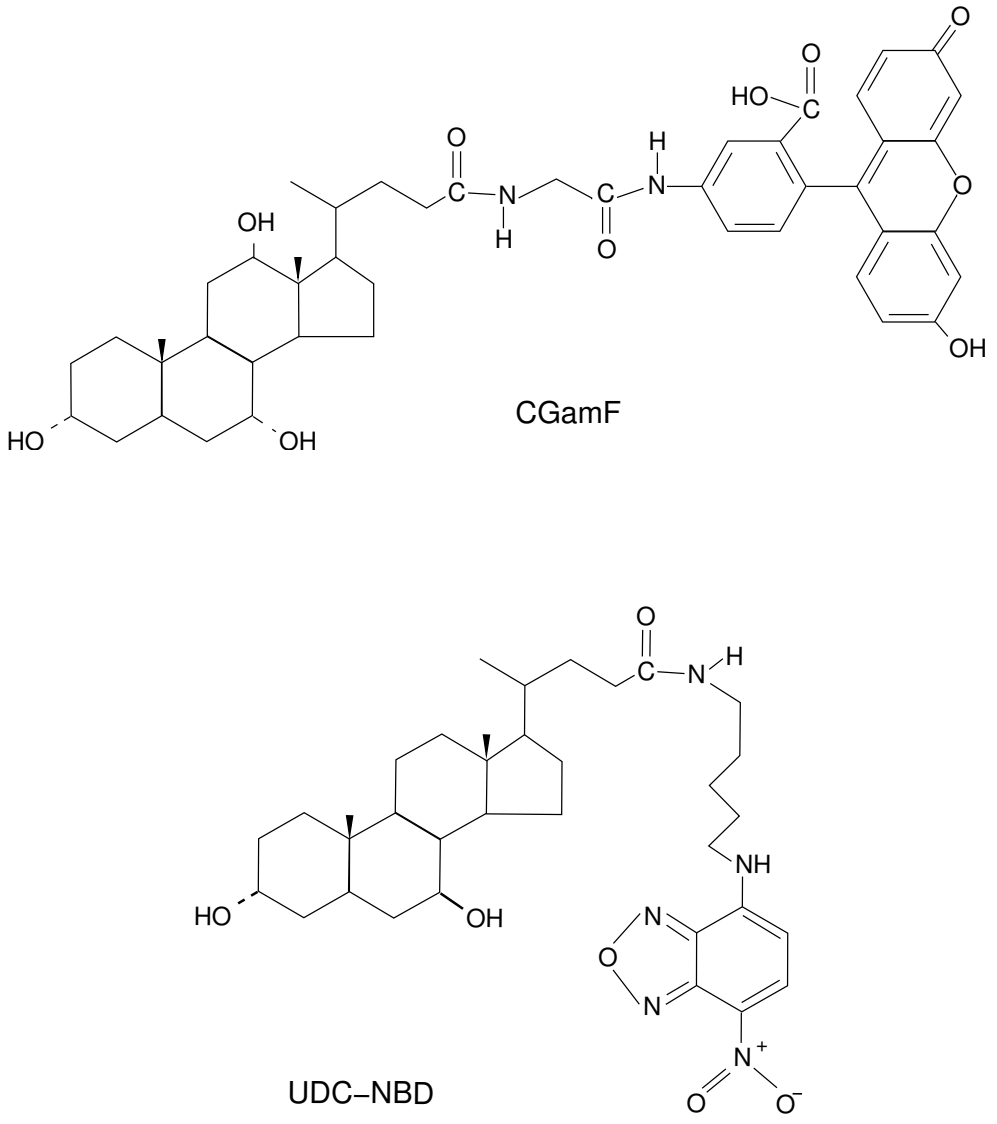

Figure 1.5: **Chemical structure of fluorescent bile salt analogues.** The structure of glycocholic acid labelled with fluorescein (CGamF) and ursodeoxycholic acid carrying the NBD reporter group (UDC-NBD) is shown. Chemical structure according to [132].

also utilised to investigate intra- and intercellular organisation of fluorescent molecules [134]. The application of fluorescence life time analysis is a very recent development to study biological questions. It is a promising technology to investigate supramolecular organisation in model systems as well as in living cells.

In this thesis fluorescence life time measurements were applied to fluorescent lipid analogues in different physico-chemical environments. The characterisation of the fluorescence properties of lipid analogues were performed in cuvette experiments using pulsed lasers as excitation source. The fluorescence life time can be determined by essentially two methods. Using pulse fluorometry the fluorescence life time is measured in the time domain, whereas applying phase and modulation fluorometry the decay time is recalculated from the frequency domain [133]. The latter is more useful to characterise longer (i. e. ten nanoseconds to microseconds) life times. Here, for characterising fluorescent lipid analogues time correlated single photon counting (TCSPC) was used.

The measurements shall be utilised to monitor the subcellular organisation of fluorescent lipid analogues on a microscopic level.

Further on, fluorescence resonance energy transfer (FRET) can be used to determine whether distinct substances (i. e. bile salts and PL) bearing appropriate fluorophores are in close neighbourhood (i. e. in the same micelle or vesicle). A typical FRET pair with a NBD-lipid as donor and a rhodamine labelled lipid as acceptor was characterised during this study.

2 Scope

The specificity of biliary lipid composition seems to play an important physiological role as changes in lipid constitution lead to severe hepatobiliary diseases as formation of gallstones and cholestasis. To identify mechanisms leading to the enrichment of specific lipids in bile, while others are shielded from biliary secretion, is a first step in developing suitable treatments or preventions for the outlined diseases. Understanding lipid specificity includes to elucidate the physico-chemical processes leading to bile formation, and the organisation of biliary lipids in the BC immediately after secretion.

Prevention of Aminophospholipid Secretion

Biliary PL composition is very different from that of cellular membranes. PS is not found and PE is only a minor constituent of the bile fluid making up about 4.5 % of biliary PL, whereas PC resembles about 95 % of the PL in bile. An APLT activity pumping PE and PS from the exoplasmic to the cytoplasmic leaflet is known from the PM of many mammalian cells. However, it has not yet been demonstrated whether APLT is also localised in the apical membrane of hepatocytes. Assuming an APLT activity in the CM, pumping PS and PE to the cytoplasmic leaflet, might prevent their solubilisation by canalicular bile salts. This would explain one component leading to biliary lipid specificity. The first part of this thesis shall demonstrate an APLT activity in the canalicular membrane of HepG2 cells and clarify if this APLT activity is sufficient to prevent biliary enrichment of aminoPL. For this reason several PL analogues which are known to differ in their affinity to APLT are applied. To probe whether these analogues are suitable for demonstration of an APLT activity, their transport rate is characterised at the basolateral membrane of HepG2 cells, in which an APLT activity has already been reported [63, 64].

To inhibit the activity of an APLT, the APLT inhibitor suramin is applied.

The APLT activity of the canalicular membrane has to be monitored indirectly by the accumulation of the different PL analogues in the BC. Absence of specific PL analogues from the lumen of the BC is related to a canalicular APLT activity.

Involvement of MDR proteins in biliary PL secretion

Mutations of the murine ABC transporter mdr2 (corresponding to human MDR3) have been shown to lead to a complete absence of PL from the bile [20]. Thus MDR3 is thought to be responsible for transporting PC to the exoplasmic leaflet of the apical membrane from where it is solubilised by canalicular bile salts. However, an ATP independent PC transport in the CM has been reported on isolated membranes [97, 99]. An ATP independent transbilayer movement of PC, however, has not yet been shown *in vivo*. Here it will be addressed whether MDR independent transport of lipids might contribute to biliary PL secretion. To investigate the influence of MDR proteins in biliary enrichment of PC and aminophospholipid analogues, different MDR inhibitors are applied.

Organisation of Lipids in Biliary Model Systems

The physico-chemical mechanisms that lead to biliary lipid secretion are still not understood. It is not yet clear if biliary lipids are secreted as vesicles or micelles. So far, the knowledge about physico-chemical organisation of early bile originates from the investigation of animal material. However, lipid composition of the widely used rodents is quite different from that of other mammals and humans especially regarding its hydrophobicity. It is therefore essential to develop a method allowing to determine the supramolecular organisation of early bile *in situ*.

To investigate the physico-chemical organisation of fluorescent lipid analogues, the analysis of the fluorescence life times of the latter is a powerful technique. The third part of this thesis was aimed at characterising the fluorescence decay of lipid analogues in possible physiological environments. This problem is addressed using different model systems as membranes or bile salt suspensions of different concentration in which fluorescent lipid analogues are incorporated. These investigations will provide the basis for a determination of lipid organisation in the BC *in vivo* in the near future.

Combining fluorescence life time measurements with FRET the neighbourhood and interaction of different lipid species can be determined. Therefore, it is a further aim of this thesis to characterise suitable FRET pairs in model experiments.

3 Materials and Methods

3.1 Materials

Fatty acid free bovine serum albumin (BSA), sodium dithionite, (±)-Verapamil hydrochloride (Verapamil), suramin, rhodamine 123 (Rho123), and the lipids (in highest purity) egg yolk phosphatidylcholine (EYPC), egg yolk sphingomyelin (EYSM), cholesterol, sodium taurocholate (TC), sodium glycocholate (GC), sodium taurolithocholate (TLC), sodium taurodeoxycholate (TDC), and sodium dehydrocholate (DHC) were obtained from Sigma (Deisenhofen, Germany). 1-Palmitoyl-2-oleoyl-sn-glycero-3-phosphocholine (POPC), 1-palmitoyl-2-[6-[(7-nitrobenz-2-oxa-1,3-diazol-4-yl)amino]caproyl]-sn-glycero-3-phosphocholine (diacyl NBD-PC), 1-palmitoyl-2-[6-[(7-nitrobenz-2-oxa-1,3-diazol-4-yl)amino]caproyl]-sn-glycero-3-phosphoserine (diacyl NBD-PS), (1-palmitoyl-2-[6-[(7-nitrobenz-2-oxa-1,3-diazol-4-yl)amino]caproyl]-sn-glycero-3-phosphoethanolamine (diacyl NBD-PE), 6-((N-(7-nitrobenz-2-oxa-1,3-diazol-4-yl)amino)hexanoyl)sphingosylphosphocholine (C_6-NBD-SM), 1,2-dioleoyl-sn-glycero-3-phosphoethanolamine-N-carboxyfluorescein (*N*-Fl-PE), and L-α-phosphoethanolamine-*N*–(lissamine rhodamine B sulfonyl (egg) (*N*-Rh-PE) were obtained from Avanti Polar Lipids (Birmingham, AL, USA). 2-(4,4-difluoro-5-(4-phenyl-1,3-butadienyl)-4-bora-3a,4a-diaza-s-indacene-3-pentanoyl)-1-hexadecanoyl-sn-glycero-3-phosphocholine (β-BODIPY-PC) was purchased from Molecular Probes (MoBiTec, Göttingen, Germany). Dulbecco's modified eagle medium (DMEM) and foetal bovine serum (FCS) were obtained from GIBCO BRL (Life Technologies, Paisley, Scotland). Collagen A, penicillin/streptomycin, HANKS' balanced salt solution (HBSS), Dulbecco's modified phosphate buffered saline (DPBS), and trypsin/EDTA solution (0.05 % (w/v) trypsin, 0.02 % (w/v) EDTA in PBS) were from Seromed

(Biochrom, Berlin, Germany). HBSS$^+$ refers to HBSS supplemented with 1.25 mM $CaCl_2 \cdot 2\ H_2O$ and 0.5 mM $MgCl_2 \cdot 2\ H_2O$. Diisopropylfluorophosphate (DFP) was obtained from Fluka (Feinchemikalien GmbH, Neu-Ulm, Germany). (3'-oxo-4-butenyl-4methyl-threonine1)-(Val^2)-cyclosporin (PSC 833) was from Novartis, Basel, Switzerland. Cholyl-glycyl-amido-fluorescein (CGamF) and ursodeoxycholyl-[N_ϵ-(7-nitro-2-1,3-benzooxadiazol-4-yl)amino]-lysine (UDC-NBD) were a generous gift from Alan F. Hofmann (MD) (University of California, San Diego, USA). 1-octadecanoxy-2-[6-[(7-nitrobenz-2-oxa-1,3--diazol-4-yl)amino]hexanoxy]-sn-glycero-3-phosphoserine (diether NBD-PS) and 1-octadecanoxy-2-[6-[(7-nitrobenz-2-oxa-1,3-diazol-4-yl)amino]hexanoxy]--sn-glycero-3-phosphocholine (diether NBD-PC), 1-O-βD-glucopyranosyl-6-((N-(7-nitrobenz-2-oxa-1,3-diazol-4-yl)amino)hexanoyl)sphingosine (C_6-NBD-GlcCer), 1-O-β-D-galactopyranosyl-6-((N-(7-nitrobenz-2-oxa-1,3-diazol-4-yl)-amino)hexanoyl)sphingosine (C_6-NBD-GalCer) were a gift from Philippe F. Devaux (Institut de Biologie Physico-Chimique, Paris, France).

3.2 Cell Culture

HepG2 cells were purchased from DSMZ, Braunschweig, Germany.

HepG2 cells were grown in DMEM containing 4.5 g/l glucose, supplemented with 10 % heat-inactivated FCS and penicillin/streptomycin. Cells were routinely passaged in 25 cm^2 plastic culture flasks coated with collagen A, medium was changed every 3–4 days.

For preparation of cell suspensions, cells were cultured in 175 cm^2 plastic culture flasks coated with collagen A, medium was changed at the day prior to experiment. Cell suspensions were prepared in that cell monolayers were rinsed two times with HBSS and harvested by incubation with trypsin/EDTA solution for 5 min at 37 °C. Subsequently, cells were resuspended in 50 ml culture medium. After keeping the suspension for 30 min on ice, the cells were washed

twice with PBS and resuspended in $DPBS^+$ (DPBS supplemented with 20 mM glucose, 1 mM sodium pyruvate and 10 mM HEPES to prevent ATP-depletion and pH-shift) for labelling.

3.3 Cell Labelling

3.3.1 Preparation of Aqueous Solutions of PL Analogues

PL marked with NBD, fluorescein, or rhodamine, were stored at -20 °C in chloroform or chloroform/methanol. Aliquots of these phospholipid analogues were transferred to a glass tube and dried under nitrogen. The analogues were then resuspended in ethanol (final ethanol concentration below 1 % v/v) and vortexed with $HBSS^+$ (for labelling adherent cells) or $DPBS^+$ (for labelling suspended cells).

Due to its higher hydrophobicity compared to NBD labelled analogues, β-BODIPY-PC was bound to fatty acid depleted BSA before labelling the cells [135]. Briefly, 75 nmole of the lipid analogue in methanol:chloroform (1:1) were evaporated under nitrogen and redissolved in 400 µl ethanol. This ethanolic solution was then carefully injected into 1 ml of PBS containing 75 nmole of fatty acid depleted BSA while vortexing the BSA-solution. To remove the ethanol, the mixture was dialysed against several changes of PBS for 16 h. Subsequently, the dialysate was centrifuged at 100,000×g for 20 min twice. The supernatant, containing the BSA bound analogue, was stored under argon at 4 °C.

3.3.2 Labelling of Adherent Cells

Before labelling, polarised cells on cover glasses were washed two times with $HBSS^+$. Labelling with the short chain diacyl and diether PL analogues of PC and PS, and the sphingolipids C_6-NBD-SM, C_6-NBD-GlcCer, and C_6-NBD-

GalCer was performed for 20 min on ice (final label concentration 4 µM in $HBSS^+$), subsequently cells were washed with $HBSS^+$ and incubated for 30 min at various temperatures (2 °C, 14 °C, and 37 °C) [94]. Taking into account the less efficient incorporation of the diacyl NBD-PE compared to PS and PC [136] labelling with this analogue was performed by incubating the cells for 30 min with the analogue at 37 °C followed by washing with $HBSS^+$ and further incubation for 30 min at 37 °C. This protocol was also applied to the head-group-labelled phospholipid analogues *N*-Fl-PE and *N*-Rh-PE. In some cases cells were further incubated with 5 % (w/v) BSA in $HBSS^+$ twice, to remove fluorescent lipids from the exoplasmic leaflet of the basolateral membrane.

The fluorescent bile salts CGamF and UDC-NBD were diluted in $HBSS^+$ from an ethanolic stock solution to a final concentration of 10 µM (final ethanol concentration about 0.1 %) and cells were labelled with this solution at 37 °C for 15 min. Subsequently cells were washed with $HBSS^+$.

3.3.3 Double-Labelling of Adherent Cells

To study the intracellular transport and canalicular enrichment of the diether analogues of PS and PC, and of diacyl PS in comparison to diacyl PC, colocalisation experiments were performed. HepG2 cells were double labelled with the red fluorescent diacyl *β*-BODIPY-PC and one of the green fluorescent lipids diether NBD-PC, diether NBD-PS, or diacyl-NBD-PS.

For double-labelling, polarised cells on cover glasses were incubated with 4 µM of a NBD labelled lipid analogue for 20 min on ice. After removing this green fluorescent analogue, the cells were labelled with 10 µM *β*-BODIPY-PC bound to BSA for 10 min at 37 °C, washed and further incubated for 30 min at 37 °C.

3.3.4 Labelling of Suspended Cells

For measurements in suspensions, cells ($4 \cdot 10^7$ cells) were incubated with 600 µl DPBS$^+$ containing the respective lipid analogue. Labelling was performed for 5 min with 12 nmole of diacyl analogues or 15 min with 24 nmole of diether analogues on ice to achieve comparable extent of labelling. To prevent hydrolysis of the diacyl lipid analogues 5 mM DFP was added to the respective samples in parallel and was present in all following steps. Subsequently, cells were washed with DPBS.

3.4 Inhibition of MDR

To inhibit the canalicular MDR transporters the non-specific MDR inhibitor Verapamil [137, 138, 139, 140, 141, 142] and the cyclosporin analogue PSC 833 which is specific for MDR1 Pgp [143, 140, 144, 145] were used. After washing, cells were preincubated with 20 µM Verapamil or 10 µM PSC 833 in HBSS$^+$ for 15 min at 37 °C followed by labelling as described in section 3.3 in the presence of the inhibitor.

As a control for the inhibition of MDR by the inhibitors the green fluorescent MDR1 Pgp substrate Rho123 was used [146, 147, 145]. Cells were labelled with 3 µM of this fluorophore in HBSS$^+$ for 30 min at 37 °C. MDR inhibited cells were preincubated with 20 µM Verapamil or 10 µM PSC 833 and the respective inhibitor was present during labelling with Rho123.

3.5 Inhibition of APLT by Suramin

A competitive inhibition of APLT by suramin was described by Devaux and coworkers [67]. Cells were incubated with 200 µM suramin in the respective incubation buffer for 30 min at 37 °C prior to labelling. The inhibitor was present during all following steps. For adherent cells, in some cases, cells were

labelled and incubated for 30 min at 37 °C to allow internalisation of analogues, and subsequently incubated with suramin for 30 min at 37 °C.

3.6 Measurements of Analogue Internalisation in Cell Suspensions

Labelled cells were incubated at 37 °C, 22 °C, or 14 °C. After various times, aliquots were transferred into a fluorescence cuvette containing 2.4 ml ice-cold DPBS$^+$. Fluorescence was monitored at 540 nm (λ_{ex}=470 nm) (Aminco Bowman Series 2 Spectrofluorometer, Polytec, Waldbronn, Germany) at 4 °C while continuously stirring the suspension. Dithionite was added from a freshly prepared 1.5 M stock solution in 100 mM Tris (pH 9.5) to give a final concentration of 50 mM as described earlier [148, 62]. Dithionite quenches the fluorescence by chemical reaction with the NBD group. Since dithionite permeates very slowly across membranes at low temperature [62], only the fluorescence of analogues on the exoplasmic leaflet is quenched. After the fluorescence intensity was reduced by dithionite to a plateau value, Triton X 100 was added to a final concentration of 2 % (w/v) making the NBD-PL on the cytoplasmic side accessible to dithionite. The amount of PL on the cytoplasmic side (PL_i) was determined according to:

$$PL_i = \frac{F_p - F_b}{F_i - F_b}$$

with F_p being the fluorescence of the plateau after dithionite reduction, F_b the background fluorescence after addition of Triton X 100, and F_i the initial fluorescence intensity before addition of dithionite.

3.7 Fluorescence Microscopy

Labelled cells grown on cover glasses were analysed with an inverted Axiovert 100 standard epifluorescence microscope (Carl Zeiss, Inc. Oberkochen, Germany) equipped with a PlanApo 100×/1.3 numerical aperture objective, a standard fluorescein filter set (BP 450 to 490 nm excitation filter, FT 510 nm dichroic mirror, and LP 520 nm emission filter), and a standard rhodamine filter set (BP 546/12 nm excitation filter, FT 580 nm dichroic mirror, and LP 590 nm emission filter) (Carl Zeiss, Oberkochen, Germany) as described previously [94]. Canalicular vacuoles (BC) were identified by phase contrast microscopy. The percentage of BC containing the fluorescent lipid analogue was quantified by counting labelled and non-labelled BC. BC having a fluorescence intensity in the BC as low as cellular autofluorescence levels were defined as non-labelled BC.

Localisation of the NBD-labelled lipid analogues in the BC was confirmed by addition of dithionite which can diffuse into the BC and react with NBD-labelled analogues in the lumen and at the lumenal membrane leaflet of the BC [149]. Remaining fluorescence of the canalicular membrane originates from PL analogues located at the cytoplasmic side of this membrane. Cells were covered with $HBSS^+$ supplemented with 20 mM HEPES (pH 7.4) to prevent any pH shift and were incubated with 30 mM sodium dithionite (added from a fresh 1 M stock solution in 100 mM Tris, pH 9.5) for 10 min on ice [94].

Photographs were taken using Kodak Ektachrome Panther P1600 films, which were push-processed to 3200 ASA and scanned using a CanoScan 2700F scanner (Canon, Tokyo, Japan) or by a cooled CCD camera (Coolsnap fx, Visitron Systems, Puchheim, Germany) using Metamorph software (Universal Imaging, Downingtown, USA).

3.7.1 Confocal Laser Scanning Microscopy

For confocal laser scanning microscopy (CLSM) of cells labelled with diacyl NBD-PS and treated with suramin a Leica Confocal laser scanning microscope (Leica Lasertechnik GmbH, Wetzlar, Germany) equipped with NPL Fluotar 40×/1.3 oil and PL Fluotar 100×/1.32 oil objectives (Leitz, Wetzlar, Germany) and an argon/krypton-ion laser emitting at 488 nm was used.

3.8 Metabolism of Diacyl NBD-Analogues

To measure hydrolysis of cell associated lipid analogues, cells in suspensions or in monolayers were labelled as described above. Subsequent to labelling, cell suspensions were incubated for 60 min, monolayers for 30 min at 37 °C (see section 3.3). For lipid extraction, monolayers were scraped from the dish and resuspended in 1 ml $HBSS^+$.

Lipids were extracted from the aqueous solution as described previously [150]. Briefly, 3.2 ml methanol:chloroform (2.2:1) were added to 1 ml of cells and incubated for 30 min at room temperature. After phase separation by adding 1 ml chloroform and 1 ml 40 mM acetic acid, lipids in the chloroform phase were collected. The aqueous phase was washed with 1 ml chloroform, and the two combined chloroform phases were dried under a nitrogen stream. The lipids were resuspended in a small volume of chloroform:methanol (1:1) and applied to a TLChr plate. Plates were developed in two dimensions using chloroform:methanol:ammonia (13:5:1) as basic solvent and acetone : chloroform : methanol : glacial acetic acid : water (8:6:2:2:1) as acidic solvents. Spots on the dried TLChr plates were analysed using a Fluorescence Image Analyser FLA-3000 (Raytest Isotopenmessgeräte GmbH, Germany) and AIDA image analysis software.

3.9 Vesicle Preparation

Aliquots of EYPC, POPC, or EYSM and cholesterol, stored at -20 °C in chloroform were transferred to a glass tube and dried under nitrogen. The lipids were resuspended in a small volume of ethanol (final ethanol concentration below 1 % (v/v)) and $HBSS^+$ was added to give a final lipid concentration of 1 mM. Small unilamellar vesicles (SUVs) were prepared by sonification of the solution 20 min on ice (Branson Sonifier 250, Schwäbisch Gmünd, Germany, intensity 2, cycle 80 %). To prepare large unilamellar vesicles (LUVs) five freeze-thaw cycles were performed followed by extrusion of the lipid solution 10× at 40 °C through two 0.1 µm polycarbonate filters (extruder from Lipex Biomembranes Inc., Vancouver, Canada, filters from Costar, Nucleopore GmbH, Tübingen, Germany). For symmetrical labelling of the two leaflets the PL analogues were added to the solution of endogenous lipid before evaporation. Fluorescent bile salts were introduced symmetrically into the LUVs by adding the respective amount of analogues in ethanol to the dried lipids on the glass surface (final ethanol concentration below 1 % (v/v)). The molar concentration of the fluorescent lipids was 1 mol% of the endogenous lipids. In the case of FRET experiments the acceptor phospholipid *N*-Rh-PE was incorporated to a molar concentration of 3 mol% of the endogenous lipids.

3.10 Measurement of Fluorescence Life Times

3.10.1 Investigated Systems

The influence of the chemical environment on the fluorescence life time of PL analogues (as diacyl C_6-NBD-PC) and of bile salt analogues (UDC-NBD and CGamF) was studied. These were either dispersed in $HBSS^+$ or incorporated into liposomes composed of EYPC, POPC, or a mixture of EYSM and cholesterol.

The influence of different bile salts on these model systems was analysed by adding the bile salts TC, TDC, GC, TLC, or DC from a 200 mM stock solution in $HBSS^+$ to the above described model solutions (analogues in vesicles or aqueous suspension). The final bile salt concentration was varied between 1 mM and 30 mM.

3.10.2 Instrumental Setup

Fluorescence life time was measured using a time correlated single photon counting (TCSPC) setup [133] as outlined in figure 3.1. Briefly, the time between excitation and emission of the first fluorescence photon was measured for a huge number of single molecules. The decay of fluorescence is represented by a histogram of these measured times.

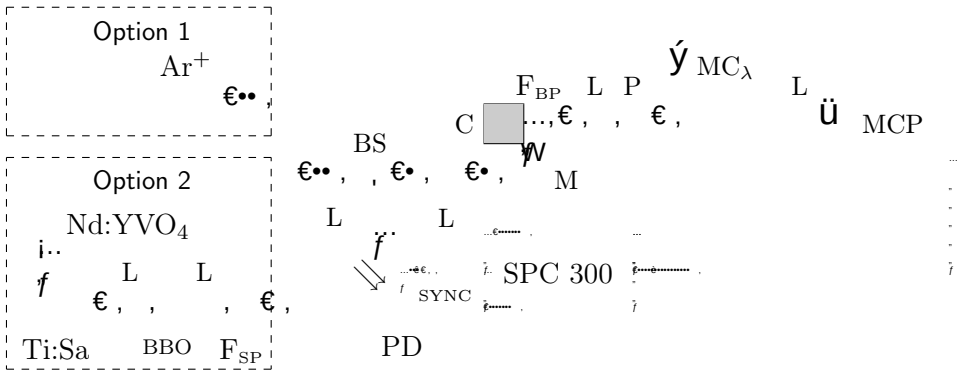

Figure 3.1: **Experimental setup of TCSPC.** The two possible excitation sources are shown in dashed boxes. L - lens, F_{SP} - shortpass filter, F_{BP} - bandpass filter, P - polariser, C - cuvette, M - mirror, BS - beam sampler, MC_λ - monochromator, MCP - micro channel plate, PD - photo diode. See text for further explanation.

Two different pulsed lasers were used to excite the samples. In one case (option 1), excitation was achieved by an actively acousto optic mode locked Ar^+-ion laser (Innova 305, COHERENT, Santa Clara, USA; APE µ 60, APE Berlin). The latter had a repetition rate of 125 MHz and a pulse width of about 150 ps, resulting in a full width of half maximum (FWHM) of the instrument

response function (IRF) of 150 ps. The laser line emitting at a wavelength of 476 nm was used.

In the second case (option 2), samples were excited by a solid state titan sapphire laser (Ti:Sa) (MIRA 900D, COHERENT, Santa Clara, USA) coupled to a home build second harmonics generation setup (SHG) using a β-barium-borate-crystal (BBO). The repetition rate of the Ti:Sa-laser was 76 MHz and pulses had a pulse width of about 100 fs, resulting in a FWHM of the IRF of about 90 ps.

During the course of this study this laser was improved by the installation of a new mirror set (XWAVE mirror set, COHERENT, Santa Clara, USA). Using the XWAVE mirror set the highest achievable wavelength was extended from 440 nm to 465 nm. As the excitation maximum of the NBD fluorophore is at about 470 nm the wavelength of 465 nm was used when available. Former measurements using an excitation at 440 nm were possible due to the broad excitation peak of NBD. Results obtained with different excitation sources were comparable as the fluorescence life time is independent of the excitation wavelength [151].

To generate the synchronisation signal a small amount of excitation light was split off (BS in figure 3.1) and focussed onto a fast photo diode determining the exact time of excitation. The intensity was adjusted by a variable grey filter to ensure excitation of only a single molecule. Attenuation was chosen in that only one percent of the laser shots resulted in excitation of a fluorophore. The resulting beam was focussed by a lens with long focal length (50 cm) into the sample. Fluorescence of the sample was detected perpendicular to excitation. A bandpass filter (F_{BP}) was used to block Rayleigh scattered excitation light. Polarisation filtering (magic angle [152]) is necessary to avoid unwanted detection of rotational polarisation effects. Due to Raman scattering of water the use of a monochromator is crucial to detect fluorescence only. Fluorescence photons were detected by a thermo electric cooled micro channel plate

(MCP) (R3809U-01, Hamamatsu Photonics Deutschland GmbH, Herrsching, Germany). Amplified MCP signals (HFAC-26dB, Becker & Hickl, Berlin, Germany) and synchronisation signals were processed by a personal computer card (SPC300, Becker & Hickl, Berlin, Germany). All measurements were performed at 22 °C. The resulting data were analysed using a home made program. Model functions were first to third order exponentials folded by the instrument response function (IRF), considering the periodicity of the IRF and a possible time shift between IRF and decay data. The Downhill Simplex Algorithm [153] was used to vary the parameters of the model functions to fit the data.

3.10.3 Determination of FRET

FRET between lipid analogues carrying the NBD group (donor) and the rhodamine group (acceptor) was investigated by the decrease of the fluorescence life time of the donor. Both lipid analogues were incorporated into LUVs or SUVs to ensure that the fluorophores were in an appropriate short distance to each other. Diacyl C_6-NBD-PC or UDC-NBD were used as donors and added in a concentration of 1 mol% of the endogenous vesicle lipids, the acceptor lipid *N*-Rh-PE was incorporated to 3 mol% of the endogenous lipids.

FRET was determined by measuring the fluorescence life time of the donor in the presence and absence of the acceptor using the instrumental setup described above.

4 Results

4.1 Enrichment of Fluorescent Bile Salts in the BC of Polarised HepG2 Cells

To verify that HepG2 cells were functionally polarised, the transport of fluorescent bile salts to the BC was investigated. Although these cells do not express all bile salt transport proteins identified in the basolateral membrane of hepatocytes [154], labelling with the two different bile salt analogues CGamF (figure 4.1 A, B) and UDC-NBD (figure 4.1 C, D) resulted in bright fluorescence of the BC. The number of BC which became enriched in the fluorescent bile salts was about 80 % for both analogues (figure 4.2).

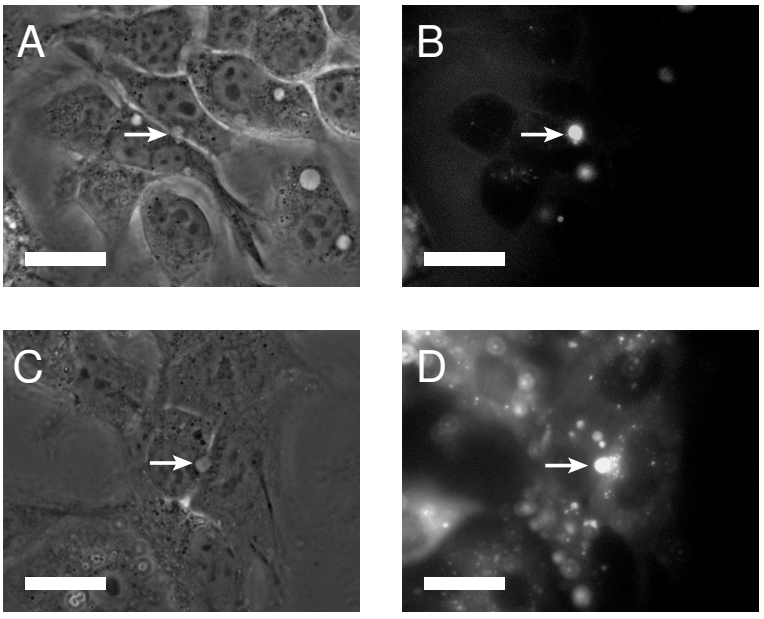

Figure 4.1: **Enrichment of fluorescent bile salt analogues in the BC of polarised HepG2 cells.** HepG2 cells were labelled with 10 µM CGamF (B; A: phase contrast to B) or 10 µM UDC-NBD (D; C: phase contrast to D) for 15 min at 37 °C. Arrows point to labelled BC. Bar, 20 µm.

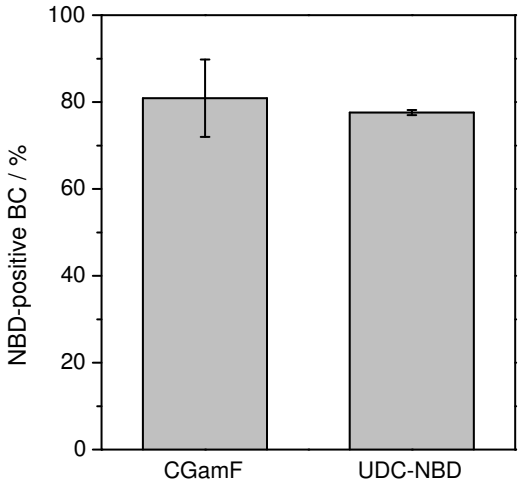

Figure 4.2: **Percentage of BC labelled with the fluorescent bile salts CGamF and UDC-NBD.** HepG2 cells were labelled with 10 µM of the fluorescent bile salt analogues for 15 min at 37 °C and the amount of fluorescent BC was determined. Data represent mean±SEM (n≥3).

4.2 Identification of an APLT Activity in the CM

To identify and characterise an APLT activity in the CM, diacyl and diether analogues of PS and PC and a diacyl analogue of PE each bearing the fluorescent NBD moiety at the short *sn2*-fatty acid chain (C_6) were used. Furthermore, two head group labelled diacyl PE analogues carrying a fluorescein or a rhodamine group were investigated. These analogues differ in their affinity to and transport by APLT which is primarily determined by the head group as well as the glycerol backbone of PL [50]. As shown for various mammalian cells, PC analogues are not transported by APLT [131, 136, 62, 155]. In contrast to PC, diacyl NBD-PS and, although to a lesser extent (see section 1.2.2) diacyl NBD-PE are substrates of APLT. However, the transport of a diether analogue of PS by APLT is very slow in comparison to diacyl NBD-PS [131].

First, the transbilayer redistribution of these analogues across the PM of suspended HepG2 cells was characterised to verify that the respective ana-

logues behave in a similar manner to that found for other mammalian cells (see section 1.5.2). Subsequently, the enrichment of aminophospholipid analogues in the BC of polarised HepG2 cells in monolayer cultures was studied.

4.2.1 Internalisation of Diacyl and Diether NBD Lipid Analogues in Suspended HepG2 Cells

Using the dithionite assay, the amount of NBD labelled lipid analogues redistributed to the cytoplasmic side of labelled HepG2 cells, being non-accessible to dithionite, was determined at 4 °C after various periods of incubation at 37 °C, 22 °C and 14 °C. In figure 4.3 a typical kinetics of the fluorescence decrease upon addition of dithionite is shown. An initial rapid decline of fluorescence intensity was observed corresponding to reduction of the analogues on the exoplasmic leaflet. Subsequently, only a very slow fluorescence decrease was observed which, very likely, is due to slow permeation of dithionite and reduction of analogues on the cytoplasmic side. To estimate the extent of reduction of analogues on the cytoplasmic side, the slow fluorescence decrease was measured over a period of 6 min and the last 100 s before addition of Triton X 100 were fitted to a linear function (see figure 4.3). The slope of the line was found to be $-7 \cdot 10^{-3}$ %/s, indicating that during kinetic measurements (which regularly took about 300 s) the reduction of intracellular localised analogues did not exceed 2 %. Thus the influence of the permeation of dithionite across the PM of HepG2 cells at 4 °C is negligible.

In figure 4.4 the kinetics of internalisation of NBD-lipid analogues in suspended HepG2 cells is shown. To differentiate between uptake by endocytic activity and by transbilayer movement from the exo- to the cytoplasmic leaflet, internalisation was measured not only at 37 °C (figure 4.4 A, B), but also at the lower temperatures 22 °C (figure 4.4 C, D), and 14 °C (figure 4.4 E, F). Endocytosis is strongly reduced at the latter temperature [156, 157]. During the

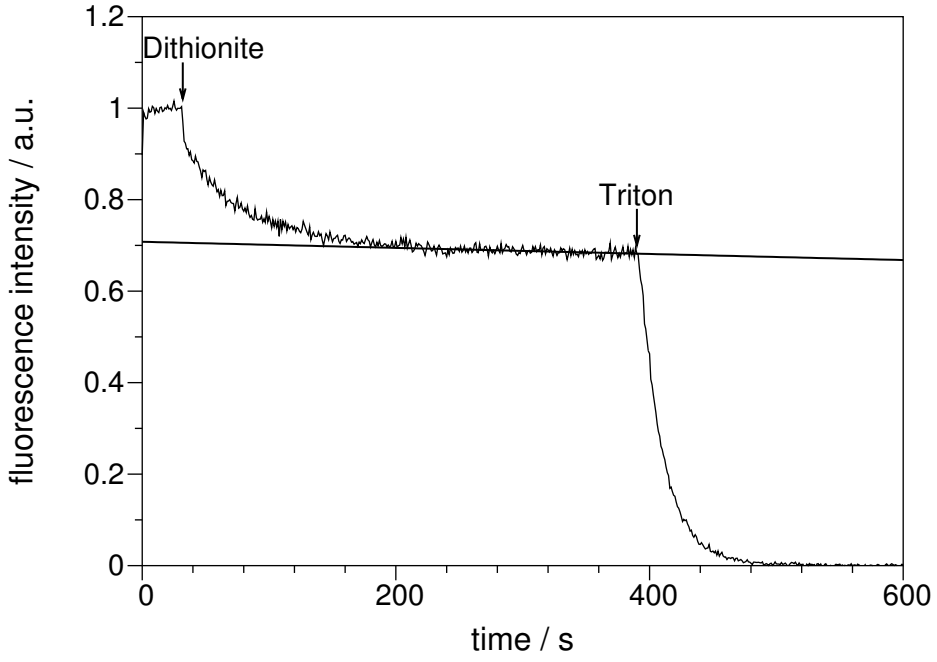

Figure 4.3: **Measurement of inward redistributed analogues by dithionite reduction of NBD at 4 °C** Cells in suspension were labelled with diacyl NBD-PS and incubated at 37 °C for 20 min. Subsequently, an aliquot of the suspension was taken and incubated at 4 °C. Fluorescence intensity was monitored and after 30 s dithionite was added. Remaining fluorescence from intracellular located analogues was reduced by adding Triton X-100 and thus solubilising the cells, after 6 min of measurement. Fitting the decrease of NBD-fluorescence intensity of the last 100 sec before addition of Triton to a linear function (solid line) reveals a slope of $-7{\cdot}10^{-3}$%/s (for details see text).

labelling procedure a low amount of NBD-analogues was lost from the exoplasmic leaflet indicated by the offset at t= 0 of the respective plots.

At 37 °C the internalisation of diacyl NBD-PS was rapid, about 75 % of the analogue was internalised with a half-time of about 5 min (figure 4.4 A). Also, a rather rapid uptake of the analogue with respect to the other analogues was observed, even at the lower temperatures (figure 4.4 C, E).

Although the internalisation of diacyl NBD-PE was slower in comparison to diacyl NBD-PS, it was still faster with respect to the PC analogue (see below). The rapid internalisation of diacyl NBD-PS and -PE across the PM

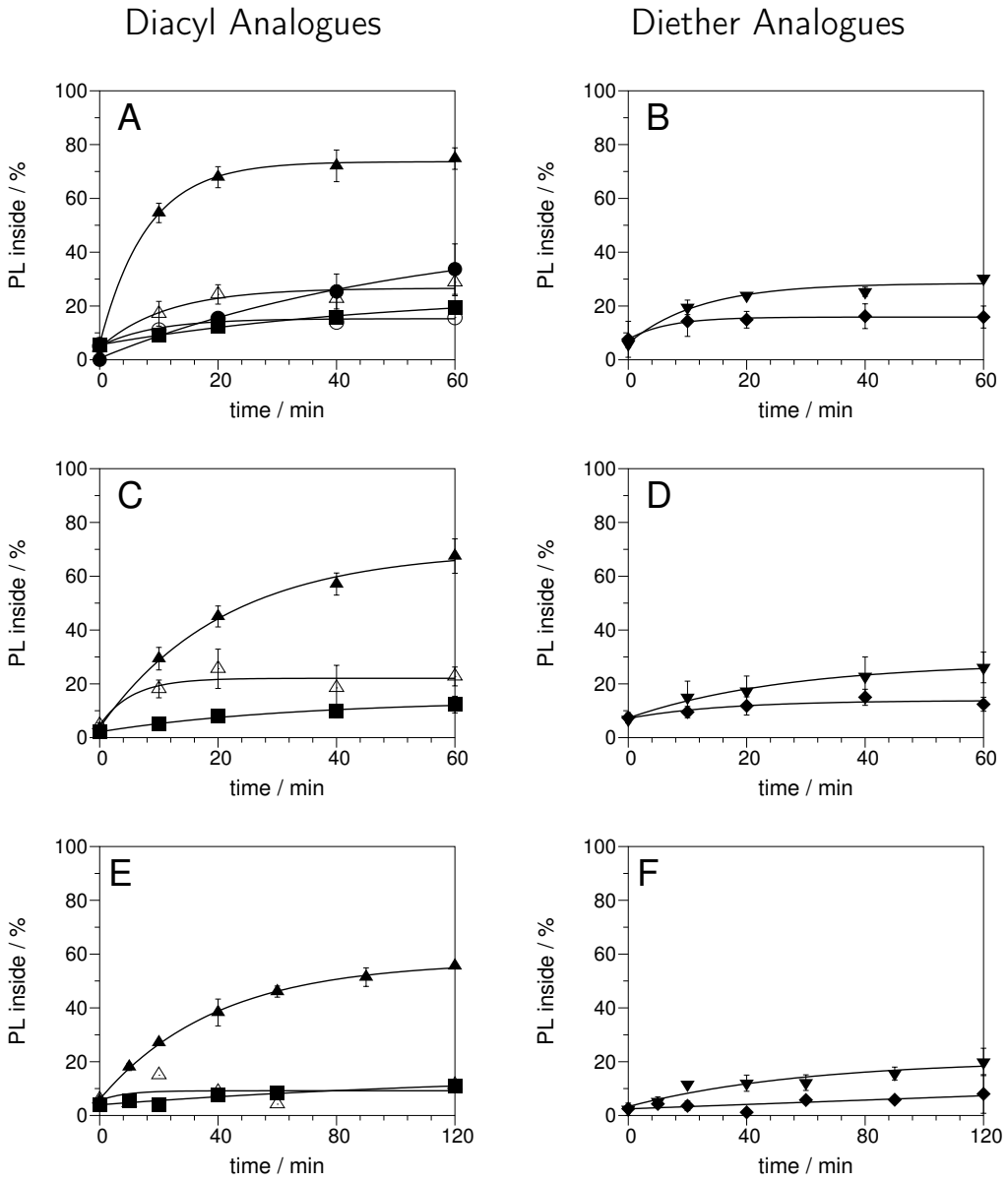

Figure 4.4: **Internalisation of NBD labelled PL analogues in suspended HepG2 cells.** HepG2 cells in suspension were labelled with NBD analogues as described in section 3.3.4. Subsequently, suspensions were incubated at 37 °C (A, B), 22 °C (C, D), and 14 °C (E, F). After various incubation periods, aliquots were taken and the percentage of analogues internalised was measured by the dithionite assay. Triangles up - diacyl NBD-PS, triangles down - diether NBD-PS, circles - diacyl NBD-PE, squares - diacyl NBD-PC, diamonds - diether NBD-PC; filled symbols without suramin, open symbols in the presence of 200 µM suramin (see section 3.5). For each analogue the mean out of 2 to 7 measurements is shown. Error bars represent the SEM, or in the case of two measurements the difference between both values. Kinetics were fitted to a monoexponential function (lines). Note the different scaling of the time axes (A–D versus E, F).

was diminished by preincubation of the cells with suramin, an inhibitor of APLT (figure 4.4 A, C, E): the plateau of redistribution kinetics was about 3–4 fold lower compared with that in the absence of suramin. These results are consistent with an APLT activity in HepG2 cells.

The internalisation of diacyl NBD-PC was different to that of the diacyl aminophospholipid analogues. The fraction of diacyl NBD-PC localised in the exoplasmic leaflet of the PM decreased much slower (figure 4.4 A). At 37 °C only about 20 % were found non-accessible to dithionite after 1 h of incubation. Again, the kinetics of internalisation were significantly reduced upon lowering the temperature (cf. figure 4.4 C, E). About 15 % and 10 % of PC analogues redistributed to cytoplasmic side within one hour at 22 °C and 14 °C, respectively. Preincubation of cells with suramin did not affect the transbilayer dynamics of diacyl NBD-PC (data not shown).

The inward redistribution of diacyl NBD-PC and -PS at 37 °C is visualised in figure 4.5. Fluorescence microscopic pictures of suspended cells immediately after labelling were taken before and after addition of dithionite. The cell membrane was bright labelled initially (figure 4.5 A, I) and almost all fluorescence was reduced by addition of dithionite (figure 4.5 B, J) for both analogues indicating that at the time point t=0 the analogues were located in the outer leaflet of the PM. Further pictures were taken after incubating the labelled cells for 30 min at 37 °C. Again the PM was brightly fluorescent by both analogues (figure 4.5 C, K) before addition of dithionite. Dithionite was added to reduce analogues associated with the outer leaflet of the PM, and in the case of PC reduced almost all of the cell associated fluorescence (figure 4.5 D). In contrast to PC, cells labelled with the diacyl PS analogue remained intracellularly fluorescent after dithionite addition (figure 4.5 L), demonstrating that this analogue became internalised and redistributed also among subcellular compartments much more efficiently than the PC analogue.

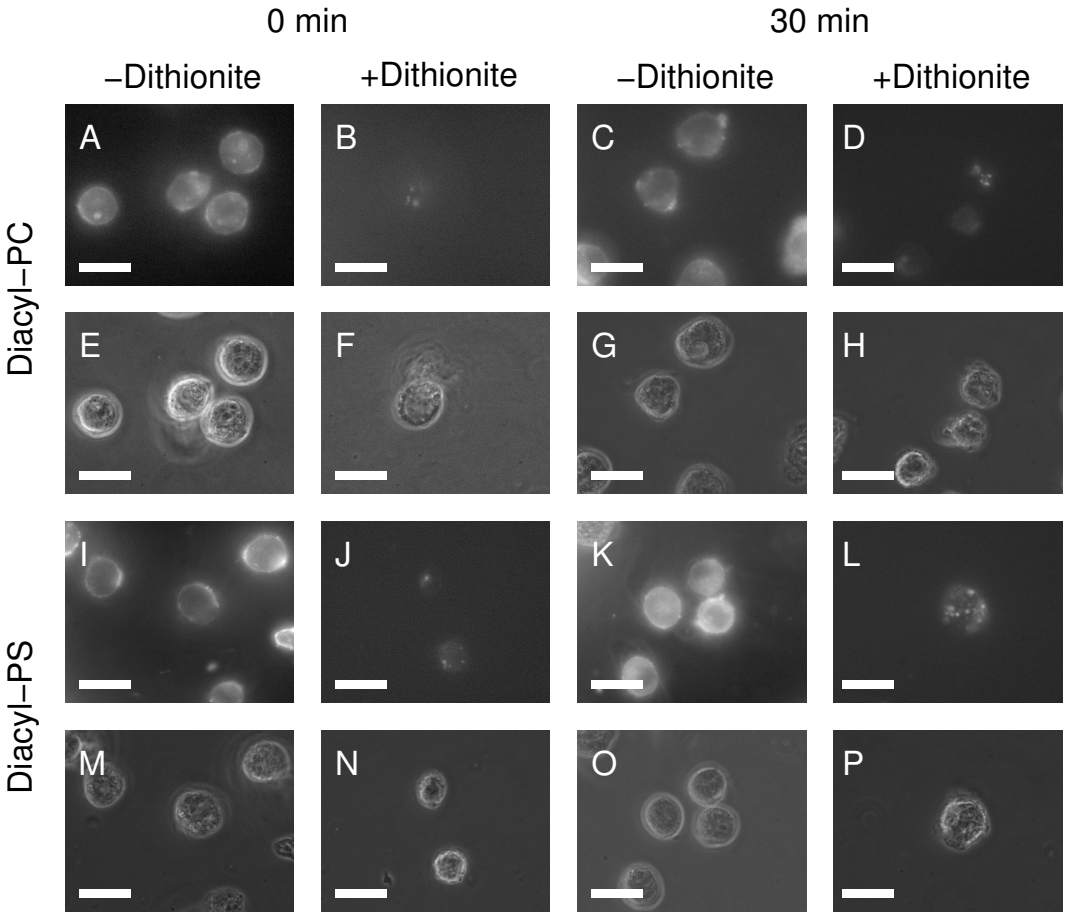

Figure 4.5: **Internalisation of diacyl NBD lipid analogues in suspended HepG2 cells.** HepG2 cells in suspension were labelled with diacyl NBD analogues as described in section 3.3.4. Immediately after labelling, aliquots were placed on a microscopy dish and photographs were taken before (A, I) or after (B, J) reducing the accessible analogues by dithionite. Labelled cells were further incubated at 37 °C for 30 min and again photographs were taken before (C, K) and after (D, L) dithionite reduction. A–D: Cells labelled with diacyl NBD-PC, E–H: phase contrast to A–D; I–L: Cells labelled with diacyl NBD-PC, M–P: phase contrast to I–L. Bar, 20 µm.

Internalisation kinetics of diether NBD-PC was very similar to that of the diacyl analogue (figure 4.4) at all investigated temperatures. However, the internalisation of diether NBD-PS was slower with respect to the diacyl analogue (figure 4.4 B, D, E) which is consistent with previous observation on fibroblasts and red blood cells indicating a very low affinity of APLT for diether NBD-PS [131]. In agreement with this, suramin only had a marginal influence on the inward reorientation of this analogue (data not shown). However, the internalisation of diether NBD-PS was still faster in comparison to both PC analogues (figure 4.4 B, D, E).

In agreement with these findings, fluorescence microscopy showed bright labelling of the plasma membrane by both diether analogues before addition of dithionite, whereas almost no fluorescence was detectable after addition of the reducing agent even after incubating the labelled cells for 30 min at 37 °C (figure 4.5).

4.2.2 Enrichment of Fluorescent NBD-PL Analogues in the BC of Polarised HepG2 Cells

Next, the enrichment of various fluorescent lipid analogues in the BC of polarised HepG2 cells was compared by fluorescence microscopy. Subsequent to labelling of the basolateral membrane on ice, the accumulation of lipid analogues in the BC was monitored after incubation of cells for 30 min at 37 °C (figure 4.7) or at 14 °C (figure 4.10). For diacyl NBD-PC, an extensive labelling of the BC was found at 37 °C (figure 4.7 A, B). About 80 % of the BC were labelled with the analogue (figure 4.8). The punctuate intracellular staining observed originates from endocytic uptake of the analogue [94, 158]. The same pattern of intracellular labelling was observed for diether NBD-PC, in particular regarding the enrichment of this analogue in the BC (figure 4.7 C, D). The amount of labelled BC was similar to that of diacyl NBD-PC (figure 4.8).

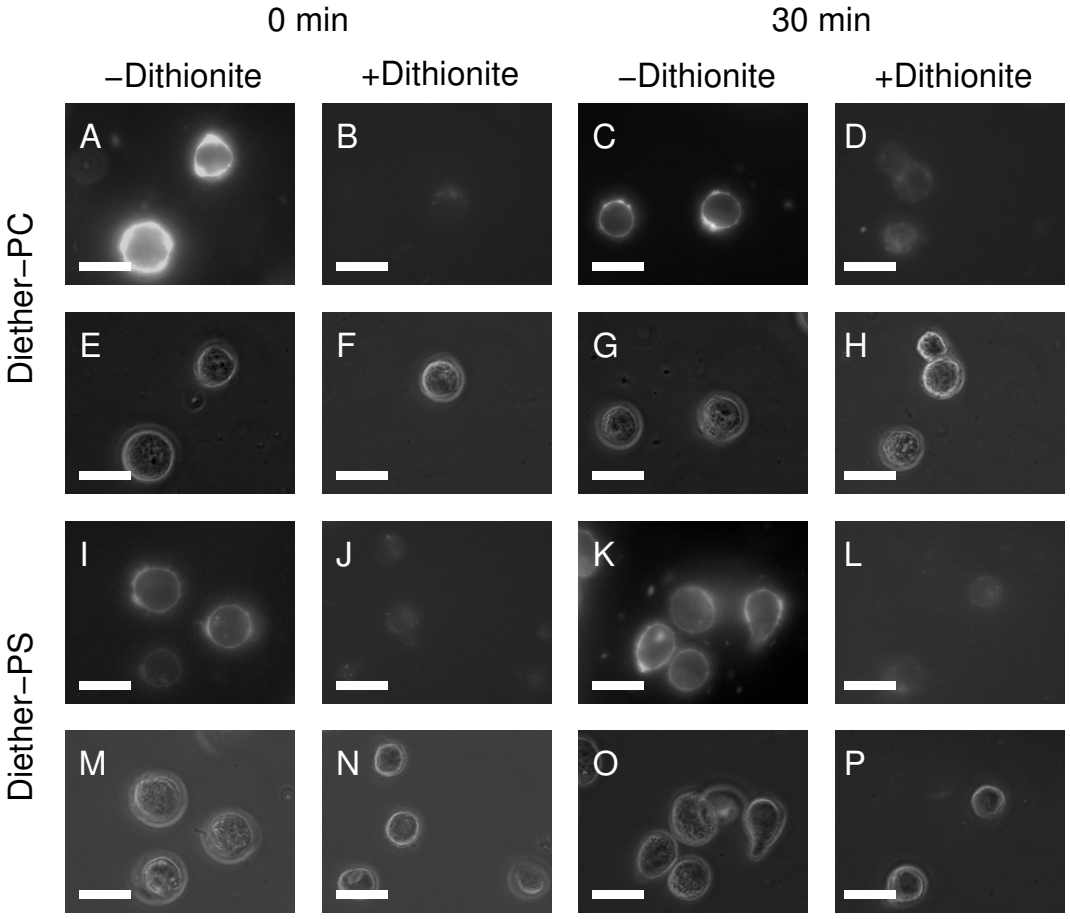

Figure 4.6: **Internalisation of diether NBD lipid analogues in suspended HepG2 cells.** HepG2 cells in suspension were labelled with diether NBD analogues as described in section 3.3.4. Immediately after labelling, aliquots were placed on a microscopy dish and photographs were taken before (A, I) or after (B, J) reducing the accessible analogues by dithionite. Labelled cells were further incubated at 37 °C for 30 min and again photographs were taken before (C, K) and after (D, L) dithionite reduction. A–D: Cells labelled with diether NBD-PC, E–H: phase contrast to A–D; I–L: Cells labelled with diether NBD-PC, M–P: phase contrast to I–L. Bar, 20 µm.

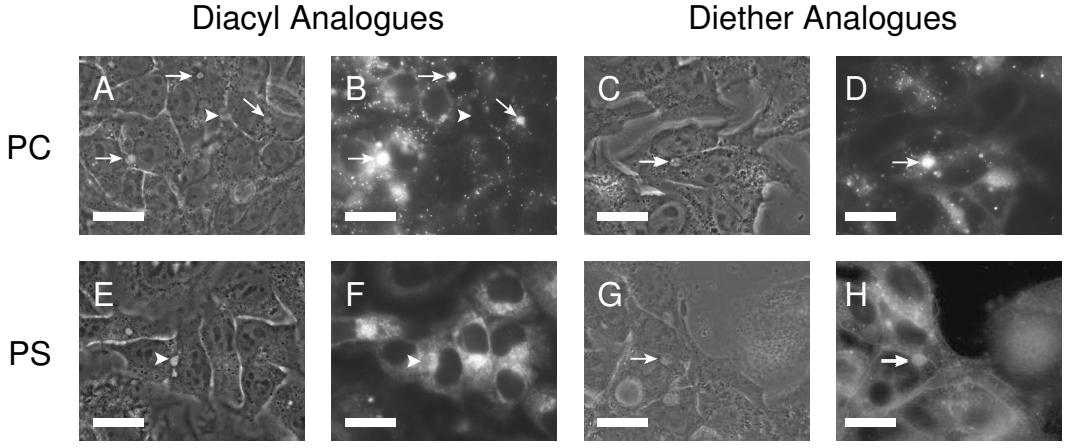

Figure 4.7: **Transport of diacyl and diether NBD-PL analogues to the BC of polarised HepG2 cells at 37 °C.** The basolateral membrane of HepG2 cells was labelled with 4 µM diacyl (A, B, E, F) or diether NBD-PL analogues (C, D, G, H) for 20 min on ice. After washing and incubation for 30 min at 37 °C, cells were washed again and incubated with 5 % (w/v) BSA in $HBSS^+$ for 10 min at room temperature twice to remove remaining label from the exoplasmic leaflet of the basolateral cell membrane. B and F - fluorescence microscopy of diacyl NBD-PC and -PS labelled cells, respectively. A and E are phase contrast images of the same field as shown in B and F, respectively. For diacyl NBD-PC, enrichment in the BC indicated by bright labelling of this structure and punctuate staining of vesicular structures were observed (B). For diacyl NBD-PS, a diffuse cytoplasmic labelling was detected, but no enrichment of the analogue in the BC. D and H - fluorescence microscopy of diether NBD-PC and -PS labelled cells, respectively. C and G are phase contrast images of the same field as shown in D and H, respectively. Both analogues enriched in the BC, although it was more pronounced for diether NBD-PC. Labelled BC are indicated by white arrows, non-labelled BC by white arrowheads. Bar, 20 µm.

The pattern of intracellular fluorescence was very different for the PC and diacyl aminophospholipid analogues. For the latter, a diffuse fluorescence distribution in the cytoplasm was observed (figure 4.7 E, F; only shown for diacyl NBD-PS). No punctuate staining of endocytic vesicles, as detected using PC analogues, was detectable using diacyl NBD-PS. In most cases no labelling of BC with the diacyl aminophospholipid analogues was found. (figure 4.7 E, F). Only about 20 % of the BC were labelled with diacyl NBD-PS after 30 min at 37 °C (figure 4.8). In these BC the fluorescence intensity was lower than that

of BC labelled with PC analogues. This indicates a reduced enrichment of the PS analogue compared to PC.

Unlike diacyl NBD-PS, diether NBD-PS became enriched in the BC (figure 4.7 G, H). The percentage of labelled BC was almost identical to that of PC analogues (figure 4.8). However, in comparison to PC analogues, the punctuate staining within the cytoplasm was less pronounced, instead a somewhat diffusive fluorescence in the cytoplasm was noted.

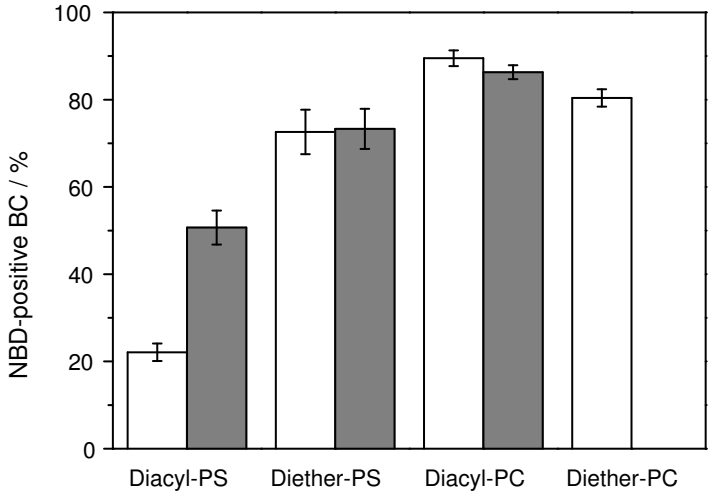

Figure 4.8: **Percentage of BC labelled with NBD-PL analogues.** The basolateral membrane of HepG2 cells was labelled with 4 µM of various NBD-PL analogues and, subsequently, treated as described in the legend to figure 4.7 and in section 3.3.2. The amount of NBD-positive BC in the absence (white bars) and in the presence of 200 µM suramin (filled bars) was determined as described in section 3.7 . Data are expressed as mean±SEM (number of experiments≥6).

Similar to diacyl NBD-PS, diacyl NBD-PE was excluded from the BC but less rigorously as diacyl NBD-PS. Enrichment of this PE analogue was found in about 30 % of the BC (figure 4.9). In contrast to this fatty acid labelled analogue, the head group labelled PE analogues *N*-Fl-PE and *N*-Rh-PE became enriched in about 80 % of the BC (figure 4.9), indicating that modifying the head group of a phospholipid by attaching a fluorophore makes that lipid unrecognisable for the head group specific transporter.

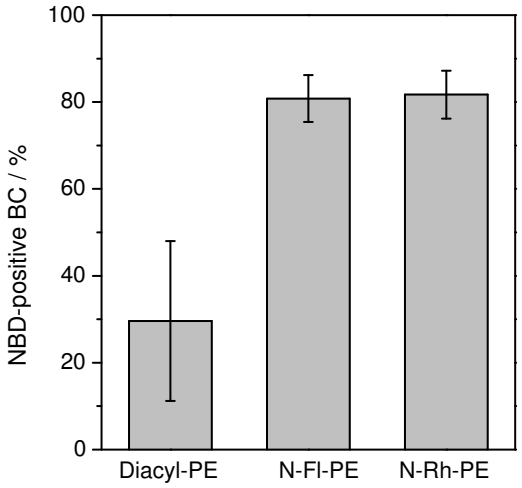

Figure 4.9: **Percentage of BC labelled with different PE analogues** The basolateral membrane of HepG2 cells was labelled with 4 µM of acyl chain (Diacyl-PE) and head group labelled analogues (*N*-Fl-PE and *N*-Rh-PE) PE analogues and the cells were further treated as described in section 3.3.2. The amount of fluorescent BC was determined as described in Materials and Methods. Data are expressed as mean±SEM (number of experiments≥5).

Endocytosis and transcytosis of vesicles from the basolateral to the apical membrane in polarised cells are temperature dependent and are strongly reduced at 14 ℃ [11]. However, also under this condition bright labelling exclusively of the BC was found for both PC analogues and diether NBD-PS (figure 4.10). In contrast, BC were not labelled by diacyl NBD-PS. Similar to the observation at 37 ℃, a bright and diffuse cytoplasmic staining was found for the PS analogue.

In the presence of suramin, a significant enrichment of diacyl NBD-PS in BC was found. Suramin treatment increased the amount of BC labelled by diacyl NBD-PS to about 50 % (figure 4.8). Interestingly, punctuate intracellular staining was observed indicating that endocytic pathways contribute significantly to the uptake of the PS analogues under those conditions. When suramin was washed out, the amount of labelled BC decreased to a value found for cells that had not been treated with the inhibitor (figure 4.11). The half time of the

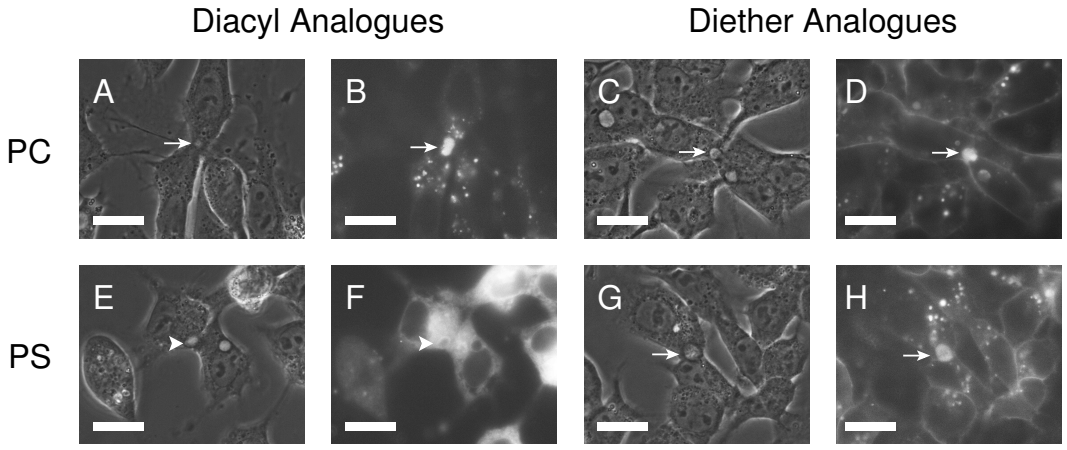

Figure 4.10: **Transport of diacyl and diether NBD-PC and -PS to the BC of polarised HepG2 cells at 14 °C.** The basolateral membrane of HepG2 cells was labelled with 4 µM diacyl (A, B, E, F) or diether NBD-PL analogues (C, D, G, H) for 20 min on ice. After washing and incubation for 30 min at 14 °C, cells were washed again and incubated with 5 % (w/v) BSA (in $HBSS^+$) for 10 min on ice twice to remove remaining label from the exoplasmic leaflet of the basolateral cell membrane. B and F - fluorescence microscopy of diacyl NBD-PC and -PS labelled cells, respectively. A and E are phase contrast images of the same field as shown in B and F, respectively. Bright labelling almost exclusively of the BC was found for diacyl NBD-PC (arrow), punctuate staining was strongly reduced in comparison to 37 °C (figure 4.7B). For diacyl NBD-PS, a diffuse cytoplasmic labelling was detected, but no enrichment of the analogue in the BC. D and H - fluorescence microscopy of diether NBD-PC and -PS labelled cells, respectively. C and G are phase contrast images of the same field as shown in D and H, respectively. Both analogues enriched in the BC, although it was more pronounced for diether NBD-PC. Labelled BC are indicated by white arrows, non-labelled by white arrowheads. Bar, 20 µm.

process was in the order of about 15 min. Suramin affected neither the number of labelled BC with diacyl NBD-PC and with diether NBD-analogues nor the punctuate staining seen for PC analogues.

The localisation of diacyl NBD-PS in the BC after suramin treatment was further confirmed using CLSM. As shown in figure 4.12 A–D diacyl NBD-PS was enriched in the lumen of BC after suramin treatment. When the inhibitor was washed out and cells were incubated for 30 min at 37 °C, the lumen of the BC appeared empty while a staining of the canalicular membrane was detectable (figure 4.12 E–H).

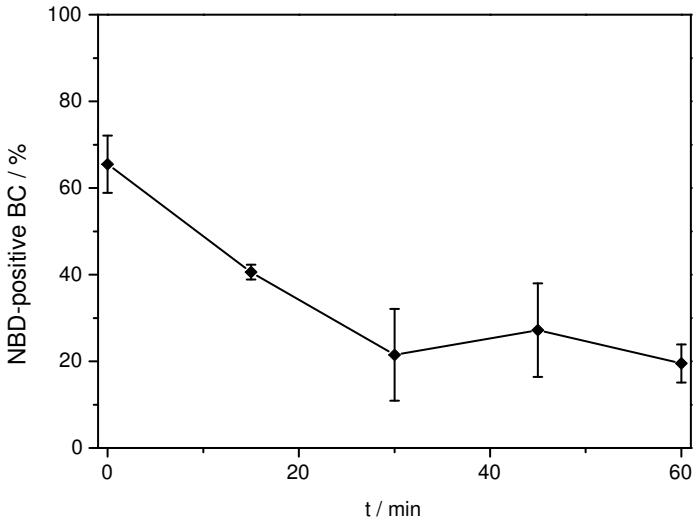

Figure 4.11: **Influence of APLT inhibitor suramin on the labelling of BC by diacyl NBD-PS.** Polarised cells on coverslips were pretreated with 200 µM suramin, labelled with diacyl NBD-PS at 4 ℃ and further incubated in the presence of the inhibitor for 30 min at 37 ℃. Subsequently suramin was washed out, and the amount of fluorescent BC was determined at distinct time points after further incubation of the cells at 37 ℃ as described in Materials and Methods. Data represent mean±SEM of three independent measurements.

Diacyl NBD-PS was also enriched in the BC when cells were treated with suramin after internalisation of the PS analogue (see Materials and Methods). To this end, cells were labelled with diacyl NBD-PS and incubated for 30 min at 37 ℃ to allow internalisation of the analogue. At this point there was only low labelling of the BC (see above). Subsequent addition of suramin led to a bright labelling of BC (data not shown).

4.2.3 Reduction of BC Associated NBD Fluorescence by Sodium Dithionite

As dithionite is able to permeate across the tight junctions and thus reduce the BC associated NBD fluorescence, it is a useful tool to investigate whether fluorescence of BC originates from analogues located in the BC lumen or on the lumenal side of the CM [149] (see section 3.7). Dithionite permeates across

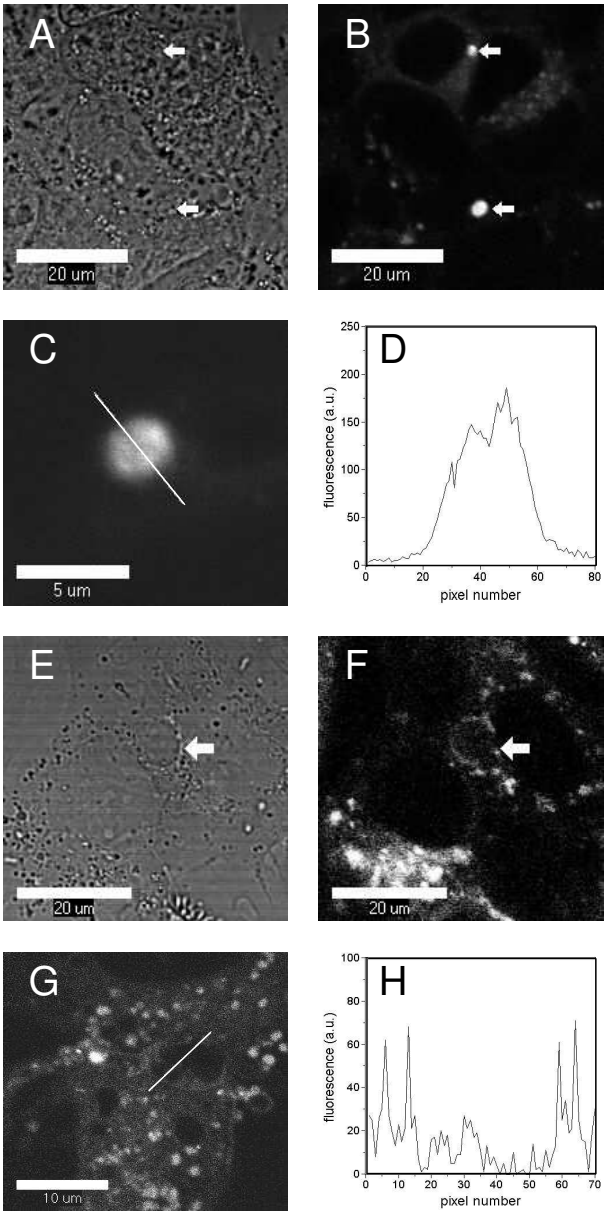

Figure 4.12: **Enrichment of diacyl NBD-PS in the lumen of BC after suramin treatment studied by confocal laser scanning microscopy.** Polarised cells on cover glass were preincubated with 200 µM suramin for 30 min at 37 °C, and labelled with 4 µM diacyl NBD-PS. Non-bound label was removed, and the cells were further incubated at 37 °C for 30 min. Subsequently, cells were back exchanged to 5 % BSA at room temperature twice. The inhibitor was present during all steps. CLSM revealed a bright labelling of BC (B, arrows; A phase contrast to B). The lower BC was scanned with a higher resolution (C). A line scan along the white line shown in C demonstrates that the analogue is enriched in the lumen of BC (D). When suramin was removed and the cells were further incubated at 37 °C only the CM but not the lumen of the BC was fluorescent (F, arrow; E phase contrast to F). Such a BC was scanned with higher resolution (G) resulting in the line scan shown in F. The fluorescence in the CM is about twice as high as in the lumen of the BC.

the PM very slowly at 4 ℃ [62], ensuring that analogues located on the cytoplasmic leaflet of the canalicular membrane are shielded from its reducing property. When cells labelled with PL analogues that are found associated to the BC (i. e. diacyl NBD-PC and diether NBD-PC and -PS) were incubated with dithionite for 10 min on ice following the labelling procedure (see section 3.3.2), the number of BC that appeared fluorescent was about 10 %, indicating that these analogues are located at the lumenal side of the BC.

4.2.4 Colocalisation of Diether and Diacyl NBD-PL Analogues with Diacyl β-BODIPY-PC

To confirm the difference in localisation between diacyl NBD-PS and diether NBD-PS as well PC analogues, cells were double labelled with NBD-PS analogues and a diacyl β-BODIPY-PC analogue. It was previously shown that β-BODIPY PC specifically enriches in the BC and colocalises with the green fluorescent diacyl NBD-PC. [94]. As labelling with both diacyl analogues bearing different fluorophores results in a similar fluorescence pattern, one can assume that their distribution reflects the intracellular allocation of endogenous lipids, too [94]. In agreement with that, β-BODIPY-PC redistributed rapidly to the lumen of the BC (figure 4.13 C), which was not observed for diacyl NBD-PS (figure 4.13 B). In contrast to this, diether NBD-PS colocalised with β-BODIPY-PC in the BC (figure 4.13 D–F).

The intracellular transport and canalicular enrichment of the diether NBD-PC analogue was compared to diacyl β-BODIPY-PC in polarised cell, too (figure 4.14. Labelling with the diether NBD-PC analogue results in virtually the same fluorescence pattern as labelling with the red fluorescent diacyl analogue.

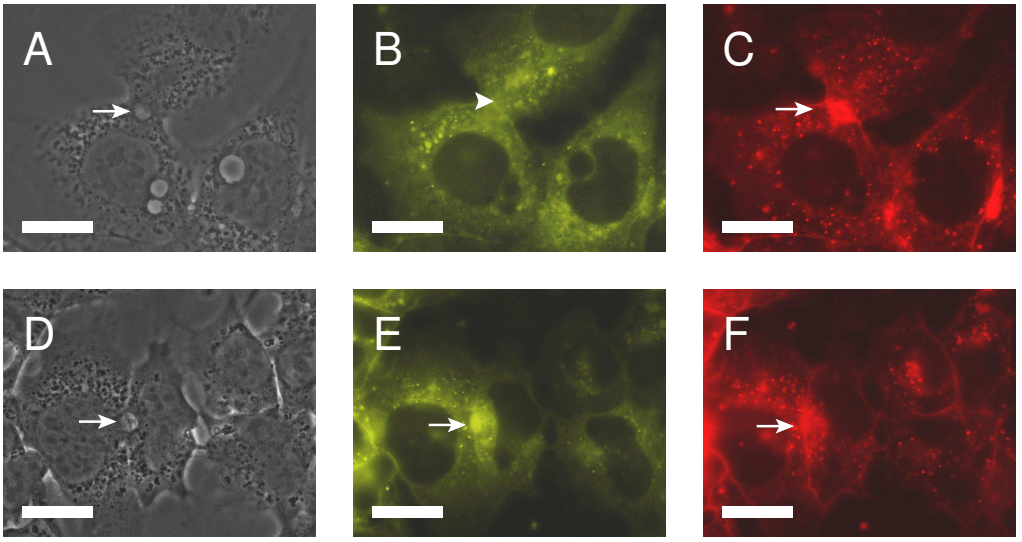

Figure 4.13: **Colocalisation of diacyl and diether NBD-PS and diacyl β-BODIPY-PC analogues.** Polarised cells on cover glasses were double labelled with diacyl NBD-PS (B) and β-BODIPY-PC (C) or diether NBD-PS (E) and β-BODIPY-PC (F) (see section 3.3.3) and further incubated at 37 °C for 30 min. A bright labelling of the BC by β-BODIPY-PC occurred (C), while diacyl NBD-PS was absent from the BC (B). A: phase contrast to B and C. In contrast, both diether NBD-PS and β-BODIPY-PC enriched in the BC (D–F).

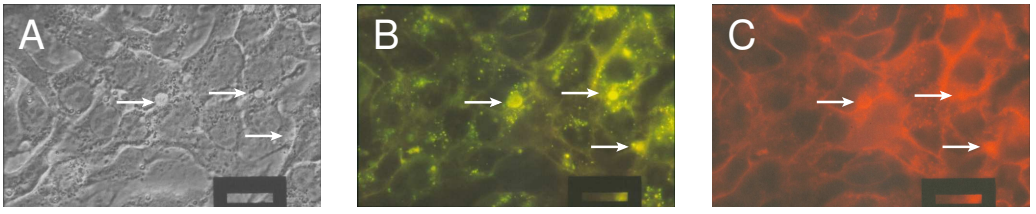

Figure 4.14: **Colocalisation of fluorescent diether and diacyl PC analogues in polarised HepG2 cells.** Cells were colabelled with diether NBD-PC (B) and diacyl β-BODIPY-PC (C) (see section 3.3.3); A: phase contrast to B and C. Arrows point to double labelled BC. Bar, 20 µm.

4.3 Influence of the MDR Inhibitors on BC Labelling Pattern

To investigate the involvement of MDR proteins, especially MDR3 in the transport of various PL from the cytoplasmic to the lumenal side of the BC the non-specific MDR inhibitor Verapamil and the MDR1 Pgp specific inhibitor PSC 833 were used. It was shown that in HepG2 cells the number of BC that were labelled with diacyl NBD-PC was reduced from about 80 % in the absence of inhibitors to about 65 % in the presence of each of the inhibitors [159]. However, the number of BC that remained fluorescent after adding dithionite to Verapamil treated cells (about 45 % of the total BC) was not significantly different from the number of BC when dithionite was absent. When cells were treated with PSC 833 the number of fluorescent BC was significantly reduced after dithionite treatment. From these data the author concluded that the detected fluorescence of the BC in the presence of Verapamil originated from analogues on the cytoplasmic leaflet of the canalicular membrane and that Verapamil strongly inhibited the transport of diacyl C_6-NBD-PC across the canalicular membrane [159].

The ability of Verapamil and PSC 833 to inhibit the transport of the diether and diacyl NBD analogues of PC and PS across the canalicular membrane was studied. The efficiency of inhibition was probed by the fluorophore Rho123 which is transported by MDR1 Pgp across the canalicular membrane and becomes highly enriched in the BC (figure 4.15). In the presence of MDR inhibitors Rho123 is excluded from the BC (figure 4.15).

Confirming previous studies [159] the number of BC that appeared fluorescent after incubation with diacyl NBD-PC was reduced from about 90 % in the absence of the inhibitor to about 65 % in the presence of Verapamil. A similar tendency of Verapamil was found for diether NBD-PC (figure 4.15). This reduction of the number of fluorescent BC was significant as tested by

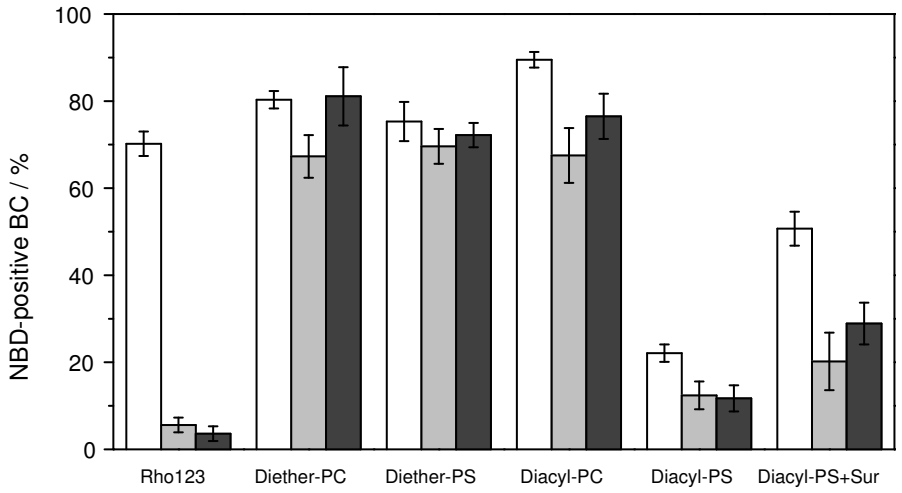

Figure 4.15: **Influence of the MDR inhibitors Verapamil and PSC 833 on the percentage of BC labelled with various PL analogues.** The basolateral membrane of HepG2 cells was labelled with the fluorophore Rho123 or various NBD-PL analogues as described in section 3.3.2. The amount of NBD positive BC in the absence (white bars) of inhibitors and in the presence of 20 µM Verapamil (light grey bars) or 10 µM PSC 833 (dark grey bars) was determined as described in section 3.7. In the case of diacyl NBD-PS additional inhibition of the APLT by suramin is indicated which was performed in the control and in the MDR inhibited cells. Data are expressed as mean±SEM (number of experiments≥ 5).

an unpaired t-test ($\alpha = 0.05$). The specific MDR1 Pgp inhibitor PSC 833 reduced the number of BC labelled with diacyl NBD-PC significantly to about 70 %. Unlike for diacyl NBD-PC no reduction of the number of diether NBD-PC labelled BC in the presence of PSC 833 compared to control was found (see figure 4.15). Only a slight decrease of NBD-positive BC in the presence of MDR inhibitors compared to control was found for both diether and diacyl NBD-PS which was significant for the diacyl analogue, but not for the diether analogue (one side unpaired t-test, $\alpha = 0.05$). When enrichment of diacyl NBD-PS was enhanced by inhibition of the APLT an effect of the MDR inhibitors became more evident. A significant reduction of the number of diacyl NBD-PS labelled BC in the presence of the APLT inhibitor suramin was observed for both MDR inhibitors. The number of labelled BC with diacyl

NBD-PS in the presence of suramin and either of the MDR inhibitors was not significantly different for Verapamil and PSC 833 treated cells (figure 4.15).

In contrast to former observations [159] the number of fluorescent BC after addition of dithionite was significantly reduced in cells that were treated with Verapamil for all investigated analogues (figure 4.16). No significant difference of the number of labelled BC after dithionite treatment in control and Verapamil inhibited cells could be observed. These data indicate that if BC appear fluorescent, the signal originates essentially from the lumenal side.

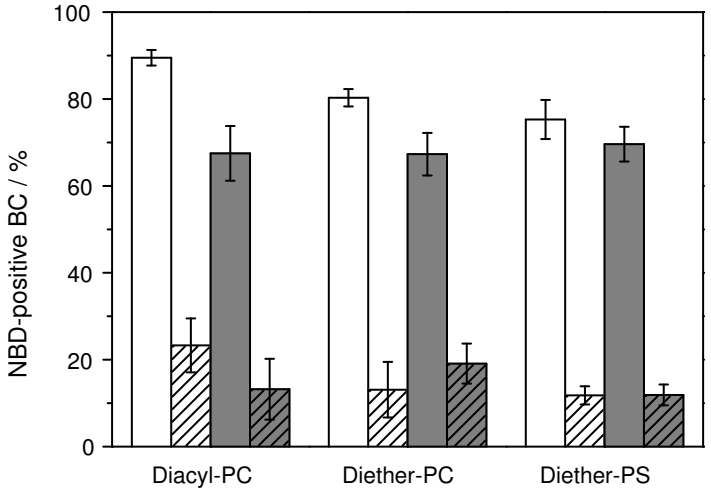

Figure 4.16: **Comparison of the number of fluorescent BC in Verapamil treated and control cells in the presence and absence of dithionite.** The basolateral membrane of HepG2 cells was labelled with diether NBD-PL analogues as described in section 3.3.2. The amount of NBD positive BC in the absence (white bars) and in the presence of 20 µM Verapamil (grey bars) was determined as described in section 3.7. Hatched bars represent the BC that remained fluorescent after 10 min incubation with 30 mM sodium dithionite on ice. Data are expressed as mean±SEM (number of experiments≥ 5).

4.4 Enrichment of Sphingolipid Analogues in the BC of HepG2 Cells

The accumulation of the NBD labelled (glyco)sphingolipid analogues C_6-NBD-SM, C_6-NBD-GlcCer, and C_6-NBD-GalCer was studied at different temperatures. In contrast to endogenous sphingolipids which are not found in bile, the transport to and accumulation in BC of NBD labelled sphingolipid analogues has been reported [149, 94, 160].

As shown in figure 4.17 labelling with the sphingolipid analogues resulted in bright fluorescence of the BC when incubated at 37 °C.

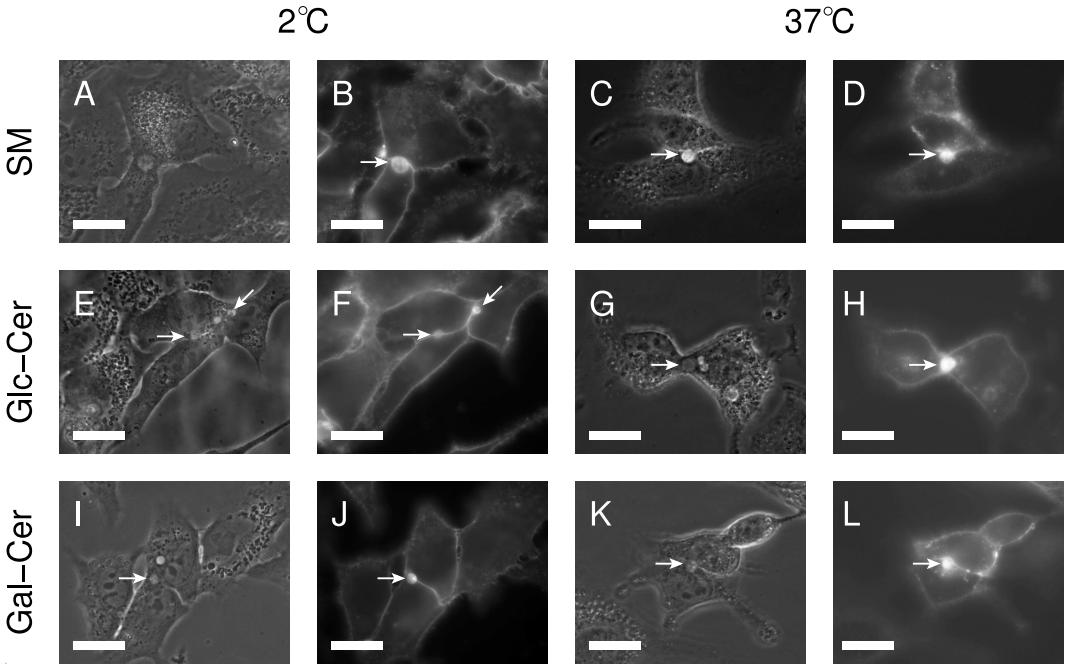

Figure 4.17: **Transport of NBD labelled sphingolipid analogues to the BC of polarised HepG2 cells at different temperatures.** The basolateral membrane of HepG2 cells was labelled with 4 µM C_6-NBD-SM (A–D), C_6-NBD-GlcCer (E–H), or C_6-NBD-GalCer (I–L) for 20 min on ice. After washing cells were further incubated for 30 min at 2 °C (A–B, E–F, I–J) or 37 °C (C–D, G–H, K–L), BC (arrows) appeared fluorescent for all investigated analogues, even when incubated at 2 °C. However, at this temperature the fluorescence intensity in the BC was lower than at 37 °C. Left panels represent phase contrast images of the corresponding right fluorescence pictures. Bar, 20 µm.

When the incubation temperature was lowered to 4 °C the fluorescence intensity in the BC was slightly reduced compared to that of incubation at 37 °C. However, the analogues were still associated with the BC indicating that they have reached the BC by a non-vesicular way, as vesicular transport is abolished at this temperature (figure 4.17).

4.5 Metabolism of the Lipid Analogues

The intracellular hydrolysis of the diacyl NBD-analogues and their metabolic conversion to other fluorescent lipids are summarised in table 4.1. For cells in suspension, between 10 and 20 % of diacyl analogues analogues were hydrolysed after incubation at 37 °C for 60 min. In monolayers of polarised cells, 6–8 % of diacyl NBD-PE and -PC and about 17 % of diacyl NBD-PS were hydrolysed after incubation for 30 min at 37 °C. In the presence of DFP, hydrolysis was reduced to a level of 2–4 % of total analogues. However, polarised cells were not treated with DFP for studying intracellular localisation of analogues, because DFP reduces the life time of adherent cells under the additional stress of microscopic observations. For both, cells in suspension and polarised cells a metabolic conversion of diacyl NBD-PS to PE and PA was observed which was not affected by DFP (table 4.1).

Table 4.1: **Metabolism of diacyl NBD-PL analogues in polarised and suspended HepG2 cells in the absence and presence of DFP.** Analysis was performed by 2D-TLChr (see section 3.8). Spots corresponding to products of analogue metabolism were quantified as percentage of the sum of all NBD containing spots. Data represent mean±deviation (in %) from the mean of two independent measurements. FA corresponds to the hydrolysed fluorescent fatty acid residue in the *sn2*-position.

		Polarised cells (monolayers)		Cells in suspension	
Analogue	Additional spot	-DFP	+DFP	-DFP	+DFP
diacyl-NBD-PC	FA	6.4±0.4	2.6±1.6	12.2±2.5	3.1±1.0
diacyl-NBD-PS	FA	16.9±2.3	3.1±2.5	17.2±2.0	1.9±1.0
	fluorescent PE*	6.6±0.8	10.6±5.5	19.2±1.5	19.4±4.1
	fluorescent PA*	5.3±0.8	6.0±2.0	3.4±0.1	6.1±2.8
diacyl NBD-PE	FA	7.9±1.8	3.2±2.5	20.8±7.5	4.1±1.3

* Spots correspond to those observed for diacyl NBD-PE and diacyl NBD-PA.

4.6 Characterisation of the Fluorescence Life Time of Lipid Analogues

The phospholipid analogue diacyl C_6-NBD-PC and the bile salt analogues UDC-NBD and CGamF were incorporated into several biliary model environments. The influence of the physico-chemical environments on the fluorescence life time(s) of the lipid analogues was monitored.

The fluorescence life time of the investigated lipid analogues was first characterised in their most suitable organic solvent at 22 ℃. The decay curves could be fitted monoexponentially. Fluorescence life times are summarised in table 4.2.

Table 4.2: **Fluorescence life times of lipid analogues in organic solvents.** τ represents the fluorescence life time and n the number of determinations. Data are expressed as mean±SEM.

Analogue	Solvent	τ / ns	n
diacyl C_6-NBD-PC	chloroform	9.21 ± 0.10	4
UDC-NBD	ethanol	6.70 ± 0.01	3
CGamF	ethanol	4.38 ± 0.01	3

4.6.1 Interaction of Bile Salts with Lipid Analogues

The interaction of bile salts with lipid analogues which were either dissolved in $HBSS^+$ or incorporated into LUVs was monitored by the change of the fluorescence life time(s) of the analogues. Data collected by TCSPC after excitation by a pulsed laser source were fitted to bi- or triexponential model functions (see section 3.10.2).

A typical biexponential fit of diacyl C_6-NBD-PC in aqueous solution is shown in figure 4.18 A. Diacyl C_6-NBD-PC incorporated into LUVs had to be

fitted to a triexponential function to give acceptable χ^2-values (figure 4.18 B), the same was true when 6 mM TC were added to both model systems (red lines in figure 4.18). The different fluorescence life times correspond to the same analogue in a different physico-chemical environment. Each organisational appearance of fluorescent analogues is termed as a "species" of analogues in the following part.

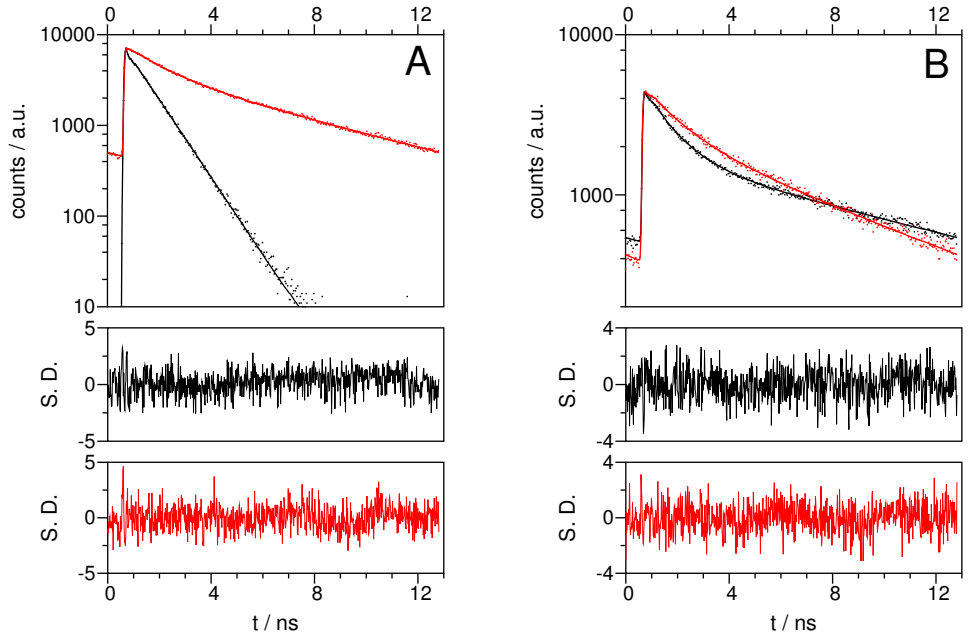

Figure 4.18: **Typical fluorescence decay curves of diacyl C_6-NBD-PC in different environments.** The fluorescence life time of diacyl C_6-NBD-PC was measured by TCSPC after excitation with a pulsed Ti:Sa laser (dots). Data points were fitted to a periodic bi- or triexponential model function (lines). The standard deviation of each point from the fitted function is given below. A: diacyl C_6-NBD-PC in aqueous solution in the absence (black) and presence (red) of 6 mM TC. B: diacyl C_6-NBD-PC incorporated into LUVs composed of EYSM:cholesterol (2:1) in the absence (black) and presence (red) of 6 mM TC.

From the bi- or triexponential fits of fluorescence decay times the contributions of the species of analogues yielding the different fluorescence life times was calculated. The total fluorescence of the solution after one single excitation by a δ-function is represented by the integral over the decay function:

$$I = \int_0^\infty \sum_n a_n \, \mathrm{e}^{-t/\tau_n} \, \mathrm{d}t$$

Thus, the contribution of the species n with the fluorescence life time τ_n to the total fluorescence intensity is given by:

$$I_n = a_n \cdot \tau_n$$

The amplitude a_n is proportional to the quantum yield Φ_n of the species n and its concentration:

$$a_n \propto \Phi_n \cdot c_n$$

Measuring the fluorescence decay time of HBSS$^+$ indicated that this buffer exhibits an autofluorescence with three different fluorescence life times. This autofluorescence, however, was much lower than that measured from any lipid analogue samples. Figure 4.19 shows the autofluorescence decay curve of HBSS$^+$ compared to that of diacyl C_6-NBD-PC in the same buffer. The contribution of the autofluorescence is even lower for diacyl C_6-NBD-PC in other environments as the quantum yield of the analogue raises when incorporated into a non-fluorescent lipid environment (see below).

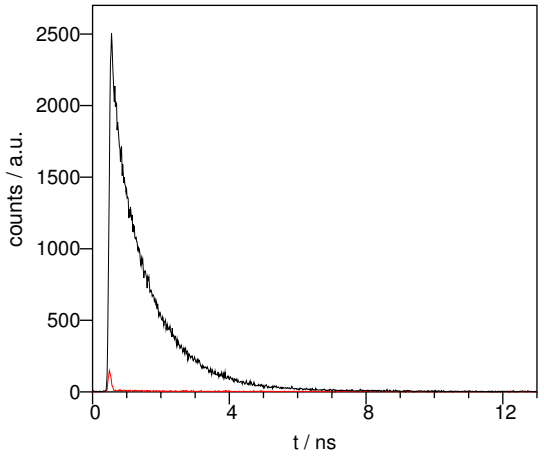

Figure 4.19: **Autofluorescence of HBSS$^+$ compared to fluorescence decay of diacyl C_6-NBD-PC in the same buffer.** The autofluorescence of HBSS$^+$ (red) is compared to the fluorescence decay of 10 µM diacyl C_6-NBD-PC in HBSS$^+$ (black). Fluorescence decay curves were obtained after excitation with a pulsed Ti:Sa laser. Excitation intensity and duration of measurement were equal for both samples.

Diacyl C_6-NBD-PC in Aqueous Solution

Diacyl C_6-NBD-PC dispersed in aqueous solution exhibited a fluorescence decay curve which was best fitted to a biexponential function (figure 4.18 A). The short time of about 0.1 ns (white diamonds in figure 4.20) was found in most samples measured (see below). Its contribution to the total fluorescence intensity is very low and decreases with increasing intensities of the other species (i. e. when bile salts are added, see below). This fluorescence life time might represent diacyl C_6-NBD-PC in self-quenching micelles. Due to the quenching process the quantum yield of this lipid species is lowered dramatically. Thus, its contribution to the total curve is very low, even in case a relatively high amount of the analogue is organised into such micelles. The second fluorescence life time of diacyl C_6-NBD-PC in an aqueous environment is about 1 ns (figure 4.20, light grey squares). It is likely that this life time represents free monomers of the analogue. Upon addition of various bile salts a third species (grey circles in figure 4.20) of fluorescent analogues with life times longer than 1 ns appeared which most likely corresponds to aggregates of diacyl C_6-NBD-PC and bile salts (mixed micelles or submicellar aggregates [161]). The fluorescence life time and the contribution to the total fluorescence intensity of this species increased with increasing bile salt concentration, and depending on the hydrophobicity of the bile salts (table 4.3). Upon stepwise bile salt addition, the fluorescence life time of the second species probably representing diacyl C_6-NBD-PC monomers in aqueous dispersion increased slightly, too.

Also, the unconjugated synthetic non-micelle forming [162] bile salt DHC induced the appearance of a third species of fluorescent analogues with a longer fluorescent life time (about 4.6 ns). Its contribution to the total fluorescence was about 50 % at 6 mM DHC concentration (data not shown).

The maximum fluorescence life times of diacyl C_6-NBD-PC incorporated into different bile salt micelles are summarised in table 4.3 and compared to the hydrophobicity of the bile salts known from the literature.

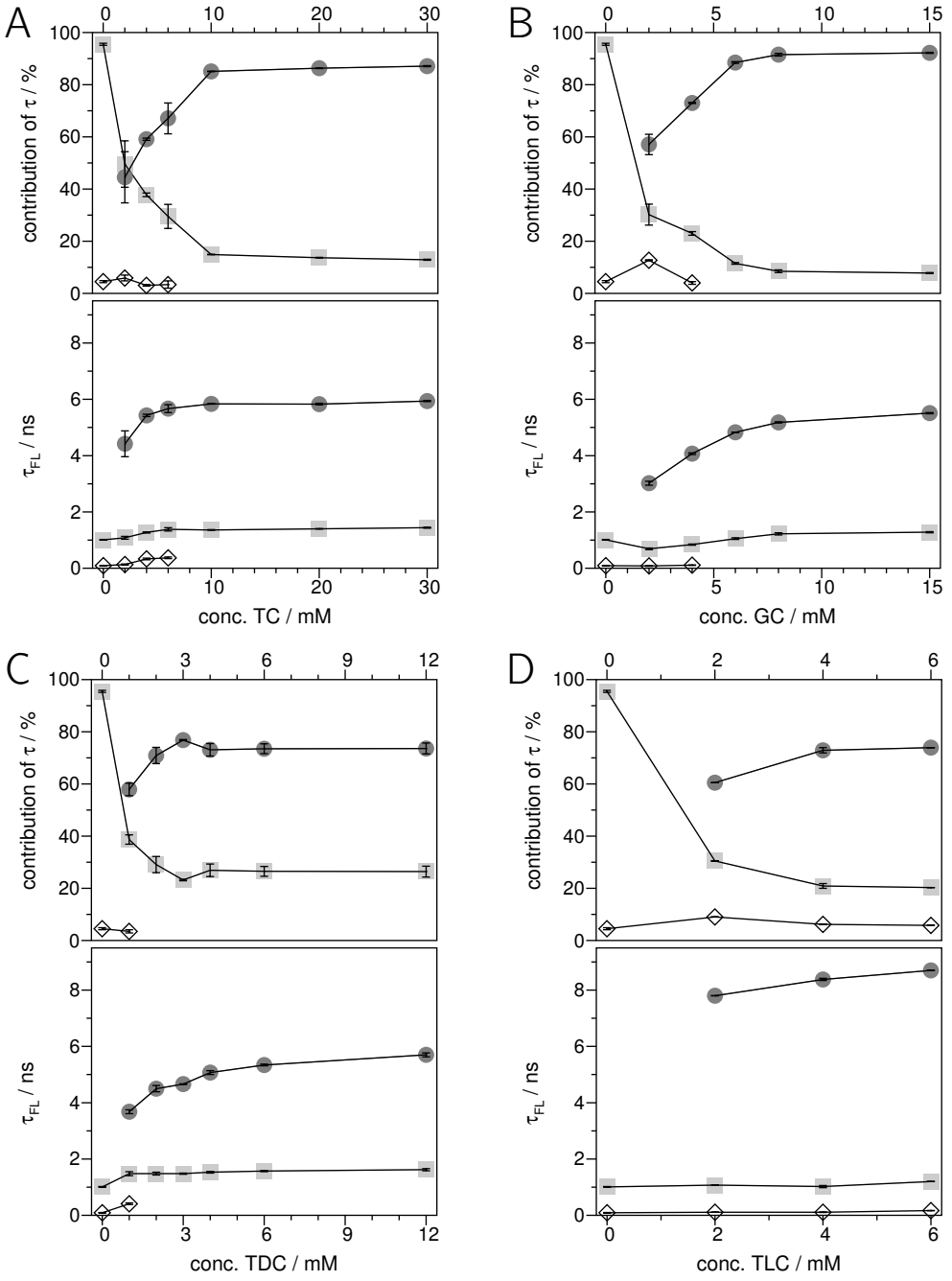

Figure 4.20: **Interaction of bile salts with diacyl C_6-NBD-PC.** The bile salts TC (A), GC (B), TDC (C), and TLC (D) were added stepwise from a stock solution to a 10 µM dispersion of diacyl C_6-NBD-PC in $HBSS^+$. Fluorescence life times were fitted to bi- or triexponential model functions. The resulting fluorescence life times and the contribution of the corresponding species of fluorophores are shown (white diamond representing diacyl C_6-NBD-PC in self-quenched micelles, light grey squares corresponding to monomeric analogue, and grey circles for analogue in bile salt complexes). Data represent mean±SEM, n≥3. Note the different scaling of the abscissae. See text for further explanation.

Table 4.3: **Maximum fluorescence life time of diacyl C_6-NBD-PC in different bile salt micelles compared to their hydrophobicity.** The maximum life time of bile salt bound diacyl C_6-NBD-PC species in bile salt suspension is compared to the hydrophobicity index (HI) of the corresponding bile salt (classified according to [84]).

Bile Salt	τ / ns	HI [84]
TC	6	+0.00
GC	5.5	+0.07
TDC	5.7	+0.59
TLC	8.7	+1.00
DHC	4.6	n.d.

Upon interaction with TC, also the head-group labelled PL analogue *N*-Fl-PE showed an increased contribution of a longer life time of about 3.5 ns to the total fluorescence compared to a shorter life time of about 0.7 ns. However, both life times were also present when TC was absent (data not shown).

Diacyl C_6-NBD-PC in LUVs

The fluorescent analogue diacyl C_6-NBD-PC was incorporated into two distinct membrane environments: vesicles composed of POPC (which represents the major biliary PC species) and vesicles composed of EYSM and cholesterol in a molar ratio of 2:1.

All decay curves were best fitted to triexponential functions. Again, a very short time with little contribution to the total intensity (white diamonds in figure 4.21) occurred. As outlined above this life time may represent diacyl C_6-NBD-PC in self quenching micelles. A second life time (about 1.2 ns, light grey squares in figure 4.21) representing monomeric analogue was found in agreement with the measurements of the analogue in aqueous solution (see above). The remaining life time (grey circles in figure 4.21) is interpreted to correspond to a species of diacyl C_6-NBD-PC incorporated into LUVs. The

latter had a life time of about 5.9 ns or 10.7 ns when LUVs were composed of POPC or EYSM/cholesterol, respectively (see figure 4.21).

Addition of bile salts as TC and TDC to the LUVs lowered the fluorescence life time of the membrane bound component to a value which is typical for the analogue bound to micelles of the corresponding bile salt (see above) in the case of EYSM/cholesterol LUVs. When LUVs were composed of POPC the fluorescence life time of the membrane bound species of diacyl C_6-NBD-PC was already very similar to that of the analogues in bile salt micelles of TC or TDC. Thus, no major changes in the fluorescence life time of this species was observed upon adding TC. However, when TDC was added, the fluorescence life time of the membrane associated component decreased at low concentrations of the bile salt and raised again at higher concentrations. The fluorescence life time of monomeric diacyl C_6-NBD-PC increased slightly upon addition of bile salts as was already found for diacyl C_6-NBD-PC in aqueous solution (see above). Also the contribution of this component increased when adding TDC (see figure 4.21).

Fluorescent Bile Salts

The fluorescence life time of the bile salt analogues CGamF and UDC-NBD was investigated.

Fluorescence decay curves of CGamF were best fitted to a monoexponential function giving a live time of 4.01±0.02 ns in $HBSS^+$. Adding TC to this solution increased the live time slightly to 4.38±0.02 ns at a concentration of 9 mM TC. Also, when the analogue was added during preparation of EYPC LUVs the fluorescence decay was still monoexponential with almost the same life time (3.93±0.02 ns) as found for the monomers in $HBSS^+$.

The decay curve of UDC-NBD in aqueous solution was biexponentially, again with a small contribution of a very short life time (white diamonds in figure 4.22), which might again be due to self-quenching effects of aggregated

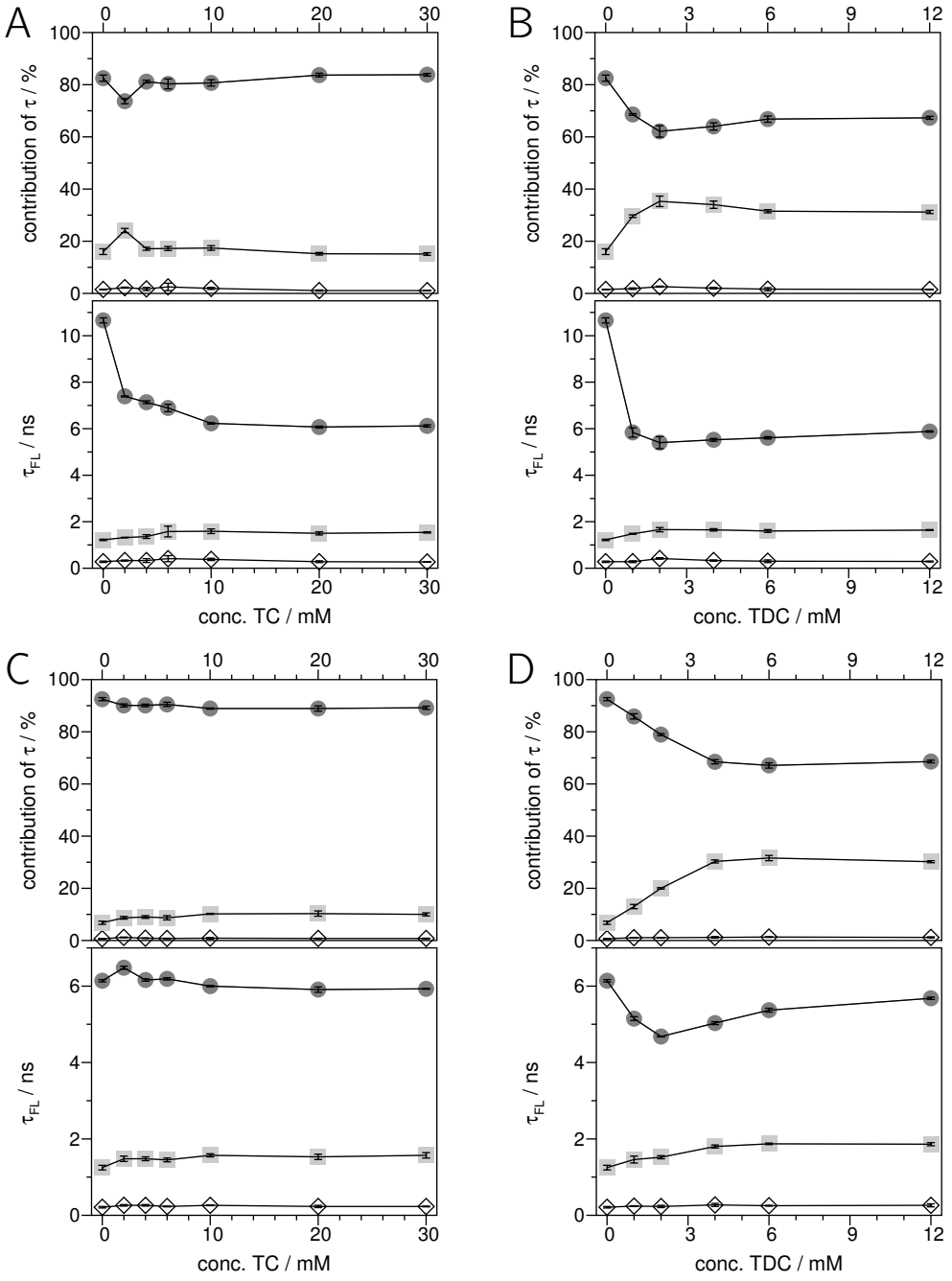

Figure 4.21: **Interaction of bile salts with diacyl C_6-NBD-PC in LUVs.** Diacyl C_6-NBD-PC was incorporated to 1 mol% into LUVs composed of EYSM:Cholesterol (2:1) (A, B) or POPC (C,D). The bile salts TC (A, C), and TDC (B, D) were added from a stock solution stepwise. Fluorescence life times were fitted to triexponential functions. The resulting fluorescence life times and the contribution of the corresponding species of fluorophores are shown (white diamond corresponding to diacyl C_6-NBD-PC in self-quenched micelles, light grey squares representing monomeric analogues, and grey circles for analogues incorporated into liposomes or in bile salt complexes). Data represent mean±SEM, n=3. Note the different scaling of the axes.

analogues. The main component of the fluorescence decay curve of UDC-NBD in HBSS$^+$ had a life time of about 2 ns (light grey squares in figure 4.22). When bile salts were added to this solution a third component appeared (grey circles in figure 4.22). The fluorescence life time of this species of UDC-NBD rose with increasing bile salt concentration to a maximum of about 5.7 ns for both TC and TDC (see figure 4.22). The fluorescence life time of about 2 ns remained rather constant upon addition of bile salts. The contribution of the latter to the total fluorescence intensity decreased with increasing concentration of endogenous bile salts (figure 4.22).

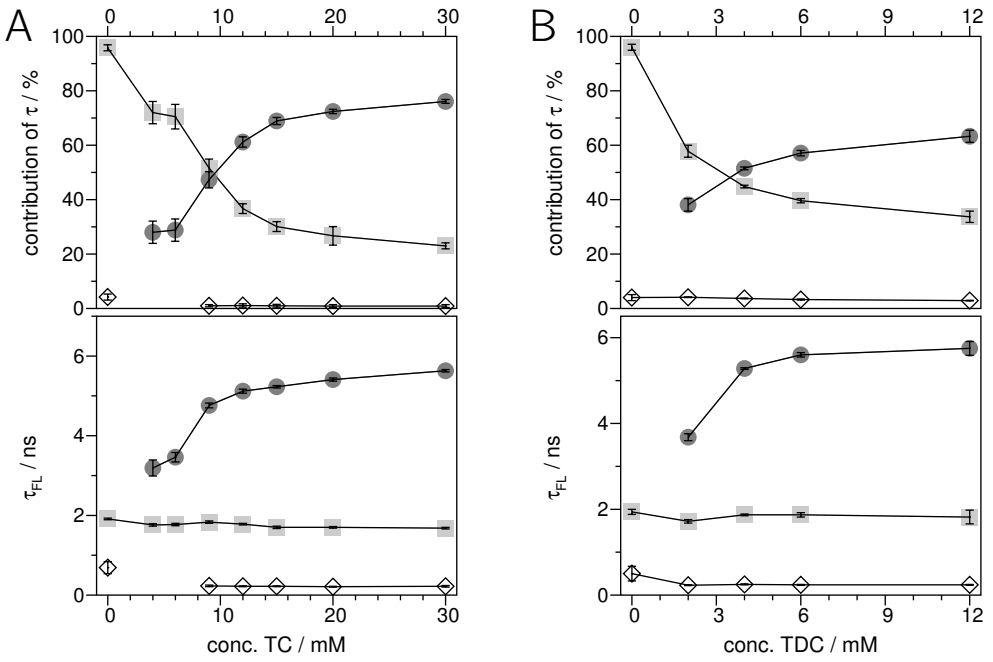

Figure 4.22: **Interaction of endogenous bile salts with UDC-NBD.** The bile salts TC (A), and TDC (B) were added stepwise from a stock solution to a 10 µM dispersion of UDC-NBD in HBSS$^+$. Fluorescence life times were fitted to bi- or triexponential model functions. The resulting fluorescence life times and the contribution of the corresponding species of fluorophores are shown (white diamond probably corresponding to complexed UDC-NBD, light grey squares representing monomeric analogue, and grey circles for membrane bound analogues or UDC-NBD in bile salt complexes). Data are expressed as mean±SEM, n=3 for TDC, n≥9 for TC. Note the different scaling of the axes. See text for further explanation.

When UDC-NBD was added to LUVs composed of EYPC, which is similar to PC of the bile fluid, fluorescence decay curves became triexponentially. The first component of the decay curve had a very short life time with little contribution to the curve (white diamonds in figure 4.23) eventually representing self-quenching analogues. The second component (light grey squares in figure 4.23) had a fluorescence life time of about 1.7 ns which is similar to that of UDC-NBD monomers in aqueous solution (see above). The third component (grey circles in figure 4.23) most likely representing membrane bound UDC-NBD had a live time of about 6.5 ns. Adding bile salts to this solution decreased the fluorescence life time of the membrane bound species at low bile salt concentrations. At higher bile salt concentrations the fluorescence life time of the third component increased again to a final value of about 5.7 ns which was also found for UDC-NBD in pure bile salt micelles (see above). The life time of the free UDC-NBD species remained almost constant upon addition of bile salts (figure 4.23).

The contribution of the putative free analogue species to the total intensity increased at low bile salt concentrations and decreased again when the concentration of TC or TDC was raised (figure 4.23). This behaviour was similar, although more pronounced to that of diacyl C_6-NBD-PC in LUVs of EYSM/cholesterol (figure 4.21 A, B).

4.6.2 FRET

FRET between NBD as donor and rhodamine as acceptor is widely used to study interaction of molecules. This FRET pair is especially useful as a membrane probe when both fluorophores are attached to lipids [163, 164].

Here, FRET between NBD attached to two different donor lipids and *N*-Rh-PE was characterised by the decrease of the fluorescence life time of the donor. Both lipid analogues were incorporated into vesicles to ensure an appropriate distance of the fluorophores well below the Förster-radius [165].

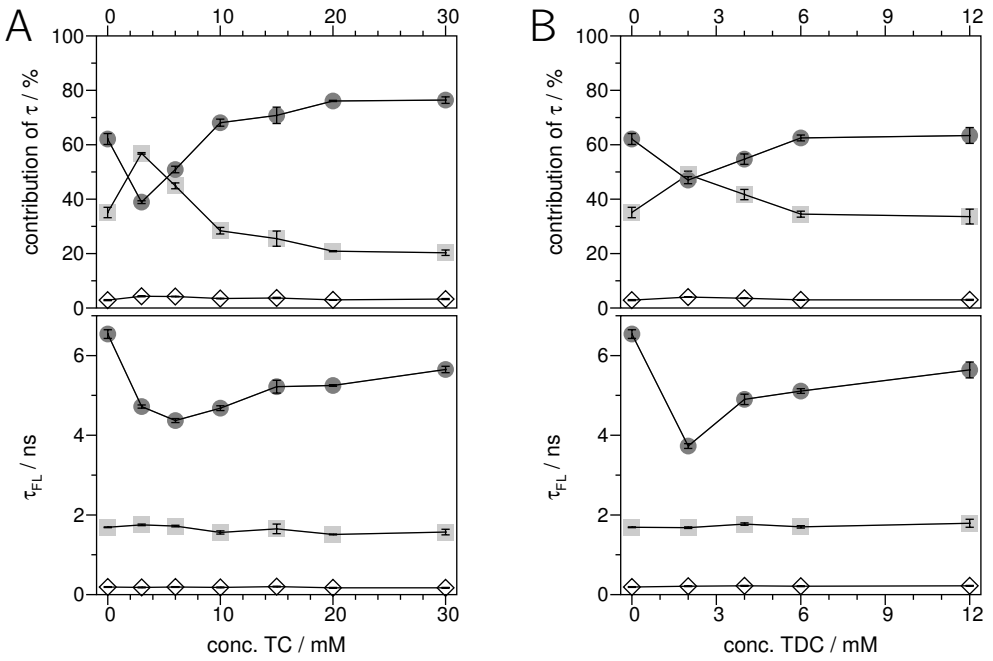

Figure 4.23: **Interaction of bile salts with UDC-NBD in LUVs.** UDC-NBD was added to 1 mol% into LUVs composed of EYPC. The bile salts TC (A), and TDC (B) were added from a stock solution stepwise. Fluorescence life times were fitted to bi- or triexponential model functions. The resulting fluorescence life times and the contribution of the corresponding species of fluorophores are shown (white diamond probably corresponding to complexed UDC-NBD, light grey squares representing monomeric analogues, and grey circles for analogue in bile salt complexes). Data represent mean±SEM, n≥3. Note the different scaling of the axes. See text for further explanation.

In figure 4.24 the fluorescence decay curves of diacyl C_6-NBD-PC in LUVs (A) and of UDC-NBD in SUVs (B) are shown in green. Both decay curves were fitted to biexponential functions (table 4.4).

When *N*-Rh-PE was incorporated into such liposomes in a concentration of 3 mol%, the fluorescence life time at the donor wavelength decreased strongly (figure 4.24, red lines). The decay curves of the vesicles containing both donor and acceptor lipid analogues were best fitted to triexponential functions (table 4.4).

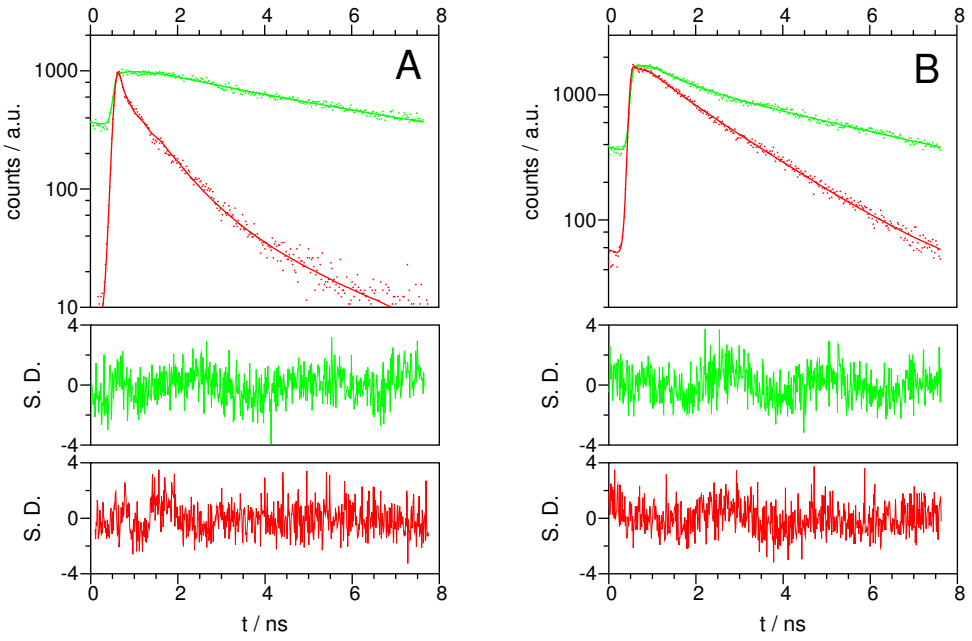

Figure 4.24: **FRET between NBD labelled lipid analogues and *N*-Rh-PE.** The fluorescence life times of the NBD group were measured by TCSPC after excitation with a pulsed Ar^+ laser (dots). Data points were fitted to a periodic bi- or triexponential model function (lines). The standard deviation of each point from the fitted function is given below. A: diacyl C_6-NBD-PC (1 mol%) in LUVs of EYPC in the absence (green) and presence (red) of 3 mol% *N*-Rh-PE in the same vesicle population. B: UDC-NBD (1 mol%) in SUVs of EYPC in the absence (green) and presence (red) of 3 mol% *N*-Rh-PE in the same vesicle population.

Table 4.4: **Fluorescence life times of NBD lipid analogues in liposomes in the presence and absence of *N*-Rh-PE.** Diacyl C_6-NBD-PC and UDC-NBD were incorporated to 1 mol% of total lipids into LUVs or SUVs, respectively. Fluorescence life times of the donor (λ_{em}=535 nm) were measured after excitation with a pulsed Ar^+ laser at 476 nm in the presence or absence of 3 mol% of the acceptor *N*-Rh-PE. Fluorescence life times (τ), contributions of the different life times (c) , and number of determinations (n) are indicated. Data are expressed as mean±SEM or as mean±deviation from mean in the case of two measurements.

	Donor			Donor+Acceptor		
Analogue	c / %	τ / ns	n	c / %	τ / ns	n
NBD-PC	94.7 ± 1.6	7.18 ± 0.07	4	32.5 ± 4.1	2.82 ± 0.18	2
	5.3 ± 1.6	1.46 ± 0.27		46.3 ± 5.1	0.66 ± 0.06	
				21.2 ± 1.0	0.10 ± 0.01	
UDC-NBD	89.0 ± 0.1	5.19 ± 0.01	3	91.0 ± 0.3	1.81 ± 0.01	3
	11.0 ± 0.1	0.73 ± 0.03		7.2 ± 0.3	0.50 ± 0.04	
				1.8 ± 0.1	0.04 ± 0.01	

5 Discussion

The present study was aimed at providing experimental evidence for mechanisms that explain the specificity in biliary lipid composition. The human derived hepatoma cell line HepG2 was used for functional studies *in vivo*. This well characterised cell line has the advantage that it is easy to handle and has an unlimited life time. Using two different fluorescent bile salt analogues the polarity of HepG2 cells and the functionality of their canalicular vacuoles was confirmed.

One essential result is the identification of an APLT activity in the canalicular membrane. This canalicular APLT was thought to be responsible for the absence of aminophospholipids from the bile for a long time. However, its activity was not proven *in vivo*. Characterising the canalicular APLT in HepG2 cells identified a mechanism that explains the almost complete absence of aminophospholipids from bile.

The involvement of MDR proteins in biliary lipid secretion was investigated employing MDR inhibitors. Especially MDR1 Pgp and MDR3 were characterised regarding their substrate specificity. One main conclusion from these experiments is that MDR proteins are not essential for the enrichment of short chain PL analogues in bile.

The interaction of PL analogues with bile salts was characterised using their fluorescence life times to access how the fluorescence life time of lipid analogues depends on their supramolecular organisation. The goal is to provide an approach which allows to determine the organisation of lipids in the BC *in vivo* by fluorescence life times of lipid analogues.

5.1 APLT Activity

The first part of this study addressed the underlying mechanism for the absence of aminophospholipids from bile. In particular, it was investigated whether the access of the aminophospholipids PS and PE to the lumen of the BC is prevented by an APLT activity in the CM by analysing the redistribution of various fluorescent analogues to the BC lumen. The main result is that aminophospholipid analogues which are not or only inefficiently transported by APLT are enriched in the BC. Analogues that represent suitable substrates of APLT are transported away from the lumen of BC, where they accumulate only when APLT activity is inhibited. It can be concluded that the CM harbours an APLT activity essential for preserving the specific phospholipid composition of the bile. This APLT activity is sufficient to explain the virtual absence of aminophospholipids from bile.

It may be asked whether the fluorescent analogues used are faithful reporters of natural PL movements because they may locally perturb the lipid bilayer (see section 1.5.2). The large differences in translocation between various lipid analogues demonstrate a selectivity to the head group/glycerol backbone and not the fluorescent NBD moiety. Indeed, the active transport of aminophospholipids in red cells first discovered using spin-labelled lipids [51] was confirmed with fluorescent probes [130] as used here, as well as with radiolabelled long-chain lipids [54]. Thus, the same conclusions could be drawn employing very different families of lipid probes. Therefore, one can be confident that in HepG2 cells studying PL translocation based on trafficking of fluorescent probes is a valid approach. This is also strongly supported by the fact, that labelling of BC by fluorescent diacyl PL analogues reflects the specific phospholipid composition of bile, while aminophospholipids are barely found, phosphatidylcholine is enriched in bile.

5.1.1 Mechanisms of Phospholipid Analogue Internalisation in HepG2 Cells

Since most of the fluorescent analogues used in this study have not been tested in HepG2 cells previously, they were first characterised regarding their internalisation from the exoplasmic leaflet to the cytoplasmic side on suspended cells. The inward movement of diacyl NBD-PS and of diacyl NBD-PE was much faster than that of diacyl NBD-PC which is consistent (i) with results of many studies on other mammalian cells (for review see [166]) and (ii) with the presence of an APLT activity in HepG2 cells [63].

The higher rate of diacyl PS internalisation with respect to PE is in agreement with a lower transport affinity of APLT for PE, in particular for diacyl NBD-PE [167, 136]. The rapid disappearance of the analogues originates neither from their hydrolysis (see section 4.5) nor from endocytic uptake since a rapid inward redistribution of the PS analogue was found even at 14 °C where endocytosis is reduced and transcytosis blocked [156, 157]. Furthermore, if endocytic activity was the main component of analogue uptake, one would not expect such great differences among the various analogues. Only after inhibition of APLT activity by suramin, endocytosis became relevant in the case of diacyl aminophospholipids at 37 °C as indicated by punctuate intracellular staining.

The inward redistribution of diacyl NBD-PS and -PE in HepG2 cells is not as fast as that of the respective spin-labelled analogues [63]. This has been also found for other mammalian cells [136, 168, 62, 66, 131]. Presumably, the bulky fluorescence moiety and its polarity reduces the affinity of NBD aminophospholipid analogues to APLT. However, this is of minor relevance as it was not the objective of this study to determine the absolute rates of PL transport across the membrane. The transport rate of endogenous PL might be different from that of any of the analogues. However, the relative rates of

PL analogue transport comparing PC to PE and PS analogues is very similar to that found for endogenous PL.

In comparison to the respective diacyl analogues, the internalisation of diether NBS-PS was significantly reduced. These data confirm previous studies on the PM of human fibroblasts and red blood cells showing a low transport activity of APLT for diether PS using NBD and spin labelled analogues [131]. They are also consistent with the fact that the glycerol backbone of PL affects the transport of lipids by APLT [50].

The uptake of diacyl NBD-PC and diether NBD-PC is similar. Apparently, the fraction of diacyl NBD-PC and diether NBD-PC on the exoplasmic leaflet decreased much slower in comparison to diacyl NBD-PS and -PE. Recently it was shown that diacyl NBD-PC is internalised in HepG2 cells at 37℃ by two routes, by endocytic uptake and by transbilayer movement facilitated by a yet unknown transporter [94]. Upon endocytosis diacyl NBD-PC was also transported into a recycling compartment containing transferrin [94]. Due to subsequent exposure of PC analogues to the PM, the fraction of analogues internalised at 37℃ is underestimated. Declining endocytosis by lowering the temperature, the amount of internalised PC analogues was reduced. However, in relation to red blood cells [62, 131] the uptake of the PC analogues was still enhanced and much faster than possible by passive diffusion alone. Indications for the existence of PC transporters in the PM of eukaryotic cells were already obtained from other cells. Experimental evidence for an ATP-dependent protein-mediated uptake of PC in polarised Va-2 cells [169] and MDCKII cells [170] was given. A screen for yeast mutants has recently led to the identification of Ros3p, an evolutionary conserved transmembrane protein whose removal caused a major reduction in the non-endocytic uptake of diacyl NBD-PC and -PE [75]. Remarkably, Ros3p is unrelated to any known ATPase and localises to multiple organelles, including the PM and ER.

Taken together, during this study a pattern of inward redistribution of

various NBD lipid analogues was found for the PM of HepG2 cells which is very similar to that of other mammalian cells. In particular a high affinity of APLT to diacyl NBD-PS, a slightly lower affinity to diacyl NBD-PE, and a very low affinity to diether NBD-PS was observed.

5.1.2 Presence of an APLT Activity in the CM

Having established this pattern of inward redistribution, the labelling of BC by fluorescence microscopy after incorporation of fluorescent analogues into the basolateral membranes of polarised HepG2 cells was analysed. Reorientation of fluorescent lipid analogues to the lumenal leaflet of the CM can be followed by the subsequent uptake of these analogues into the BC lumen [94]. A strong correlation between a low degree of BC labelling and APLT mediated internalisation of the analogue could be demonstrated (see table 5.1). Analogues that were not or only inefficiently transported by APLT such as the PC analogues and diether NBD-PS were rapidly enriched in the BC. Remarkably the labelling pattern for diacyl and diether NBD-PC was very similar. This was also confirmed by colocalisation experiments of diether NBD-PC with diacyl β-BODIPY-PC. The latter was shown to colocalise with diacyl NBD-PC in the BC [94]. Thus the transport and biliary enrichment of PC might be independent of the kind of linkage of the fatty acid chains. For the aminophospholipid analogues diacyl NBD-PS and -PE that were shown to be transported efficiently by an APLT activity in HepG2 cells (see above), only a low percentage of BC were enriched in the respective analogue (see table 5.1). Importantly, the diacyl PE analogue was less rigorously excluded from the BC. This can be explained by the lower affinity of APLT to PE (see section 1.2.2), which can also rationalise the small amount of PE found in bile [89] (see table 1.2). In contrast to diacyl PE which carried the label group on its fatty acid chain, head group labelled PE was highly enriched in the BC. This can be explained by the inability of the transporter to recognise analogues with modified head-groups.

The metabolic conversion of diacyl NBD-PS (table 4.1) cannot account for the low degree of BC labelling. Even after incubation for 30 min at 37 °C, about 70 % of internalised diacyl NBD-PS were not metabolised.

Table 5.1: **Qualitative correlation between inward movement of analogues at the basolateral membrane (BM) of suspended HepG2 cells and percentage of labelled BC in polarised HepG2 cells.** +++ high, ++ medium, + low. The inward movement of analogues is a combined process of APLT mediated transport and APLT independent (passive) transport. If low, it is probably independent of APLT activity, whereas if fast inward movement is detected APLT mediated movement accounts for most of it. The correlation between APLT mediated inward movement and absence of these analogues from the BC is evident. See text for further details.

analogue	inward movement at BM	number of labelled BC
diacyl NBD-PS	+++	+
diacyl NBD-PS + suramin	+	++
diacyl NBD-PE	++	++
diether NBD-PS	+	+++
diacyl NBD-PC	+	+++
diether NBD-PC	+	+++

Labelling of BC by diacyl NBD-PS increased upon treatment of cells with suramin, an inhibitor of APLT. Suramin did not influence the labelling pattern of PC analogues and their enrichment in BC indicating that the transport pathways of PC [94] are not affected by the inhibitor. These results strongly suggest that low labelling of BC by diacyl NBD-aminophospholipids is related to an APLT activity in the CM pumping aminophospholipids from the lumenal to the cytoplasmic leaflet, and that inhibition of this APLT activity, e.g. by suramin, leads to labelling of the BC by the analogues.

One may wonder whether the rapid inward movement of diacyl NBD-PS and -PE by an APLT activity on the basolateral membrane may specifically

prevent the access of the analogues to the BC. First of all, it should be emphasised that tight junctions prevent both lateral diffusion of analogues from the basolateral to the apical membrane on the exoplasmic leaflet and access of the analogues to the BC by aqueous space [94, 171, 172]. Thus, analogues have to be delivered to the BC via intracellular pathways, or at least by accessing the cytoplasmic leaflet of the plasma membrane. During this study bright diffuse intracellular staining for both diacyl NBD-PS and -PE, but no labelled endocytic vesicles were found. This shows that the major route of intracellular uptake of these analogues is the rapid transport from the exoplasmic to the cytoplasmic leaflet by APLT, while the endocytic pathway plays only a minor role if at all. Once on the inner leaflet of the PM, both analogues equilibrate rapidly with the cytoplasmic leaflet of subcellular membranes presumably by monomer diffusion [167]. Thus, these analogues have access to the canalicular/apical membrane by lateral diffusion in the cytoplasmic leaflet of the PM and/or by diffusion through the cytoplasm. The diffuse intracellular labelling observed in the case of diether NBD-PS suggests that this analogue may have access to the canalicular membrane in a similar manner.

It might be argued, that enrichment of diacyl aminophospholipid analogues in the BC upon treatment with suramin is related solely to an inhibition of APLT activity of the basolateral membrane but does not argue for an APLT activity of the CM. This concern is ruled out by the following observations. Firstly, when cells were treated with suramin after internalisation of diacyl NBD-PS or -PE, the original low labelling of BC changed to a bright labelling of BC indicating strongly that APLT activity of the CM was inhibited. Secondly, bright labelling of the BC by diacyl aminophospholipid analogues of suramin treated HepG2 cells was reversed upon removal of suramin suggesting that the restored APLT activity of the CM caused a redistribution of the analogues from the lumenal to the cytoplasmic leaflet of the CM. However, the process is slower in comparison to that found for APLT-mediated inward re-

distribution of diacyl aminophospholipid analogues in suspended HepG2 cells (compare figure 4.4 and figure 4.11). Several reasons may account for this: (i) A lower surface density of APLT in the canalicular membrane. (ii) The concentration of enriched analogues in the BC may cause saturation of APLT. (iii) Transport from the cytoplasmic to the lumenal side of the canalicular membrane counterbalancing APLT activity. (iv) The partition behaviour of the analogues between the lumen and the membrane of the BC may affect the kinetics of analogue depletion in the BC. (v) The recovery of full APLT activity after removing the inhibitor might slow down the transport of PS.

The clearance of BC labelling after removal of the inhibitor indicates that the solubilisation of PL from the CM by bile salts is a reversal process. Most likely PL of the exoplasmic leaflet of the CM and that solubilised in the BC are at equilibrium. This repartition of PL to the PM might be enhanced by the use of the short chain PL analogues.

Notably, the repartition of PC analogues, of diether NBD-PS and - in the presence of suramin - of diacyl NBD-aminophospholipids to the BC lumen is in agreement with previous observation that solubilisation of analogues by bile salts is independent of their head group [65, 66]. Thus, low labelling of the BC by diacyl aminophospholipid analogues in the absence of suramin cannot be explained by a failure of bile components to solubilise these analogues from the lumenal leaflet.

Direct evidence for an APLT activity in the apical membrane would require incorporation of phospholipid analogues directly into the BC and subsequent observation of their redistribution to the cytoplasmic side. While BC of fixed cells have been labelled by microinjection [173], labelling of BC of living HepG2 cells by this method was not successful despite strong efforts.

In conclusion, this study provides evidence for an APLT activity in the canalicular/apical membrane of polarised HepG2 cells. In the light of the finding, that solubilisation of PL from the membrane by bile salts is indepen-

dent of the PL head group, and thus, does not offer a mechanism to ensure the specific PL composition of bile fluid (see section 1.3.2), the presence of an APLT activity in the canalicular membrane may provide an alternative explanation for the absence of aminophospholipids from bile. This activity excludes aminophospholipids from the lumenal leaflet of the BC in a very efficient manner. Remarkably, this activity is even sufficient to prevent BC enrichment of diacyl NBD-PS which can be solubilised by bile salts much more efficiently than endogenous PS having two long fatty acid chains [65]. It remains to be established if APLT of the canalicular membrane is encoded by the *Fic1* gene as previously suggested [78] or if this P-type ATPase carries out other functions in the process of biliary lipid secretion. The physiological relevance of the absence of aminophospholipids from the bile remains unclear. It seems unlikely that partly substitution of the biliary PC by aminophospholipids causes such severe defects as found in patients with PFIC I. On the other hand, it was demonstrated that aminophospholipids incorporated into PC LUVs reduce the binding of bile salts to thess vesicles [174]. Thus, the asymmetric distribution of aminophospholipids in the CM might facilitate the secretion of PC by lightening the access of bile salts to this phospholipid.

5.2 Influence of ABC Proteins on Biliary PL Enrichment

Several ABC transporters are localised in the CM of hepatocytes [175] (see section 1.2.1). ABC transporters, e. g. MDR1 Pgp and MDR3 have been shown to transport PL including PC and PE as well as ether lipids [11, 176, 177]. Recently, it was shown that MDR1 Pgp is also able to transport diacyl NBD-PS and endogenous PS [14]. However, the transport activity of MDR1 Pgp was much lower in comparison to that of APLT.

To investigate the role of MDR proteins in biliary PL secretion two MDR inhibitors were applied. PSC 833 which is a specific inhibitor of MDR1 Pgp had no influence on the secretion of diether NBD-PC and reduced the secretion of diacyl NBD-PC slightly. Using the non-specific MDR inhibitor Verapamil, which was shown to block MDR1 Pgp and MDR3, a reduction of canalicular enrichment was found for both diacyl and diether NBD-PC in agreement with previous observations on diacyl NBD-PC [159]. Both inhibitors significantly reduced the secretion of diacyl NBD-PS which became even more evident after inhibition of APLT. However, no significant reduction of diether NBD-PS enrichment in the BC was found in the presence of Verapamil or PSC 833.

Addition of dithionite reduced the number of BC labelled with diacyl NBD-PC as well as with the diether NBD analogues significantly in the presence of Verapamil. This is in contrast to a recent report [159]. Using diacyl NBD-PC, in the presence of Verapamil a small reduction from about 65 % NBD positive BC in the absence of dithionite to about 40 % in the presence of dithionite was found which was not considered to be significant [159]. To test whether this reduction is significant or not would have required more experiments. The results presented here, clearly indicate also in the presence of Verapamil a significant reduction of the number of fluorescent BC when dithionite is added for each of the analogues that accumulate in the BC, similar to that found in the absence of inhibitors.

As the number of labelled BC was unchanged by PSC 833 for the diether PC analogue it is unlikely that MDR1 Pgp is involved in the translocation of this analogue. Verapamil had a small but significant effect on the number of BC labelled with diether NBD-PC indicating that probably MDR3 influences secretion of this analogue. Diacyl NBD-PC secretion was partly inhibited by both PSC 833 and Verapamil. However, the effects of the non-specific inhibitor Verapamil were higher than that of the MDR1 Pgp specific inhibitor PSC 833. Assuming that MDR1 Pgp is equally blocked by PSC 833 and Verapamil (as

shown by inhibiting the enrichment of Rho 123 in BC), the stronger inhibition in the case of Verapamil is due to inhibition of another protein, which is very likely MDR3. Thus, both MDR1 Pgp and MDR3 are probably involved in the transport of diacyl NBD-PC.

Both PSC 833 and Verapamil had about similar effects on the secretion of diacyl NBD-PS. Thus, it is likely that MDR1 Pgp is involved in the secretion of this analogue. However, this becomes only relevant when APLT is blocked. MDR1 Pgp mediated translocation of PS was recently reported in human gastric carcinoma cells, too [14]. None of the inhibitors had a significant influence on the secretion of diether NBD-PS.

The conclusions on the involvement of MDR proteins in the secretion of various lipid analogues into the BC are summarised in table 5.2. From the inhibition pattern of secretion of various analogues into the BC one can conclude that MDR1 Pgp is not markedly involved in secretion or transport of diether analogues. PC secretion is supported by MDR1 Pgp and another protein inhibited by Verapamil which probably represents MDR3. PS secretion is only influenced by MDR1 Pgp which is in agreement with previous studies [11]. However, each of the inhibitors had only a small effect on the secretion of PL analogues into BC.

Table 5.2: **Comparison of the involvement of MDR proteins in secretion of various PL analogues.** + influence on secretion, – no influence on secretion.

analogue	MDR1 Pgp	MDR3
diacyl NBD-PC	+	+
diether NBD-PC	–	+
diacyl NBD-PS	+	–
diether NBD-PS	–	–

The enrichment of PC in bile fluid was shown to be absolutely dependent on human MDR3 or murine mdr2 [20, 21] (see section 1.2.1). However, the

reduction of the number of BC that were labelled with diether or diacyl NBD-PC upon addition of Verapamil was low. Two reasons could account for this: Firstly, Verapamil might not efficiently block MDR3 and represent a better inhibitor for MDR1 Pgp than for MDR3. At least MDR1 Pgp was sufficiently blocked as tested by exclusion of Rho123 from the BC. Secondly, other (ATP independent) transporters might be essentially responsible for PC translocation across the canalicular membrane as suggested previously [97, 98, 99]. But if other proteins are essential for transport of PC to the lumenal side of BC, what could be the function of mdr2/MDR3 in specific lipid enrichment in bile? As mentioned before mdr2 deficiency leads to a complete absence of PL from bile in mice [20].

An alternative function of mdr2/MDR3 would be that the ABC transporter acts as a "liftase" rather than as a membrane transporter making PC accessible for solubilisation by canalicular bile salts. A similar function in exposing cholesterol was recently suggested for the ABC transporters ABCG5/ABCG8 [102] (see section 1.3.3). The activity as an ATP-dependent "liftase" would explain why the absence of mdr2/MDR3 has a dramatic effect on biliary enrichment of endogenous lipids but not on lipid analogues. The solubilisation of NBD-labelled PL by bile salts should be more efficient than that of endogenous lipids due to their lower hydrophobicity. A "liftase" activity might therefore be necessary to solubilise endogenous PL but not their NBD labelled analogues which were used here.

Previous studies identified MDR3 mediated transbilayer movement of lipid analogues in MDR3 transfected cells. It might be that mdr2/MDR3 possesses both a "liftase" and a flippase activity. When overexpressed the flippase activity might become relevant which may not be the case when other ATP independent transporters facilitate transbilayer movement with a faster kinetics, as it is probably the case in hepatocytes.

A MDR1 Pgp mediated transbilayer movement was reported for a variety

of lipid analogues including PS [11, 14]. MDR1 Pgp mediated flipping might be the reason for enrichment of PS in the BC after blocking APLT, as PS is generally found at the cytoplasmic leaflet of the PM. It can not be stated at this point whether MDR1 Pgp might act as a "liftase", too.

5.3 Interplay of APLT and MDR Transporters

An APLT mediated transport of diacyl NBD-PS and NBD-PE analogues from the lumenal to the cytoplasmic leaflet in HepG2 cells was demonstrated. On the other hand MDR1 Pgp is involved in the outward transport of diacyl aminophospholipids as shown for diacyl NBD-PS here. Thus, two ATP dependent transport proteins operate in opposite direction raising the question if APLT activity is sufficient to compensate for MDR1 Pgp mediated outward movement of PS. This problem shall be addressed by a quantitative consideration.

Evaluating the inward movement of PL analogues at the basolateral membrane (see section 4.2.1) of suspended cells, cells were labelled with about 300 pmole of diacyl analogue per million cells. Assuming that about 80 % of the analogue incorporated into the membrane during the labelling procedure cells were labelled with about 250 pmole of the respective analogue per one million of cells. As the PL contents of HepG2 cells is about 64 nmole per million cells [63], and the plasma membrane of hepatocytes resembles about 8 % of cellular membrane surface [178] the amount of internalised analogue corresponds to about 5 % of PM phospholipids. In the erythrocyte membrane APLT activity was shown to be saturated by such concentrations of PS analogues [49]. Assuming a similar saturation behaviour of APLT in HepG2 cells this would mean that the initial velocity of PS translocation corresponds to the maximum velocity of APLT mediated transport. However, APLT activity in HepG2 cells was found to be higher than in erythrocytes [63], so using the initial velocity of APLT mediated inward movement might somewhat underestimate the

maximum velocity of APLT mediated transport.

The initial velocity of translocation of various analogues was recalculated from the inward movement which was fitted to a monoexponential function. Knowing the amount of PL analogues in the PM the initial velocity of APLT mediated transport was estimated as 22 pmole per minute and million cells and 2.3 pmole per minute and million cells for diacyl NBD-PS and diacyl NBD-PE, respectively. This is in agreement with an about 10 fold lower affinity of the APLT for PE compared to PS [49]. After inhibition of the APLT with suramin the initial velocity of inward transport of diacyl NBD-PS decreased to about 3.6 pmole per minute and million cells. For comparison, the inward movement of diacyl NBD-PC was about 0.1 pmole per minute and million cells.

As discussed above (section 5.1) the inward movement of PS in the apical membrane after removal of the APLT inhibitor suramin was found to be somewhat lower than that in the basolateral membrane. However it was in the same order of magnitude and thus one can be confident that the data obtained at the basolateral membrane can also provide a good estimation of the APLT activity in the apical membrane.

The MDR3 mediated PC secretion in intact liver is about 50 pmole per minute and million cells (R. P. J. Oude Elferink, personal communication). Thus, the MDR3 mediated PC secretion is about 500 times higher than the spontaneous inward movement of PC.

The kinetics of MDR1 Pgp mediated transport was not thoroughly investigated in general and has not been studied at the apical membrane of HepG2 cells. Characterisation of MDR1 Pgp mediated transport of NBD labelled phospholipid analogues led to controversial results using different approaches. While during one study no MDR1 Pgp mediated translocations of diacyl NBD-PC could be detected [141], others find that MDR1 Pgp is as efficient as MDR3 in translocating diacyl NBD-PC [11]. According to the kinetics of outward movement of diacyl NBD-PS in a MDR1 Pgp overexpressing gastric

carcinoma cell line published recently [14] the initial velocity of MDR1 Pgp mediated movement is about 1.7 % of available lipid analogues per minute. Applying this kinetics to the HepG2 system described above would mean that the MDR1 Pgp mediated transport of diacyl NBD-PS is about 4 pmole per minute and million cells. Certainly, this can only be a rough estimation. Of course, the MDR1 Pgp mediated outward movement depends critically on the concentration of this protein in the membrane. It is, however, likely that the activity of MDR3 in lipid transport is higher than that of MDR1 Pgp as the latter is a very unspecific transporter which mainly serves in detoxification of the cell.

As has been pointed out recently [14], it is very likely that APLT transport efficiency is much higher than that of MDR1 Pgp at least for PS. Furthermore, it is not reasonable that two ATP consuming processes operate in opposite directions on the same substrate, thus MDR1 Pgp might mainly serve in drug elimination and lipid translocation may represent rather a side effect.

As APLT affinity for PE is lower than that for PS, MDR1 Pgp mediated transport may significantly account for its transbilayer distribution, and thus, higher exposure of PE to the lumenal side of the CM compared to PS. This might explain that PE is found to minor levels in bile [89]. It could also account for the higher amounts of diacyl NBD-PE compared to diacyl NBD-PS located in the BC of HepG2 cells described in this study. Also, the APLT inhibitor suramin lowered the initial velocity of diacyl NBD-PS transport to a level at which MDR1 Pgp mediated outward movement might show similar kinetics. In fact, inhibition of HepG2 cells with suramin led to an enrichment of diacyl NBD-PS in about 50 % of the BC compared to about 80–90 % labelled BC by analogues which are no substrates of APLT. This could be due to a compensation of APLT mediated inward movement, and MDR1 Pgp mediated outward movement if both transporters exhibit similar transport kinetics.

5.4 Enrichment of Sphingolipid Analogues in the BC

The exoplasmic leaflet of the PM is especially enriched in PC and sphingolipids (see section 1.2.2). However, PC contributes to about 95 % of biliary PL and only trace amounts of SM are found in bile. One hypothesis to explain this phenomenon is the preferential localisation of sphingolipids in detergent resistant rafts [6] which are not solubilised by lumenal bile salts and thus prevent a complete solubilisation of the apical membrane [110].

Confirming earlier studies [149, 94, 160] it could be demonstrated here that NBD-labelled (glycol)sphingolipids enrich in the BC of HepG2 cells. This is in contrast to the absence of sphingolipids from bile. Even at 4 °C, where vesicular trafficking is inhibited, NBD-labelled sphingolipids became enriched in the BC. Thus, NBD labelled sphingolipid analogues are able to reach the BC either by diffusion from the basolateral membrane on the cytoplasmic leaflet or by monomer exchange through the cytoplasm. This would, however, result in an enrichment of these analogues at the cytoplasmic leaflet of the CM preventing a secretion into the BC.

One can assume that NBD labelled sphingolipids do not represent endogenous SM properly as they might be excluded from sphingolipid-cholesterol rich rafts due to their lower hydrophobicity. This lower hydrophobicity could also facilitate a non-vesicular movement of these analogues to the BC which might not be the case for endogenous lipids.

A detergent soluble SM pool was identified at the cytoplasmic leaflet of the PM of mammalian cells [179, 180] which is most likely involved in signalling processes. NBD labelled sphingolipid analogues are more likely to behave like those signalling lipids due to their reduced hydrophobicity. Also the trace amounts of SM in the bile fluid which are mainly enriched in palmitic acid are more hydrophilic than the sphingolipids of the CM [181].

Sphingolipids carrying a NBD marker were shown to be transported by various ABC transporters [11, 182, 29]. Only NBD labelled sphingolipids but not radiolabelled short chain analogues were identified as substrates of MRP1 [29]. This again indicates that NBD analogues might not be suitable for representing the behaviour of endogenous sphingolipids.

Transport by MDR1 Pgp or MRP1 can explain the enrichment of NBD labelled lipid analogues in the lumen of the BC assuming an otherwise preferential cytoplasmic orientation of these analogues.

Taken together these data question the suitability of NBD labelled analogues to represent the behaviour of endogenous sphingolipids which are very hydrophobic and preferentially located in sphingolipid-cholesterol rafts. It is unlikely that endogenous sphingolipids are enriched in the BC like their NBD-labelled analogues. However, the absence of sphingolipids from bile could alternatively be explained by the presence of a canalicular sphingomyelinase which might rapidly degrade solubilised sphingolipids. Indeed, an alkaline sphingomyelinase was identified in human and guinea pig bile [183, 184], but was absent in bile of rat, pig, sheep, and cow [184]. The activity of this enzyme was shown to be dependent on bile salts [185]. However its function is the degradation of dietary sphingomyelin [184] rather then degradation of secreted sphingolipids from the canalicular membrane.

5.5 Fluorescence Life Times of Lipid Analogues

Fluorescence life times of lipid analogues were measured using TCSPC. As expected, the fluorescence decay of lipid analogues in organic solvents was monoexponential, as all fluorescent analogues experience the same physicochemical environment. Fluorescence decay curves of NBD labelled lipid analogues in aqueous solution were bi- or triexponential indicating that more than one species of analogues was present, differing in their molecular organisation.

In most cases a component with a short fluorescence life time of 0.05–0.3 ns appeared in addition to other life times. The contribution of this component was quite low, it never exceeded 10 % of the total fluorescence intensity of a sample. It could be excluded that this component was due to Rayleigh scattering of vesicles or to Raman scattering of water by measuring a solution of unlabelled vesicles or pure buffer. One can explain the short life time of diacyl C_6-NBD-PC as representing molecules that are organised at self-quenching conditions, i. e. micelles of the analogue [129, 161]. This conclusion is justified by the following observation: the contribution of the short time component to the total decay curves was lowest when diacyl C_6-NBD-PC was below its CMC (40 nanomolar) compared to measurements using diacyl C_6-NBD-PC well above its CMC (i. e. 1–10 micromolar). As the quantum yield of the self-quenched species of diacyl C_6-NBD-PC is very low, the contribution of this time to the decay curve is minimal. Nevertheless, it is likely that most of the molecules are organised into micelles in aqueous solution above the CMC of diacyl C_6-NBD-PC.

5.5.1 Incorporation of Lipid Analogues into Bile Salt Micelles

As discussed above, diacyl C_6-NBD-PC forms micelles in aqueous solution in which NBD fluorescence is self-quenched [129, 161]. Upon addition of bile salts the fluorescence intensity increased as mixed micelles between the analogues and bile salts were formed [66]. This is due to spatial separation of diacyl C_6-NBD-PC molecules by bile salts leading to a dequenching.

The fluorescence life time of diacyl C_6-NBD-PC monomers in aqueous solution was much shorter then in organic solvents or when incorporated into a membrane. This may be caused by the reduced hydrophobicity of the solvent as well as vibrational relaxation due to hydrogen bounding between the

fluorophore and the solvent [186]. The fluorescence life time of about 1 ns presented here is very similar to that of other NBD labelled PL analogues or fatty acids found in previous studies [187, 186].

When adding bile salts to a suspension of diacyl C_6-NBD-PC in aqueous solution a third fluorescence life time appeared which was longer than that of the analogue in aqueous solution. The fluorescence life time and the contribution of this third component to the total intensity increased with increasing bile salt concentration both reaching a maximum which seems to depend on bile salt hydrophobicity and CMC. The concentration dependency of this process was very similar to that found by a dequenching assay for TC, GC, and TDC [66].

As demonstrated before [66] the fluorescence intensity increased by adding bile salts to diacyl C_6-NBD-PC in aqueous solution due to dequenching. Also, the quantum yield of monomer diacyl C_6-NBD-PC in aqueous solution is lower than that of mixed micelles with bile salts or when incorporated into a membrane [187]. For this reason, the fraction of diacyl C_6-NBD-PC which is not incorporated into mixed micelles is underestimated by the evaluation procedure used here.

Also the fluorescence life time which corresponds to diacyl C_6-NBD-PC monomers (see above) not incorporated into mixed micelles increased slightly with increasing bile salt concentration. The reason for this behaviour might be a loose association of diacyl C_6-NBD-PC with bile salt molecules reducing the number of hydrogen bound to the solvent or increasing the solvent hydrophobicity.

Surprisingly, also addition of DHC, which is known as non-micelle forming bile salt [162], generated a species of diacyl C_6-NBD-PC analogues with a longer fluorescence life time. The contribution of this species to the total fluorescence intensity was lower than for the other investigated bile salt, however. Probably this bile salt is able to intercalate into micelles of diacyl C_6-NBD-PC

or form submicellar aggregates with the analogues [161], and thus stabilises the S_1-state of lipid analogues.

As demonstrated in table 4.3, the fluorescence life time is not solely dependent on the hydrophobicity of the utilised bile salt. More hydrophobic bile salts generally yield longer fluorescence life times. But probably also the size of the micelles influences the fluorescence life time of the incorporated lipid analogues. Primary bile salt micelles are formed by 2-9 molecules. The aggregation number is dependent on the chemical structure of the bile salt and is higher for TDC than for TC [188]. Secondary micelles are aggregates of primary bile salts and are only found for dihydroxy bile salts [162]. The concentration of bile salts, needed to reach highest life times and maximum contribution of the longer life time to the total intensity, is also dependent on the hydrophobicity of the bile salt and is strongly reduced for TDC and TLC compared to TC. This concentration might be near or above the CMC of the respective bile salt. However, different methods to measure the CMC of bile salts yield very different results (range of 0.5–20 mM) [188], therefore an exact value of the respective CMC is not available. Most investigation revealed a lower CMC for TDC compared to TC, however [188, 189].

Investigating the interaction of the fluorescent bile salt UDC-NBD with the bile salts TC and TDC resulted in a similar picture as found for diacyl C_6-NBD-PC. In aqueous solution UDC-NBD exhibits a fluorescence life time of about 2 ns. Also, a species with a shorter fluorescence life time was found which might correspond to aggregates of UDC-NBD. The CMC of endogenous UDC was determined to be in the range of 1–6 mM depending on the method used [190]. NBD labelled UDC might exhibit a lower CMC. Thus, one can not predict if the analogue in the concentration range used here (10–20 µM) forms micelles. However, also submicellar aggregates of bile salts have been reported [161], making an interaction between UDC-NBD analogues at this concentration reasonable. Self-quenching of UDC-NBD is much lower as found for diacyl

C_6-NBD-PC as judged by the quantum yield of the substances (not shown). Adding endogenous bile salts to this solution results in an additional fluorescent species with a longer fluorescence life time which probably corresponds to mixed micelles between UDC-NBD and TC or TDC.

The fluorescence decay curve of the bile salt CGamF which is labelled with fluorescein was monoexponential with a live time of about 4 ns. Adding TC to this solution only slightly increased the fluorescence life time of CGamF which was still fitted by a single exponential function to a value very close to that of CGamF in ethanol. The effects of bile salts on the fluorescein labelled phospholipid *N*-Fl-PE were also less pronounced than on diacyl C_6-NBD-PC. These data indicate that the fluorescein fluorophore is less sensitive to environmental changes probably due to the lack of hydrogen bounds between the fluorophore and the solvent.

5.5.2 Release of Lipid Analogues from LUVs by Bile Salts

Incorporating diacyl C_6-NBD-PC into LUVs of different composition yielded three different life times of the fluorophore, which derive from different species of diacyl C_6-NBD-PC. Two species exhibited a life time of about 0.1–0.3 ns and 1 ns as was already found for the analogue in aqueous solution. These life times represent analogues organised as self-quenched micelles or monomeric diacyl C_6-NBD-PC, respectively. The third fluorescence life time which contributed to most of the total intensity originates from diacyl C_6-NBD-PC incorporated into the membrane and was dependent on the lipid composition of the LUVs. For LUVs composed of the relatively hydrophilic POPC this live time was about 5.9 ns, when LUVs where made of EYPC the life time increased to 7.2 ns. Diacyl C_6-NBD-PC in LUVs composed of EYSM/cholesterol displayed a life time which was even longer than that of the analogue in chloroform indicating that this vesicular environment is very hydrophobic and rigid. The fluorescence life time of diacyl C_6-NBD-PC in LUVs of EYPC was again similar to that

found for a head group labelled NBD-PL analogue in EYPC liposomes in a previous study [187]. This is consistent with the localisation of the NBD moiety of diacyl C_6-NBD-PC close to the membrane surface [191]. A dependency of the fluorescence life time of NBD labelled PL on the molar concentration of the analogues in vesicles was found before [187], which is probably due to quenching. At the concentration used here (analogue concentration 1 mol% of endogenous lipids), the fluorescence life time of the analogue was almost at maximum [187].

When UDC-NBD was incorporated into LUVs of EYPC, the fluorescence decay curve of this solution indicated the presence of two or three species with different supramolecular organisation, too. Concluding from the behaviour of UDC-NBD in aqueous solution, the first species with a live time of about 1.7 ns should represent UDC-NBD not associated with vesicle. In some cases also a very short life time of 0.2–0.5 ns was found probably representing UDC-NBD aggregates. The part of analogue that was incorporated into LUVs displayed a fluorescence life time of about 6.5 ns. The contribution of this longer life time to the total fluorescence intensity was only 65 % compared to about 80–90 % when diacyl C_6-NBD-PC was incorporated into LUVs. These differences most likely represent the different partitions of the analogues between the aqueous phase and the membrane.

Addition of bile salts to the liposomes containing NBD labelled lipid analogues resulted in a decrease of the longer fluorescence life time at low concentrations of the bile salt. At higher bile salt concentrations the fluorescence life time increased again to reach a value which was similar to that of mixed bile salt analogue micelles at the same bile salt concentration (see above). The contribution of the longer life time decreased upon addition of bile salts. In EYPC-LUVs containing UDC-NBD incubated with TC the contribution of the longer life time decreased dramatically upon addition of low amounts of bile salt and increased again at higher concentrations. This effect was also found

for diacyl C_6-NBD-PC in LUVs composed of EYSM/cholesterol upon addition of both TC or TDC, although less pronounced. A possible explanation of this phenomenon might be that low bile salt concentrations loosen the membrane integrity and thus lower the thermodynamical barrier for exchange of the analogues to the aqueous phase [192]. This might force a higher percentage of the relatively hydrophilic analogues into the aqueous phase. At increasing bile salt concentrations the vesicles might become completely solubilised and the diacyl C_6-NBD-PC molecules are integrated into mixed micelles as discussed above. Remarkably, at high bile salt concentrations the fluorescence life times, and their contributions to total fluorescence intensity are very similar for samples originally containing the lipid analogues (diacyl C_6-NBD-PC or UDC-NBD) in LUVs or in aqueous solution. The final organisation of analogues that were incorporated into LUVs after addition of large amounts of bile salts seems to be similar to that of analogues with bile salts in aqueous solution. These findings indicates that LUVs become completely solubilised at high bile salt concentrations or that the lipid analogue is completely extracted from the vesicle. As bile salt concentration in the BC is high [193] it is likely that lipids in the BC are organised into an environment that is mainly determined by bile salts, i. e. mixed micelles of bile salts with PL.

The shorter live time of the analogues corresponding to the non-membrane bound species was constant upon addition of bile salts in the case of UDC-NBD and increased slightly for diacyl C_6-NBD-PC probably due to a loose association of this analogue with bile salt micelles (see above).

Surprisingly, the bile salts TC and TDC had similar or even higher effects on the solubilisation of diacyl C_6-NBD-PC from LUVs composed of EYSM/cholesterol compared to LUVs of POPC. One would expect a rapid solubilisation of POPC LUVs, as they have a similar composition as biliary PL. The composition of liposomes from EYSM/cholesterol should, however, rather represent the behaviour of detergent resistant rafts. This controversy might be explained by

the fact that the high affinity of cholesterol to SM is lost in the presence of bile salts [194], allowing a cholesterol secretion into bile. Diacyl C_6-NBD-PC might alternatively be easily extracted from EYSM/cholesterol LUVs leaving the liposome intact. It shall be emphasised that by the technique of fluorescence life time analysis one can only receive clear predictions for the environment of the investigated fluorescent molecule, which was in any case a short chain phosphatidylcholine analogue. Solubilisation of short chain lipid analogues from a membrane is much easier than that of endogenous lipids due to the lower hydrophobicity of the analogue. Statements about the membrane of endogenous lipids from which the analogue is solubilised can only be assumptions.

The data presented here also point out the limits of the fluorescence life time technique in investigating organisation of lipid analogues. As the fluorescence life time of diacyl C_6-NBD-PC in TC micelles and in LUVs of POPC is very similar, one would not be able to discriminate these species *in vivo*. On the other hand biliary PC does not solely comprise POPC and different bile salts exist in the BC. It is thus likely that one can distinguish between vesicles and micelles in the BC. However, for proper interpretation of future *in vivo* experiments probably more cuvette experiments are necessary using bile salt and PL mixtures.

5.5.3 Characterisation of FRET between NBD and Rhodamine

Fluorescence resonance energy transfer between the NBD-fluorophore attached to lipids and *N*-Rh-PE was characterised by the decrease of the fluorescence life time of the donor. To ensure that FRET pairs were in close neighbourhood both lipid analogues were incorporated into liposomes composed of EYPC. In the absence of the acceptor two distinct fluorescence life times of the donor were identified corresponding to free and membrane bound analogues (see above).

In the presence of the acceptor the fluorescence decay at the donor wavelength became triexponential. The distribution of the life times in the presence of the acceptor indicates that also the analogue species with the shorter life time, i. e. the analogues in aqueous dispersion were able to perform FRET indicating that they are somehow associated with the membrane, too.

The FRET efficiency and thus the lowering of the fluorescence life time of the donor is dependent on the distance between donor and acceptor. The distances between the various FRET-pairs are distributed statistically. A tri-exponential model functions can therefore only estimate for the mean distances between FRET pairs and will not fit the experimental data appropriate. The distance between donor and acceptor in the liposomal system investigated here is estimated to about 3 nm assuming an area of 96 $Å^2$ per PL molecule and 3 % acceptor concentration. This distance is well below the Förster radius as the donor fluorescence life time decreases by a factor greater than two.

5.6 Conclusions

The specificity of biliary PL composition is strikingly in that mainly PC, carrying palmitic acid in *sn1*-position and oleic, linoleic, or arachidic acid in *sn2*-position [88], is found in bile. This study revealed physiological mechanisms that are responsible for this specificity (summarised in figure 5.1). It could be demonstrated that an APLT activity in the CM of hepatocytes is responsible for the almost complete absence of aminophospholipids from bile.

The involvement of the ABC transporters MDR1 Pgp and MDR3 in biliary phospholipid secretion was studied applying different MDR inhibitors. The data presented here question the previously reported function of mdr2/MDR3 as a lipid flippase [141, 20]. It seems more likely that the MDR proteins function as a “liftase” making endogenous PC accessible for secretion by bile salts that act as detergents.

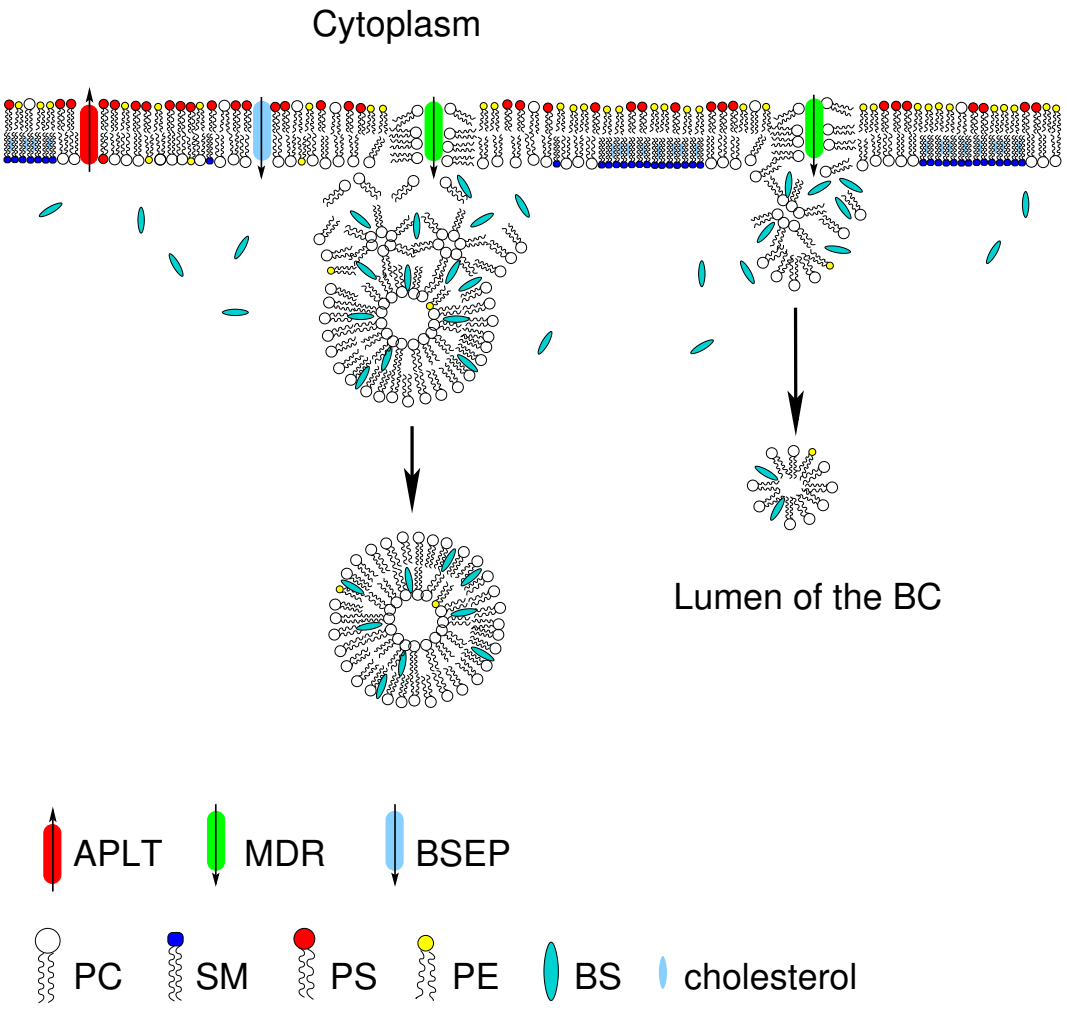

Figure 5.1: **Mechanisms of to achieve biliary lipid specificity.** A canalicular APLT is pumping aminophospholipids PS and PE to the cytoplasmic leaflet of the CM preventing their solubilisation by lumenal bile salts. MDR proteins (especially mdr2/MDR3) make PC accessible to solubilisation by bile salts. The physico-chemical way of biliary lipid secretion (i. e. vesicular or micellar) is not yet understood. This thesis introduces a method to investigate molecular mechanisms of biliary secretion by the use of the fluorescence life times of lipid analogues. Applying this method on a microscopic level to hepatocytes with BC enriched in fluorescent lipid analogues could reveal underlying physico-chemical processes.

Enrichment of NBD-labelled (glyco)sphingolipids could be demonstrated in the BC of HepG2 cells. Aware of the absence of sphingolipids from bile, the suitability of NBD-labelled sphingolipid analogues is questioned especially as they turn out to be more hydrophilic then the endogenous sphingolipids. The strong hydrophobicity of the latter is the reason for their preferential localisation in detergent insoluble rafts [6].

Although the identification of lipid transport processes across the CM reveals mechanisms for specific enrichment of lipids in bile, they are not able to address the supramolecular organisation of lipids in the BC. For this reason, the interaction of bile salts with lipid analogues has been studied by their fluorescence life times. These investigations on lipid analogues in a panel of model environments provide the basis for future studies in an *in vivo* system. Investigating fluorescence life times of lipid analogues enriched in the BC on a microscopic scale will reveal the molecular organisation of lipids in the early canalicular bile fluid. To interpret future data from an *in vivo* system, knowledge about the behaviour of lipid analogues in certain model system, as presented here, is crucial. For this reason FRET-pairs were characterised in this study, too. Measuring FRET between different lipid analogues *in vivo* allows to predict about distances between the analogues.

Previous investigations on the mechanism of biliary PL secretion were mainly performed using rats or mice. The hydrophobicity of their bile salts is much lower than that of humans. Furthermore the cholesterol content of human bile is much higher than that of rodents (see table 1.1) [85]. It is thus risky to conclude from the results obtained with animal material on the behaviour of human cells, as has been done sometimes. Therefore, when concluding about mechanisms of lipid secretion one has to be careful about the investigated system. The use of the fluorescence life time techniques might provide a method for investigating different model systems (as human and animal cell lines) and compare them.

5.7 Future Prospects

This study provided evidence that an APLT located in the apical membrane of hepatocytes is sufficient to prevent the enrichment of aminophospholipids in bile by maintaining membrane asymmetry. It remains to be established how PC is specifically extracted from the exoplasmic leaflet of the BC from a mixture of PL that comprise mainly PC and sphingolipids.

The role of sphingolipids and their preferential localisation in detergent resistant rafts has been discussed in section 5.4. As NBD labelled SM enriches in the BC of HepG2 cells one could prove a possible canalicular sphingomyelinase applying fluorescence life time studies on NBD-SM and its degradation products. Measurement of the fluorescence life time of NBD-SM analogues and its degradation products *in vitro* and comparison with the fluorescence life time of NBD-SM labelled BC *in vivo* would then reveal if this analogue is degraded.

The role of the Fic1 protein which was supposed to represent the canalicular APLT remains to be established. The expression of Fic1 in HepG2 cells could be blocked using iRNA. Investigations whether this blocking shows similar effects on the accumulation of aminophospholipid analogues in the BC as described for suramin in this thesis would clarify the role of Fic1 in aminophospholipid translocation.

The fluorescence life time measurements of lipid analogues in different environments provide a basis for *in vivo* measurements of fluorescence life times of lipid analogues in the BC. Comparing the fluorescence life time of fluorescent bile salts and PLs measured on the microscopic level in the BC with that of the same analogues in model systems as used here, the physico-chemical environment of lipids in the BC can be evaluated. Furthermore, FRET between different PL analogues or bile salt and PL analogues in the BC can be utilised to analyse which lipids are in close neighbourhood in the BC.

The measurement of fluorescence anisotropy of lipid analogues in different

environments (i. e. micelles and vesicles) in cuvette experiments and its comparison to the anisotropy of the same analogue in the BC would provide an even better tool to elucidate the canalicular lipid organisation. So far, fluorescence anisotropy was not applied to the investigate lipid analogues because of their photo instability. A setup which allows quasi simultaneous recording of both polarisation states (parallel and perpendicular to excitation) of the fluorescence light could overcome this problem. This setup is presently in preparation.

The role of cholesterol in the physico-chemical composition of the canalicular lipids should be further investigated. The fluorescent cholesterol analogue DHE is a widely used cholesterol analogue as its structure is very similar to that of endogenous cholesterol. The only modifications to cholesterol are three additional double bounds making it fluorescent, and a methyl group. This natural yeast sterol is very similar to cholesterol regarding its physico-chemical behaviour in model membranes [195, 196, 197]. Even though differences between cholesterol and DHE in the ability to be extracted by cyclodextrins were reported [198], DHE remains one of the best fluorescent cholesterol analogues as it does not carry a bulky reporter group. The accumulation of DHE in the BC of HepG2 cells has already been investigated [101]. FRET between DHE and PL carrying a dansyl group has been reported [199, 200] and might be used to measure interaction of DHE with PL in the BC. It has to be elucidated whether DHE is able to perform FRET with other fluorescent lipid analogues. Furthermore measurements of the fluorescence life time of DHE in cuvette experiments (as performed for other fluorescent lipid analogues during this study) and *in vivo* could enable a description the complex interplay of different lipids in bile. It is evident that this interplay of lipids is altered in hepatobiliary disease like gallstone formation [201, 202, 203]. With the measurement of fluorescence life time of lipid analogues *in vivo* and its comparison to that of the well defined system *in vitro*, a method to elucidate the changes in bile

composition in affected individuals can be established. The knowledge of the changes in the mechanism of biliary lipid secretion in healthy and unhealthy individuals might lead to a therapy of hepatobiliary diseases.

References

[1] Rehner, G. & Daniel, H. (2001). *Biochemie der Ernährung*, chap. 9. Spektrum Akademischer Verlag, Heidelberg, Berlin.

[2] Alberts, B., Bray, D., Lewis, J., Raff, M., Roberts, K., & Watson, J. D. (1994). *Molecular biology of the cell*, chap. 22, 1147–1149. 3rd edn. Garland Publishing, Inc. New York & London.

[3] Kahle, W., Leonhardt, H., & Platzer, W. (1986). *Taschenatlas der Anatomie. Band 2: Innere Organe*, vol. 2, 234–235. 5th edn. Georg Thieme Verlag Stuttgart, New York.

[4] Welsch, U. (ed.) (2002). *Sobotta Atlas Histologie*, 152–156. 6th edn. Urban & Fischer, München, Jena.

[5] Schiebler, T. H. (1996). *Histologie*, chap. 21, 531–546. 4th edn. Springer-Verlag Berlin, Heidelberg, New York.

[6] Simons, K. & Ikonen, E. (1997). Functional rafts in cell membranes. *Nature* 387:569–572.

[7] Sprong, H., van der Sluijs, P., & van Meer, G. (2001). How proteins move lipids and lipids move proteins. *Nature reviews/Molecular cell biology* 2:504–513.

[8] Raggers, R. J., Pomorski, T., Holthuis, J. C. M., Kälin, N., & van Meer, G. (2000). Lipid Traffic: The ABC of transbilayer movement. *Traffic* 1:226–234.

[9] Klein, I., Sarkadi, B., & Varadi, A. (1999). An inventory of the human ABC proteins. *Biochim. Biophys. Acta* 1461:237–262.

[10] Bosch, I. & Croop, J. (1996). P-glycoprotein multidrug resistance and cancer. *Biochim. Biophys. Acta* 1288:F37–F54.

[11] van Helvoort, A., Smith, A. J., Sprong, H., Fritzsche, I., Schinkel, A. H., Borst, P., & van Meer, G. (1996). MDR1 P-glycoprotein is a lipid translocase of broad specifity, while MDR3 P-glycoprotein specifically translocates phosphatidylcholine. *Cell* 87:507–517.

[12] Bosch, I., Dunussi-Joannopouluo, K., Wu, R., & Furlong, J., S.and Croop (1997). Phosphatidylcholine and phosphatidylethanolamine behave as substrates of the human MDR1 P-glycoprotein. *Biochemistry* 36:5685–5694.

[13] Abulrob, A. G. & Gumbleton, M. (1999). Transport of phosphatidylcholine in MDR3-negative epithelial cell lines via drug-induced MDR1 P-glycoprotein. *Biochem. Biophys. Res. Comm.* 262:121–126.

[14] Pohl, A., Lage, H., Müller, P., Pomorski, T., & Herrmann, A. (2002). Transport of phosphatidylserine via MDR1 (multidrug resistance 1) P-glycoprotein in a human gastric carcinoma cell line. *Biochem. J.* 365:259–268.

[15] Garrigues, A., Escargueil, A. E., & Orlowski, S. (2002). The multidrug transporter, P-glycoprotein, actively mediates cholesterol redistribution in the cell membrane. *Proc. Natl. Acad. Sci. USA* 99:10347–10352.

[16] Meijer, D. K. F., Smit, J. W., & Müller, M. (1997). Hepatobiliary elimination of cationic drugs: the role of P-glycoproteins and other ATP-dependent transporters. *Adv. Drug Deliv. Rev.* 25:159–200.

[17] Luker, G. D., Pica, C. M., Kumar, A. S., Covey, D. F., & Piwnica-Worms, D. (2000). Effects of cholesterol and enantiomeric cholesterol on P-glycoprotein localization and function in low-density membrane domains. *Biochemistry* 39:7651–7661.

[18] Smith, A. J., Timmermans-Hereijegers, J. L., Roelofsen, B., Wirtz, K. W., van Blitterswijk, W. J., Smit, J. J. M., Schinkel, A. H., & Borst, P. (1994). The human MDR3 P-glycoprotein promotes translocation of phosphatidylcholine through the plasma membrane of fibroblasts from transgenic mice. *FEBS Lett.* 354:263–266.

[19] de Vree, J. M., Jacquemin, E., Sturm, E., Cresteil, D., Bosma, P. J., Aten, J., Deleuze, J.-F., Desrochers, M., Burdelski, M., Bernard, O., Oude Elferink, R. P. J., & Hadchouel, M. (1998). Mutations in the MDR3 gene cause progressive familial intrahepatic cholestasis. *Proc. Natl. Acad. Sci. USA* 95:282–287.

[20] Smit, J. J. M., Schinkel, A. H., Oude Elferink, R. P. J., Groen, A. K., Wagenaar, E., van Deemter, L., Mol, C. A. A. M., Ottenhoff, R., van der Lugt, N. M. T., van Roon, M. A., van der Valk, M. A., Offerhaus, G. J. A., Berns, A. J. M., & Borst, P. (1993). Homozygous disruption of the murine mdr2 P-glycoprotein gene leads to a complete absence of phospholipid from bile and to liver disease. *Cell* 75:451–462.

[21] Oude Elferink, R. P. J., Tytgat, G. N. J., & Groen, A. K. (1997). The role of mdr2 P-glycoprotein in hepatobiliary lipid transport. *FASEB J.* 11:19–28.

[22] Deleuze, J. F., Jacquemin, E., Dubuisson, C., Cresteil, D., Dumont, M., Erlinger, S., Bernard, O., & Hadchouel, M. (1996). Defect of multidrug-resistance 3 gene expression in a subtype of progressive familial intrahepatic cholestasis. *Hepatology* 23:904–908.

[23] Gerloff, T., Stieger, B., Hagenbuch, B., Madon, J., Landmann, L., Roth, J., Hofmann, A. F., & Meier, P. J. (1998). The sister of P-glycoprotein represents the canalicular bile salt export pump of mammalian liver. *J. Biol. Chem.* 273:10046–10050.

[24] Kullak-Ublick, G.-A., Stieger, B., Hagenbuch, B., & Meier, P. J. (2000). Hepatic transport of bile salts. *Sem. Liv. Disease* 20:273–291.

[25] Kullak-Ublick, G.-A. & Meier, P. J. (2000). Mechanisms of cholestasis. *Pathophysiol. Liv. Disease* 4:357–385.

[26] Keppler, D. & König, J. (1997). Expression and localization of the conjugate export pump encoded by the *MRP2* (*cMRP/cMOAT*) gene in liver. *FASEB J.* 11:509–516.

[27] Kool, M., van der Linden, M., den Haas, M., Baas, F., & Borst, P. (1999). Expression of human MRP6, a homologue of the multidrug resistance protein gene MRP1, in tissues and cancer cells. *Cancer Research* 59:175–182.

[28] Keppler, D., Leier, I., & Jedlitschky, G. (1997). Transport of glutathione conjugates and glucuronides by the multidrug resistance protein MRP1 and MRP2. *Biol. Chem.* 378:787–791.

[29] Raggers, R. J., van Helvoort, A., Evers, R., & van Meer, G. (1999). The human multidrug resistance protein MRP1 translocates sphingolipid analogs across the plasma membrane. *J. Cell Sci.* 112:415–422.

[30] Kamp, D. & Haest, C. W. M. (1998). Evidence for a role of the multidrug resistance protein (MRP) in the outward translocation of NBD-phospholipids in the erythrocyte membrane. *Biochim. Biophys. Acta* 1372:91–101.

[31] Dekkers, D. W. C., Comfurius, P., Schroit, A. J., Bevers, E. M., & Zwaal, R. F. A. (1998). Transbilayer movement of NBD-labeled phospholipids in red blood cell membranes: outward-directed transport by the multidrug resistance protein 1 (MRP1). *Biochemistry* 37:14833–14837.

[32] Roelofsen, H., Vos, T. A., Schippers, I. J., Kuipers, F., Koning, H., Moshage, H., Jansen, P. L. M., & Müller, M. (1997). Increased levels of the multidrug resistance protein in lateral membranes of proliferating hepatocyte-derived cells. *Gastroenterology* 112:511–521.

[33] König, J., Nies, A. T., Cui, Y., Leier, I., & Keppler, D. (1999). Conjugate export pumps of the multidrug resistance protein (MRP) family: localization, substrate specificity, and MRP2-mediated drug resistance. *Biochim. Biophys. Acta* 1461:377–394.

[34] Müller, M. & Jansen, P. L. M. (1998). The secretory function of the liver: new aspects of hepatobilary transport. *J. Hepatology* 28:344–354.

[35] Madon, J., Eckhardt, U., Gerloff, T., Stieger, B., & Meier, P. J. (1997). Functional expression of the rat liver canalicular isoform of the multidrug resistance-associated protein. *FEBS Lett.* 406:75–78.

[36] Akita, H., Suzuki, H., Ito, K., Kinoshita, S., Sato, N., Takikawa, H., & Sugiyama, Y. (2001). Characterization of bile acid transport mediated by multidrug resistance associated protein 2 and bile salt export pump. *Biochim. Biophys. Acta* 1511:7–16.

[37] König, J., Rost, D., Cui, Y., & Keppler, D. (1999). Characterization of the human multidrug resistance protein isoform MRP3 localized to the basolateral hepatocyte membrane. *Hepatology* 29:1156–1163.

[38] Hirohashi, T., Suzuki, H., Takikawa, H., & Sugiyama, Y. (2000). ATP-dependent transport of bile salts by rat multidrug resistance-associated protein 3 (Mrp3). *J. Biol. Chem.* 275:2905–2910.

[39] Bergen, A. A. B., Plomp, A. S., Schuurman, E., Terry, S., Breuning, M., Dauwerse, H., Swart, J., Kool, M., van Soest, S., Baas, F., ten Brink, J. B., & de Jong, P. T. V. M. (2000). Mutations in ABCC6 cause pseudoxanthoma elasticum. *Nat. genetics* 25:228–231.

[40] Madon, J., Hagenbuch, B., Landmann, L., Meier, P. J., & Stieger, B. (2000). Transport function and hepatocellular localization of mrp6 in rat liver. *Mol. Pharmacol.* 57:634–641.

[41] Wang, J., Near, S., Young, K., Connelly, P. W., & Hegele, R. A. (2001). ABCC6 gene polymorphism associated with variation in plasma lipoproteins. *J. Hum. Genet.* 46:699–705.

[42] Klucken, J., Büchler, C., Orsó, E., Kaminski, W. E., Porsch-Özcürümez, M., Liebisch, G., Kapinsky, W., M.and Diederich, Drobnik, W., Dean, M., Allikmets, R., & Schmitz, G. (2000). ABCG1 (ABC8), the human homolog of the *Drosophila white* gene, is a regulator of macrophage cholesterol and phospholipid transport. *Proc. Natl. Acad. Sci. USA* 97:817–822.

[43] Schmitz, G., Langmann, T., & Heimerl, S. (2001). Role of ABCG1 and other ABCG family members in lipid metabolism. *J. Lipid Res.* 42:1513–1520.

[44] Yu, L., Hammer, R. E., Li-Hawkins, J., von Bergmann, K., Lutjohann, D., Cohen, J. C., & Hobbs, H. H. (2002). Disruption of Abcg5 and Abcg8 in mice reveals their crucial role in biliary cholesterol secretion. *Proc. Natl. Acad. Sci. USA* 99:16237–16242.

[45] Malicpaard, M., Scheffer, G. L., Fancyte, I. F., van Gastelen, M. A., Pijnenborg, C. L. M., Schinkel, A. H., van de Vijver, M. J., Scheper, R. J., & Schellens, J. H. M. (2001). Subcellular localization and distribution of the breast cancer resistance protein transporter in normal human tissues. *Canc. Res.* 61:3458–3464.

[46] Janvilisri, T., Venter, H., Shahi, S., Reuter, G., Balakrishnan, L., & van Veen, H. W. (2003). Sterol transport by the human breast cancer resistance protein (ABCG2) expressed in *Lactococcus lactis*. *J. Biol. Chem.* 278(23):20645-51:20645–20651.

[47] Zachowski, A. (1993). Phospholipids in animal eukaryotic membranes: transverse asymmetry and movement. *Biochem. J.* 294:1–14.

[48] Beleznay, Z., Zachowski, A., Devaux, P. F., Puente Navazo, M., & Ott, P. (1993). ATP-dependent aminophospholipid translocation in erythrocyte vesicles: stoichiometry of transport. *Biochemistry* 32:3146–3152.

[49] Zachowski, A., Favre, E., Paraf, A., & Devaux, P. F. (1986). Outside-inside translocation of aminophospholipids in the human erythrocyte membrane is mediated by a specific enzyme. *Biochemistry* 25:2585–2590.

[50] Morrot, G., Hervé, P., Zachowski, A., Fellmann, P., & Devaux, P. F. (1989). Aminophospholipid translocase of human erythrocytes: Phospholipid substrate specificity and effect of cholesterol. *Biochemistry* 28:3456–3462.

[51] Seigneuret, M. & Devaux, P. F. (1984). ATP-dependent asymmetric distribution of spin-labeled phospholipids in the erythrocyte membrane: Relation to shape changes. *Proc. Natl. Acad. Sci. USA* 81:3751–3755.

[52] Seigneuret, M., Zachowski, A., Herrmann, A., & Devaux, P. F. (1984). Asymmetric lipid fluidity in human erythrocyte membrane: New spin-label evidence. *Biochemistry* 23:4271–4275.

[53] Daleke, D. L. & Huestis, W. H. (1985). Incorporation and translocation of aminophospholipids in human erythrocytes. *Biochemistry* 24:5406–5416.

[54] Tilley, L., Cribier, S., Roelofsen, B., Op den Kamp, J. A. F., & van Deenen, L. L. M. (1986). ATP-dependent translocation of amino phospholipids across the human erythrocyte membrane. *FEBS Lett.* 194:21–27.

[55] Martin, O. C. & Pagano, R. E. (1987). Transbilayer movement of fluorescent analogs of phosphatidylserine and phosphatidylethanolamine at the plasma membrane of cultured cells. Evidence for a protein-mediated and ATP-dependent process(es). *J. Biol. Chem.* 262:5890–5898.

[56] Sune, A., Bette-Bobillo, P., Bienvenüe, A., Fellmann, P., & Devaux, P. F. (1987). Selective outside-inside translocation of aminophospholipids in human platelets. *Biochemistry* 26:2972–2978.

[57] Zachowski, A., Herrmann, A., Paraf, A., & Devaux, P. F. (1987). Phospholipid outside-inside translocation in lymphocyte plasma membranes is a protein mediated phenomenon. *Biochim. Biophys. Acta* 897:197–200.

[58] Zachowski, A. & Gaudry-Talarmain, Y. M. (1990). Phospholipid transverse diffusion in synaptosomes: evidence for the involvement of the aminophospholipid translocase. *J. Neurochem.* 55:1352–1356.

[59] Comfurius, P., Senden, J. M., Tilly, R. H., Schroit, A. J., Bevers, E. M., & Zwaal, R. F. (1990). Loss of membrane phospholipid asymmetry in platelets and red cells may be associated with calcium-induced shedding of plasma membrane and inhibition of phospholipid translocase. *Biochim. Biophys. Acta* 1026:153–160.

[60] Chahine, J. M. E. H., Cribier, S., & Devaux, P. F. (1993). Phospholipid transmembane domains and lateral diffusion in fibroblasts. *Proc. Natl. Acad. Sci. USA* 90:447–451.

[61] Tilly, R. H., Senden, J. M., Comfurius, P., Bevers, E. M., & Zwaal, R. F. (1990). Increased aminophospholipid translocase activity in human platelets during secretion. *Biochim. Biophys. Acta* 1029:188–190.

[62] Pomorski, T., Müller, P., Zimmermann, B., Burger, K., Devaux, P. F., & Herrmann, A. (1996). Transbilayer movement of fluorescent and spin-labeled phospholipids in the plasma membrane of human fibroblasts: A quantitative approach. *J. Cell Sci.* 109:687–698.

[63] Müller, P., Pomorski, T., Porwoli, S., Tauber, R., & Herrmann, A. (1996). Transverse movement of spin-labeled phospholipids in the plasma membrane of a hepatocytic cell line (HepG2): implications for biliary lipid secretion. *Hepatology* 24:1497–1503.

[64] Buton, X., Hervé, P., Kubelt, J., Tannert, A., Burger, C. N. J., Fellmann, P., Müller, P., Herrmann, A., Seigneuret, M., & Devaux, P. F. (2002). Transbilayer movement of monohexosyl sphingolipids in endoplasmic reticulum and Golgi membranes. *Biochemistry* 41:13106–13115.

[65] Wüstner, D., Pomorski, T., Herrmann, A., & Müller, P. (1998). Release of phospholipids from erythrocyte membranes by taurocholate is determined by their transbilayer orientation and hydrophobic backbone. *Biochemistry* 37:17093–17103.

[66] Wüstner, D., Herrmann, A., & Müller, P. (2000). Head group-independent interaction of phospholipids with bile salts: a fluorescence and EPR study. *J. Lipid. Res.* 41:1–10.

[67] Beleznay, Z., Zachowski, A., Devaux, P. F., & Ott, P. (1997). Characterization of the correlation between ATP-dependent aminophospholipid translocation an Mg^{2+}-ATPase activity in red blood cell membranes. *Eur. J. Biochem.* 243:58–65.

[68] Tang, X., Halleck, M. S., Schlegel, R. A., & Williamson, P. (1996). A subfamily of P-type ATPases with aminophospholipid transporting activity. *Science* 272:1495–1497.

[69] Gomès, E., Jakobsen, M. K., Axelsen, K. B., Geisler, M., & Palmgren, M. G. (2000). Chilling tolerance in Arabidopsis involves ALA1, a member of a new family of putative aminophospholipid translocases. *Plant Cell* 12:2441–2454.

[70] Siegmund, A., Grant, A., Angeletti, C., Malone, L., Nichols, J. W., & Rudolph, H. K. (1998). Loss of Drs2p does not abolish NBD-labeles phospholipid transfer across the plasma membrane of *Saccharomyces cerevisiae*. *J. Biol. Chem.* 273:34399–34405.

[71] Marx, U., Polakowski, T., Pomorski, T., Lang, C., Nelson, H., Nelson, N., & Herrmann, A. (1999). Rapid transbilayer movement of fluorescent phospholipid analogues in the plama membrane of endocytosis-deficient yeast cells does not require the Drs2 protein. *Europ. J. Biochem.* 263:254–263.

[72] Chen, C. Y., Ingram, M. F., Rosal, P. H., & Graham, T. R. (1999). Role of Drs2p, a P-type ATPase and potential aminophospholipid translocase, in yeast late Golgi function. *J. Cell Biol.* 147:1223–1236.

[73] Pomorski, T., Lombardi, R., Riezman, H., Devaux, P. F., van Meer, G., & Holthuis, J. C. M. (2003). Drs2p-related P-type ATPases Dnf1p and Dnf2p are required for phospholipid translocation across the yeast plasma membrane and serve a role in endocytosis. *Mol. Biol. Cell* 14:1240–1254.

[74] Grant, A. M., Hanson, P. K., Malone, L., & Nichols, J. W. (2001). NBD-labeled phosphatidylcholine and phosphatidylethanolamine are internalized by transbilayer transport across the yeast plasma membrane. *Traffic* 2:37–50.

[75] Kato, U., Emoto, K., Frederiksson, C., Nakamura, H., Ohta, A., Kobayashi, T., Murakami-Murofushi, K., Kobayashi, T., & Umeda, M. (2002). A novel membrane protein, Ros3p, is required for phospholipid translocation across the plasma membrane in *Saccharomyces cerevisiae*. *J. Biol. Chem.* 277:37855–37862.

[76] Bull, L. N., van Eijk, M. J. T., Pawlikowa, L., DeYoung, J. A., Juijn, J. A., Liao, M., Klomp, L. W. J., Lomri, N., Berger, R., Scharschmidt, B. F., Knisely, A. S., Houwen, R. H. J., & Freimer, N. B. (1998). A gene encoding a P-type ATPase mutated in two forms of hereditary cholestasis. *Nature genetics* 18:219–224.

[77] Eppens, E. F., van Mil, S. W. C., de Vree, J. M. L., Mok, K. S., Juijn, J. A., Oude Elferink, R. P. J., Berger, R., Houwen, R. H. J., & Klomp, L. W. J. (2001). FIC1, the protein affected in two forms of hereditary cholestasis, is localized in the cholangiocyte and the canalicular membrane of the hepatocyte. *J. Hepatol.* 35:436–443.

[78] Ujhazy, P., Oritz, D., Misra, S., Li, S., Moseley, Jones, H., & Arias, I. M. (2001). Familial intrahepatic cholestasis 1: studies of localization and function. *Hepatology* 34:768–775.

[79] Jacquemin, E., Dumont, M., Bernard, O., Erlinger, S., & Hadchouel, M. (1994). Evidence for defective primary bile acid secretion in children with progressive familial intrahepatic cholestasis (Byler disease). *Eur. J Pediatr.* 153:424–428.

[80] Oude Elferink, R. & Groen, A. K. (2002). Genetic defects in hepatobilary transport. *Biochim. Biophys. Acta* 1586:129–145.

[81] Stieger, B. (2001). FIC1: another bile salt carrier within enterohepatic circulation? *J. Hepatol.* 35:522–524.

[82] Abe, T., Kakyo, M., Tokui, T., Najagomi, R., Nishio, T., Nakai, D., Nomura, H., Unno, M., Suzuki, M., Naitoh, T., Matsuno, S., & Yawo, H. (1999). Identification of a novel gene family encoding human liver-specific organic anion transporter LST-1. *J. Biol. Chem.* 274:17159–17163.

[83] Kullak-Ublick, G.-A., Beuers, U., & Paumgartner, G. (2000). Hepatobilary transport. *J. Hepatol.* 32:3–18.

[84] Heuman, D. M. (1989). Quantitative estimation of the hydrophillic-hydrophobic balance of mixed bile salt solutions. *J. Lipid Res.* 30:719–730.

[85] Kuipers, F., Oude Elferink, R. P. J., Verkade, H. J., & Groen, A. K. (1997). Mechanisms of (patho)physiological significance of biliary cholesterol secretion. *Subcellular Biochemistry* 28:295–318.

[86] Thompson, M. B. (1996). Bile acids in the assessment of hepatocellular function. *Toxicologic Pathology* 24:62–71.

[87] Meier, P. J. (1995). Molecular mechanisms of hepatic bile salt transport from sinusoidal blood into bile. *Am. J. Physiol.* 269:G801–G812.

[88] Crawford, J. M. (1996). Intracellular traffic and plasma membrane secretion of small organic solutes involved in hepatocellular bile formation. *Comp. Biochem. Physiol.* 115B:341–354.

[89] Rigotti, A., Marzolo, M. P., & Nervi, F. (1994). Lipid transport from hepatocyte into the bile. *Current Topics in Membranes* 40:579–615.

[90] Robins, S. J. & Brunengraber, H. (1982). Origin of bilary cholesterol and lecithin in the rat: contribution of new synthesis and preformed hepatic stores. *J. Lipid Res.* 23:604–608.

[91] Chanussot, F., Lafont, H., Hauton, J., Tuchweber, B., & Yousef, I. (1990). Studies on the origin of biliary phospholipid. *Biochem. J.* 270:691–695.

[92] Portal, I., Clerc, T., Sbarra, V., Portugal, H., Pauli, A.-M., Lafont, H., Tuchweber, B., Yousef, I., & Chanussot, F. (1993). Importance of high-density lipoprotein-phosphatidylcholine in secretion of phospholipid and cholesterol in bile. *Am J. Physiol.* 264:G1052–G1056.

[93] Patton, G. M., Fasulo, J. M., & Robins, S. J. (1994). Evidence that hepatic triglycerides provide acylglycerides for synthesis of bile phosphatidylcholines. *Am. J. Physiol.* 267:G1028–G1034.

[94] Wüstner, D., Mukherjee, S., Maxfield, F. R., Müller, P., & Herrmann, A. (2001). Vesicular and nonvesicular transport of phosphatidylcholine in polarized HepG2 cells. *Traffic* 2:277–296.

[95] Cohen, D. E., Leonard, M. R., & Carey, M. C. (1994). In vitro evidence that phospholipid secretion into bile may be coordinated intracellularly by the combined actions of bile salts and the specific phosphatidylcholine transfer protein of liver. *Biochemistry* 33:9975–9980.

[96] van Helvoort, A., de Brouwer, A., Ottenhoff, R., Brouwers, J. F. H. M., Wijnholds, J., Beijnen, J. H., Rijnveld, A., van der Poll, T., van der Valk, M., Majoor, D., Voorhout, W., Wirtz, K. W. A., Oude Elferink, R. P. J., & Borst, P. (1999). Mice without phosphatidylcholine transfer

protein have no defects in the secretion of phosphatidylcholine into bile or into lung airspaces. *Proc. Natl. Acad. Sci. USA* 96:11501–11506.

[97] Berr, F., Meier, P. J., & Stieger, B. (1993). Evidence for the presence of a phosphatidylcholine translocator in isolated rat liver canalicular membrane vesicles. *J. Biol. Chem.* 268:3976–3979.

[98] Kullak-Ublick, G.-A., Gerloff, T., Hagenbuch, B., Berr, F., Meier, P. J., & Stieger, B. (1996). Expression of a rat liver phosphatidylcholine translocator in *Xenopus laevis* oocytes. *Hepatology* 23:1254–1259.

[99] Fuchs, M., Carey, M. C., & Cohen, D. E. (1997). Evidence for an ATP-independent long-chain phosphatidylcholine translocator in hepatocyte membranes. *Am. J. Physiol.* 273:G1312–G1319.

[100] Robins, S. J., Fasulo, J. M., Collins, M. A., & Patton, G. M. (1985). Evidence for separate pathways for transport of newly synthesized and preformed cholesterol into bile. *J. Biol. Chem.* 260:6511–6513.

[101] Wüstner, D., Herrmann, A., Hao, M., & Maxfield, F. R. (2002). Rapid nonvesicular transport of sterols between the plasma membrane domains of polarized hepatic cells. *J. Biol. Chem.* 277:30325–30336.

[102] Small, D. M. (2003). Role of ABC transporters in secretion of cholesterol from liver into bile. *Proc. Natl. Acad. Sci. USA* 100:4–6.

[103] Bell, R. M., Ballas, L. M., & Coleman, R. A. (1981). Lipid topogenesis. *J. Lipid Res.* 22:391–403.

[104] Jeckel, D., Karrenbauer, A., Birk, R., Schmidt, R. R., & Wieland, F. (1990). Sphingomyelin is synthesized in the cis Golgi. *FEBS Lett.* 261:155–157.

[105] Jeckel, D., Karrenbauer, A., Burger, K. N. J., van Meer, G., & Wieland, F. (1992). Glucosylceramide is synthesized at the cytosolic surface of various Golgi subfractions. *J. Cell Biol.* 117:259–267.

[106] Hoekstra, D. & Kok, J. W. (1992). Trafficking of glycosphingolipids in eukaryotic cells; sorting and recycling of lipids. *Biochim. Biophys. Acta* 1113:277–294.

[107] Futerman, A. H. & Pagano, R. E. (1991). Determination of the intracellular sites and topology of glucosylceramide synthesis in rat liver. *Biochem. J.* 280:295–302.

[108] Lannert, H., Bünning, C., Jeckel, D., & Wieland, F. T. (1994). Lactosylceramide is synthesized in the lumen of the Golgi apparatus. *FEBS Lett.* 342:91–96.

[109] Burger, K. N., van der Bijl, P., & van Meer, G. (1996). Topology of sphingolipid galactosyltransferases in ER and Golgi: transbilayer movement of monohexosyl sphingolipids is required for higher glycosphingolipid biosynthesis. *J. Cell Biol.* 133:15–28.

[110] Zegers, M. M. P. & Hoekstra, D. (1998). Mechanisms and functional features of polarized membrane traffic in epithelial and hepatic cells. *Biochem. J.* 336:257–269.

[111] Bishop, W. R. & Bell, R. M. (1985). Assembly of the endoplasmic reticulum phospholipid bilayer: the phosphatidylcholine transporter. *Cell* 42:51–60.

[112] Buton, X., Morrot, G., Fellmann, P., & Seigneuret, M. (1996). Ultrafast glycerophospholipid-selective transbilayer motion mediated by a protein in the endoplasmic reticulum membrane. *J. Biol. Chem.* 271:6651–6657.

[113] Marx, U., Lassmann, G., Holzhütter, H.-G., Wüstner, D., Müller, P., Höhlig, A., Kubelt, J., & Herrmann, A. (2000). Rapid flip-flop of phospholipids in endoplasmic reticulum membranes studied by a stopped-flow approach. *Biophysical J.* 78:2628–2640.

[114] Kobayashi, T., Pimplikar, S. W., Parton, R. G., Bhaki, S., & Simons, K. (1992). Sphingolipid transport from trans-Golgi network to the apical surface in permeabilized MDCK cells. *FEBS Lett.* 300:227–231.

[115] Ruetz, S. & Gros, P. (1995). Enhancement of Mdr2-mediated phosphatidylcholine translocation by the bile salt taurocholate. *J. Biol. Chem.* 270:25388–25395.

[116] Cohen, D. E., Angelico, M., & Carey, M. C. (1989). Quasielastic light scattering evidence for vesicular secretion of biliary lipids. *Am. J. Physiol.* 257:G1–G8.

[117] Crawford, J. M., Möckel, G.-M., Crawford, A. R., Hagen, S. J., Hatch, V. C., Barnes, S., Godleski, J. J., & Carey, M. C. (1995). Imaging biliary lipid secretion in the rat: ultrastructural evidence for vesiculation of the hepatocyte canalicular membrane. *J. Lipid Res.* 36:2147–2163.

[118] Verkade, H. J., de Bruijn, M. A. C., Brink, M. A., Talsma, H., Vonk, R. J., Kuipers, F., & Groen, A. K. (1996). Interactions between organic anions, micelles and vesicles in model bile systems. *Biochem. J.* 320:917–924.

[119] Eckhardt, E. R. M., Moschetta, A., Renooij, W., Goerdayal, S. S., van Berge-Henegouwen, G. P., & van Erpecum, K. J. (1999). Asymmetric distribution of phosphatidylcholine and sphingomyelin between micellar

and vesicular phases: potential implications for canalicular bile formation. *J. Lipid Res.* 40:2022–2033.

[120] Verkade, H. J., Vonk, R. J., & Kuipers, F. (1995). New insights into the mechanism of bile acid-induced bilary lipid secretion. *Hepatology* 21:1174–1189.

[121] Gilat, T. & Sömjen, G. J. (1996). Phospholipid vesicles and other carriers in bile. *Biochim. Biophys. Acta* 1286:95–115.

[122] Coleman, R. & Roma, M. G. (2000). Hepatocyte couplets. *Biochemical Society Transactions* 28:136–140. Review.

[123] Aden, D. P., Fogel, A., Plotkin, S., Damjanov, I., & Knowles, B. B. (1979). Controlled synthesis of HBsAG in a differentiated human liver carcinoma-derived cell line. *Nature* 282:615–616.

[124] Sormunen, R., Eskelinen, S., & Lehto, V. P. (1993). Bile canaliculus formation in cultured HEPG2 cells. *Lab. Invest.* 68:652–662.

[125] Zegers, M. M. P. & Hoekstra, D. (1997). Sphingolipid transport to the apical plasma membrane domain in human hepatoma cells is controlled by PKC and PKA activity: a correlation with cell polarity in HepG2 Cells. *J. Cell Biol.* 138:307–321.

[126] Lian, W.-N., Tsai, J.-W., Yu, P.-M., Wu, T.-W., Yank, S.-C., Chau, Y.-P., & Lin, C. (1999). Targeting of aminopeptidase N to bile canaliculi correlates with secretory activities of the developing canalicular domain. *Hepatology* 30:748–760.

[127] Cooper, A. D., Craig, W. Y., Tangiguchi, T., & Everson, G. T. (1994). Characteristics and regulation of bile salt synthesis and secretion by human hepatoma HepG2 cells. *Hepatology* 20:1522–1531.

[128] Javitt, N. B. (1990). Hep G2 cells as a resource for metabolic studies: lipoprotein, cholesterol, and bile acids. *FASEB J.* 4:161–168.

[129] Chattopadhyay, A. (1990). Chemistry and biology of *N*-(7-nitrobenz-2-oxa-1,3-diazol-4-yl)-labeled lipids: fluorescent probes of biological and model membranes. *Chem. Phys. Lipids* 53:1–15.

[130] Connor, J. & Schroit, A. J. (1987). Determination of lipid asymmetry in human red cells by resonance energy transfer. *Biochemistry* 26:5099–5105.

[131] Fellmann, P., Hervé, P., Pomorski, T., Müller, P., Geldwerth, D., Herrmann, A., & Devaux, P. F. (2000). Transmembrane movement of diether phospholipids in human erythrocytes and human fibroblasts. *Biochemistry* 39:4994–5003.

[132] Holzinger, F., Schteingardt, C. D., Ton-Nu, H.-T., Eming, S. A., Monte, M. J., Hagay, L. E., & Hofmann, A. F. (1997). Fluorescent bile acid derivatives: relationship between chemical structure and hepatic and intestinal transport in the rat. *Hepatology* 26:1263–1271.

[133] Birch, D. J. S. & Imhof, R. E. (1991). Time-domain fluorescence spectroscopy using time-correlated single-photon counting. In *Topics in Fluorescence Spectroscopy* (edited by J. R. Lackowitz), vol. 1: Techniques, chap. 1, 1–95. Plenum Press, New York and London.

[134] Stubbs, C. D. & Williams, B. W. (1992). Fluorescence in membranes. In *Topics in Fluorescence Spectroscopy* (edited by J. R. Lackowitz), vol. 3: Biochemical Applications, chap. 5, 231–271. Plenum Press, New York and London.

[135] Mukherjee, S., Soe, T. T., & Maxfield, F. R. (1999). Endocytic sorting of lipid analogues differing solely in the chemistry of their hydrophobic tails. *J. Cell Biol.* 144:1271–1284.

[136] Colleau, M., Herve, P., Fellmann, P., & Devaux, P. F. (1991). Transmembrane diffusion of fluorescent phospholipids in human erythrocytes. *Chem. Phys. Lipids* 57:29–37.

[137] Tsuruo, T., Iida, H., Tsukagoshi, S., & Sakurai, Y. (1981). Overcoming of vincristine resistance in P388 leukemia in vivo and in vitro through enhanced cytotoxicity of vincristine and vinblastine by verapamil. *Cancer Res.* 41:1967–1972.

[138] Yusa, K. & Tsuro, T. (1989). Reversal mechanism of multidrug resistance by verapamil: direct binding of verapamil to P-glycoprotein on specific sites and transport of verapamil outward across the plasma membrane of K562/ADM cells. *Cancer Res.* 49:5002–5006.

[139] Ford, J. M. & Hait, W. N. (1990). Pharmacology of drugs that alter multidrug resistance in cancer. *Pharmacol. Rev.* 42:155–199.

[140] Piwnica-Worms, D., Rao, V. V., Kronauge, J. F., & M., C. J. (1995). Characterization of multidrug resistance P-glycoprotein transport function with an organotechnetium cation. *Biochmistry* 34:12210–12220.

[141] Ruetz, S. & Gros, P. (1994). Phosphatidylcholine translocase: a physiological role for the mdr2 gene. *Cell* 77:1071–1081.

[142] Kwon, Y., Kamath, A. V., & Morris, M. E. (1996). Inhibitors of P-glycoprotein-mediated daunomycin transport in rat liver canalicular membrane vesicles. *J. Pharmac. Sci.* 85:935–939.

[143] Boesch, D., Gaveériaux, C., Jachez, B., Portier-Manzanedo, A., Bollinger, P., & Loor, F. (1991). In vivo circumvention of P-glycoprotein-mediated multidrug resistance of tumor cells with SDZ PSC 833. *Cancer Res.* 51:4226–4233.

[144] Mayer, U., Wagenaar, E., Dorobek, B., Beijnen, J. H., Borst, P., & Schinkel, A. H. (1997). Full blockade of intestinal P-glycoprotein and extensive inhibition of blood-brain barrier P-glycoprotein by oral treatment of mice with PSC833. *J. Clin. Invest.* 100:2430–2436.

[145] van der Pol, M. A., Pater, J. M., Feller, N., Westra, A. H., van Stijn, A., Ossenkoppele, G. J., Broxterman, H. J., & Schuurhuis, G. J. (2001). Functional characterization of minimal residual disease for P-glycoprotein and multidrug resistance protein activity in acute myeloid leukemia. *Leukemia* 15:1554–1563.

[146] Neyfakh, A. A. (1988). Use of fluorescent dyes as molecular probes for the study of multidrug resistance. *Exp. Cell Res.* 174:168–176.

[147] Efferth, T., Löhrke, H., & Volm, M. (1989). Reciprocal correlation between expression of P-glycoprotein and accumulation of rhodamine 123 in human tumors. *Anticancer Res.* 9:1633–1638.

[148] McIntyre, J. C. & Sleight, R. G. (1991). Fluorescence assay for phospholipid membrane asymmetry. *Biochemistry* 30:11819–11827.

[149] van IJzendoorn, S. C. D., Zegers, M. M. P., Kok, J. W., & Hoekstra, D. (1997). Segregation of glucosylceramide and sphingomyelin occurs in the apical to basolateral transcytotic route in HepG2 cells. *J. Cell Biol.* 137:347–357.

[150] Bligh, E. G. & Dyer, W. J. (1959). A rapid method of total lipid extraction and purification. *Can. J. Biochem. Physiol.* 37:911–917.

[151] Röder, B. (1999). *Einführung in die molekulare Photobiophysik*, chap. 2, 58–62. Teubner.

[152] Spencer, R. D. & Weber, G. (1970). Influence of Brownian rotation and energy transfer upon the measurements of fluorescence life time. *J. Chem. Phys.* 52:1654–1663.

[153] Nelder, J. A. & Mead, R. (1965). A simplex method for function minimization. *Computer Journal* 7:308–315.

[154] Kullak-Ublick, G. A., Beuers, U., & Paumgartner, G. (1996). Molecular and functional characterization of bile acid transport in human hepatoblastoma HepG2 cells. *Hepatology* 23:1053–1060.

[155] Connor, J., Pak, C., Zwaal, R. F. A., & Schroit, A. J. (1992). Bidirectional transbilayer movement of phospholipid analogs in human red blood cells - evidence for an ATP-dependent and protein-mediated process. *J. Biol. Chem.* 267:19412–19417.

[156] van Meer, G., Stelzer, E. H., Wijnaends-van Resandt, R. W., & Simons, K. (1987). Sorting of sphingolipids in epithelial (Madin-Darby canine kidney) cells. *J. Cell Biol.* 105:1623–1635.

[157] Oka, J. A. & Weigel, P. H. (1989). The pathways for fluid phase and receptor mediated endocytosis in rat hepatocytes are different but thermodynamically equivalent. *Biochem. Biophys. Res. Comm.* 159:488–494.

[158] Sleight, R. G. & Pagano, R. E. (1984). Transport of a fluorescent phosphatidylcholine analog from the plasma membrane to the Golgi apparatus. *J. Cell Biol.* 99:742–751.

[159] Wüstner, D. (2000). Investigation of the mechanism of the specific phospholipid enrichment in the bile. Ph.D. thesis, Institut für Biologie, Humboldt-Universität zu Berlin, Germany.

[160] Maier, O. & Hoekstra, D. (2003). Trans-Golgi network and subapical compartment of HepG2 cells display different properties in sorting and exiting of sphingolipids. *J. Biol. Chem.* 278:164–173.

[161] Shoemaker, D. G. & Nichols, J. W. (1990). Hydrophobic interaction of lysophospholipids and bile salts at submicellar concentrations. *Biochemistry* 29:5837–5842.

[162] Small, D. M. (1968). The size and structure of bile salt micelles. *Advances Chem.* 84:31–52.

[163] Struck, D. K., Hoekstra, D., & Pagano, R. E. (1981). Use of resonance energy transfer to monitor membrane fusion. *Biochemistry* 20:4093–4099.

[164] Nichols, J. W. & Pagano, R. E. (1982). Use of resonance energy transfer to study the kinetics of amphiphile transfer between vesicles. *Biochemistry* 21:1720–1726.

[165] Förster, T. (1948). Zwischenmolekulare Energieumwanderung und Fluoreszenz. *Annalen der Physik* 6:55–75.

[166] Daleke, D. L. & Lyles, J. V. (2000). Identification and purification of aminophospholipid flippases. *Biochim. Biophys. Acta* 1486:108–127.

[167] Devaux, P. F., Fellmann, P., & Hervé, P. (2002). Investigation on lipid asymmetry using lipid probes. Comparision between spin-labeled lipids and fluorescent lipids. *Chem. Phys. Lip* 116:115–134.

[168] Müller, K., Pomorski, T., Müller, P., Zachwoski, A., & Herrmann, A. (1994). Protein-dependent translocation of aminophospholipids and asymmetric transbilayer distribution of phospholipids in the plasma membrane of ram sperm cells. *Biochemistry* 33:9968–9974.

[169] Sleight, R. G. & Abanto, M. N. (1989). Differences in intracellular transport of a fluorescent phosphatidylcholine analog in established cell lines. *J. Cell Sci.* 93:363–374.

[170] Pomorski, T., Herrmann, A., Müller, P., van G., Meer, & Burger, K. (1999). Protein-mediated inward translocation of phospholipids occurs in both the apical and basolateral membrane domains of epithelial cells. *Biochemistry* 38:142–150.

[171] Dragsten, P. R., Handler, J. S., & Blumenthal, R. (1982). Fluorescent membrane probes and the mechanism of maintenance of cellular asymmetry in epithelia. *Federation Proceedings* 41:48–53.

[172] van Meer, G. & Simons, K. (1986). The function of tight junctions in maintaining differences in lipid composition between the apical and the basolateral cell surface domains of MDCK cells. *EMBO J.* 5:1455–1464.

[173] Ihrke, G., Martin, G. V., Shanks, M. R., Schrader, M., Schroer, T. A., & Hubbard, A. L. (1998). Apical plasma membrane proteins and endolyn-78 travel through a subapical compartment in polarized WIF-B hepatocytes. *J. Cell Biol.* 141:115–133.

[174] Schubert, R. & Schmidt, K.-H. (1988). Structural changes in vesicle membranes and mixed micelles of various lipid compositions after binding of different bile salts. *Biochemistry* 27:8787–8794.

[175] Smit, J. J. M., Schinkel, A. H., Mol, C. A. A. M., Majoor, D., Mooi, W. J., Jongsma, A. P. M., Lincke, C. R., & Borst, P. (1994). Tissue distribution of the human MDR3 P-glycoprotein. *Lab. Invest.* 71:638–649.

[176] Kipp, H. & Arias, I. M. (2002). Trafficking of canalicular ABC transporters in hepatocytes. *Annu. Rev. Physiol.* 64:595–608.

[177] Ernest, S. & Bello-Reuss, E. (1999). Secretion of platelet-activating factor is mediated by MDR1 Pglycoprotein in cultured human mesangial cells. *J. Am. Soc. Nephrol.* 10:2306–2313.

[178] Blouin, A., Bolender, R. P., & Weibel, E. R. (1977). Distribution of organelles and membranes between hepatocytes and nonhepatocytes in the rat liver parenchyma. *J. Cell Biol.* 72:441–455.

[179] Linardic, C. M. & Hannun, Y. A. (1994). Identification of a distinct pool of sphingomyelin involved in the sphingomyelin cycle. *J. Biol. Chem.* 269:23530–23537.

[180] Andrieu, N., Salvayre, R., & Levade, T. (1996). Comparative study of the metabolic pools of sphingomyelin and phosphatidylcholine sensitive to tumor necrosis factor. *Eur. J. Biochem.* .

[181] Nibbering, C. P. & Carey, M. C. (1999). Sphingomyelins of rat liver: biliary enrichment with molecular species containing 16:0 fatty acids as compared to canalicular enriched plasma membranes. *J. Membrane Biol.* 167:165–171.

[182] van Helvoort, A., Giudici, M. L., Thielemans, M., & van Meer, G. (1997). Transport of sphingomyelin to the cell surface is inhibited by brefeldin A and in mitosis, where C_6-NBD-sphingomyelin is translocated across the plasma membrane by a multidrug transporter activity. *J. Cell Sci.* 110:75–83.

[183] Nyberg, L., Duan, R.-D., Axelson, J., & Nilsson, Å. (1996). Identification of an alkaline sphingomyelinase activity in human bile. *Biochim. Biophys. Acta* 1300:42–48.

[184] Duan, R.-D., Hertervig, E., Nyberg, L., Hauge, T., Sternby, B., Lillienau, J., Farooqi, A., & Nilson, Å. (1996). Distribution of alkaline sphingomyelinase activity in human beings and animals. *Digestive Diseases and Sciences* 41:1801–1806.

[185] Duan, R.-D. & Nilson, Å. (1997). Purification of a newly identified alkaline sphingomyelinase in human bile and effects of bile salts and phosphatidylcholine on enzyme activity. *Hepatology* 26:823–830.

[186] Lin, S. & Struve, W. S. (1991). Time-resolved fluorescence of nitrobenzoxadiazole-aminohexanoic acid: effect of intermolecular hydrogen-bonding on non-radiative decay. *Photochem. Photobiol.* 54:361–365.

[187] Arvinte, T., Cudd, A., & Hildenbrand, K. (1986). Fluorescence studies of the incorporation of *N*-(7-nitrobenz-2-oxa-1,3-diazol-4-yl)-labeled phosphatidylethanolamines into liposomes. *Biochim. Biophys. Acta* 860:215–228.

[188] Coello, A., Meijide, F., Núñez, E. R., & Tato, J. V. (1996). Aggregation behavior of bile salts in aqueous solution. *J. Pharm. Sci.* 85:9–15.

[189] Lake, M. & Organisciak, D. T. (1984). Determination of the composition of mixed micelles of bile salts by kinetic dialysis. *Lipids* 19:553–557.

[190] Carey, M. C., Montet, J.-C., Phillipis, M. C., Armstrong, M. J., & Mazer, N. A. (1981). Thermodynamic and molecular basis for dissimilar cholesterol-solubilizing capacities by micellar solutions of bile salts: Cases of sodium chenodeoxycholate and sodium ursodeoxycholate and their glycine and taurine conjugates. *Biochemistry* 20:3637–3648.

[191] Huster, D., Müller, P., Arnold, K., & Herrmann, A. (2003). The distribution of lipid chain attached NBD in negatively charged membranes determined by NMR spectroscopy. *Eur. Biophys. J.* 32:47–54.

[192] Nichols, J. W. (1985). Thermodynamics and kinetics of phospholipid monomer-vesicle interaction. *Biochemistry* 24:6390–6398.

[193] Coleman, R. & Rahman, K. (1992). Lipid flow in bile formation. *Biochim. Biophys. Acta* 1125:113–133.

[194] van Erpecum, K. J. & Carey, M. C. (1997). Influence of bile salts on molecular interactions between sphingomyelin and cholesterol: relevance to bile formation and stability. *Biochim. Biophys. Acta* 1345:269–282.

[195] Rogers, J., Lee, A. G., & Wilton, D. C. (1979). The organisation of cholesterol and ergosterol in lipid bilayers based on studies using non-perturbing fluorescent sterol probes. *Biochim. Biophys. Acta* 552:23–37.

[196] Yeagle, P. L., Bensen, J., Boni, L., & Hui, S. W. (1982). Molecular packing of cholesterol in phospholipid vesicles as probed by dehydroergosterol. *Biochim. Biophys. Acta* 692:139–146.

[197] Hale, J. E. & Schroeder, F. (1982). Asymmetric transbilayer distribution of sterol across plasma membranes determined by fluorescence quenching of dehydroergosterol. *Eur. J. Biochem.* 122:649–661.

[198] Ohvo-Rekilä, H., Åkerlund, B., & Slotte, J. P. (2000). Cyclodextrin-catalyzed extraction of fluorescent sterols from monolayer membranes and small unilamellar vesicles. *Chem. Phys. Lipids* 105:167–178.

[199] Wrenn, S. P., Kaler, E. W., & Lee, S. P. (1999). A fluorescence energy transfer study of lecithin- cholesterol vesicles in the presence of phospholipase C. *J. Lipid Res.* 40:1483–1494.

[200] John, K., Kubelt, J., Müller, P., Wüstner, D., & Herrmann, A. (2002). Rapid transbilayer movement of fluorescent dehydroergosterol in lipid membranes. *Biophys. J.* 83:1525–1534.

[201] Armstrong, M. J. & Carey, M. C. (1982). The hydrophobic-hydrophillic balance of bile salts. Inverse correlation between reverse-phase high performance liquid chromatographic mobilities and micellar cholesterol solubilising capacities. *J. Lipid Res.* 23:70–80.

[202] Harvey, P. R. C., Somjen, G., Gilat, T., Gallinger, S., & Strasberg, S. M. (1988). Vesicular Cholesterol in bile. Relationship to protein concentration and nucleation time. *Biochim. Biophys. Acta* 958:10–18.

[203] van Erpecum, K. J., Portincasa, P., Gadellaa, M., van der Heijning, B. J. M., van Berge Henegouwen, G. P., & Renooij, W. (1996). Effects of bile salt hydrophobicity on crystallization of cholesterol in model bile. *Eur. J. Clin. Invest.* 26:602–608.

Acknowledgement

This work would not have been possible without the support of a number of people, to whom I want to express my special thanks.

First of all I want to thank Prof. Andreas Herrmann for introducing me into that very interesting field of research and his offer to work on this topic. His excellent supervision, best support, and encouragement as well as his care about my scientific progress made working in his lab enjoyable and fruitful.

I want to express my thanks to Dr. Peter Müller and Prof. Thomas Pomorski for helpful discussions about experimental setup. Their suggestions and comments on the topic of this thesis were very useful. Dr. Thomas Korte was always prepared to help me with any problems in fluorescence microscopy and image analysis. Bärbel Hillebrecht introduced me into cell culture techniques and gave many useful technical advises. My thanks goes to Janek Kubelt and Stefanie Vehring for fruitful discussions. I want to thank all members of the lab of "Molecular Biophysics" for the outstanding working atmosphere.

I am indebted to Dr. Ekkehardt Richter and Petra Klein for their help with CLSM.

I want to thank Prof. Beate Röder for the opportunity to carry out experiments in her lab. My special thanks goes to Sebastian Tannert for introducing me into the theory and the experimental setup of TCSPC. All the hours he spent in adjusting lasers and preparing a suitable software for data analysis so that I could hand in this thesis in time will never be forgotten. He was also helpful with any computer problems even though he drove me to despair with his request to learn programming in the C language (maybe I will some time). Szeretlek!

I would like to thank Prof. Phillippe Devaux for providing me with fluorescent ether lipid analogues and analogues of glycosphingolipids and Prof. Allan

Hofmann for donating the fluorescent bile salts CGamF and UDC-NBD.

This thesis was supported financially by the Graduate Program "Dynamics and Evolution of Cellular and Macromolecular Processes" of the Deutsche Forschungsgemeinschaft. The opportunity to give talks and to discuss with members of this graduate program were very important for the progress of this thesis.

Lebenslauf

Name:	Astrid Tannert, geb. Höhlig
Geburtsdatum:	7. April 1976
Geburtsort:	Wolfen (Kr. Bitterfeld)
Nationalität:	deutsch
Familienstand:	verheiratet

Ausbildung und Tätigkeiten

09/1982 – 08/1990	POS „Herrmann Matern“ Raguhn
09/1983 – 02/1985	Schule bei der Botschaft der DDR in der ČSSR, Prag
09/1990 – 07/1992	Gymnasium Bitterfeld (Abschluss Abitur)
10/1994 – 09/1996	Studium der Biochemie an der Martin-Luther-Universität Halle-Wittenberg
09/1996 – 06/1997	Studium der Biochemie an der University of Wales, Cardiff, UK
07/1997 – 08/1996	Praktikum bei Bayer Bitterfeld
10/1997 – 07/2000	Studium an der Freien Universität Berlin in der Fachrichtung Biochemie, Anschluss Diplom
02/2000 – 07/2000	Diplomarbeit zum Thema „Translokation von Phospholipidanaloga im ER von Hefezellen“ Betreuer: Prof. Dr. Andreas Herrmann (HU Berlin)
seit 08/2000	Promotionsstudium an der Humboldt-Universität zu Berlin, Lehrstuhl Prof. Dr. Andreas Herrmann Institut für Biologie

Publikationen

Marx, U., Lassmann, G., Holzhütter, H.-G., Wüstner, D., Müller, P., **Höhlig, A.**, Kubelt, J., & Herrmann, A. (2000). Rapid flip-flop of phospholipids in the endoplasmic reticulum membranes studied by a stopped-flow approach. *Biophys. J.* 78:2628-2640.

Libera, J., Pohl, A., **Tannert, A.**, Müller, P. & Herrmann, A. (2001). Biologische Membranen - Wie ›lebendig‹ sind Lipide?. *Humboldt-Spektrum*, 3–4: 58–63.

Buton, X., Herve, P., Kubelt, J., **Tannert, A.**, Burger, K. N. J., Fellmann, P., Müller, P., Herrmann, A., Seigneuret, M., & Devaux, P. F. (2002). Transbilayer movement of monohexosyl sphingolipids in endoplasmic reticulum and Golgi membranes. *Biochemistry*, 41: 13106-13115.

Tannert, A., Pohl, A., Pomorski, T., & Herrmann, A. (2003). Protein Mediated Transbilayer Movement of Lipids in Eukaryotes and Prokaryotes: The Relevance of ABC Transporters. *Int. J. Antimicrob. Agents*, in press.

Tannert, A., Wüstner, D., Bechstein, J., Müller, P., Devaux, P. F., & Herrmann, A. (2003). Aminophospholipids have no access to the lumenal side of the biliary canaliculus - Implications for the specific lipid composition of the bile fluid. *J. Biol. Chem.*, in press.

Poster und Vorträge

Tannert, A., Tannert, S., Kemnitz, K., Röder, B., & Herrmann, A. Fluorescence life time determination of fluorescent lipid analogs in different environments. A Method for Determination of the Localization and Organization of Phospholipids in the Bile. Poster und Vortrag, Joint Workshop "Biophysics and Bioinformatics", August 2001, Berlin.

Tannert, A., Tannert, S., Kemnitz, K., Röder, B., & Herrmann, A. Determination of Lipid Organization in the Canalicular Lumen of HepG2 Cells by Fluorescence Life Times of Lipid Analogs. Poster, 46^{th} Annual Meeting of the Biophysical Society, February 2002, San Francisco.

Tannert, A. Mechanisms of specific lipid enrichment in the bile fluid. Vortrag, „International Workshop Cell System Biology“, November 2002, Berlin.

Selbständigkeitserklärung

Hiermit erkläre ich, die vorliegende Arbeit selbständig ohne fremde Hilfe verfaßt zu haben und nur die angegebene Literatur verwendet zu haben.

Ich besitze keinen entsprechenden Doktorgrad und habe mich anderwärts nicht um einen Doktorgrad beworben.

Die dem Promotionsverfahren zugrundeliegende Promotionsordnung vom 19.06.2002 ist mir bekannt.

Astrid Tannert
2. September 2003